Chapter 2
Chemical Bond

2.1 Historical Development of the Concept

The concept of the *chemical bond* is central to modern chemistry. Its classical form, which gradually and painstakingly developed in the course of the 19th century, described molecules as a combinations of linked atoms. The idea proved extremely useful for interpreting, systematizing and predicting chemical facts, although for a long time it developed without any understanding of the underlying physics. This 'black box' situation began to change towards the close of the century. G. J. Stoney in 1881 calculated the elementary charge of electricity and in 1891 named it 'electron'. In 1894, W. Weber suggested that the atom consists of positive and negative electric charges. In 1897, W. Wiechert, J. J. Thomson, and J. S. Townsend measured the charge of the electron. In 1902–1904, William Thomson (Lord Kelvin) and J. J. Thomson developed the 'plum cake' atomic model, with electrons distributed within the homogenous sphere of positive electricity. In 1904, H. Nagaoka suggested that the positive charge is located in the center of the atom, the electrons orbiting around it. Finally, in 1911 E. Rutherford proved this planetary model experimentally.

In 1904, R. Abegg proposed that the valence of an atom corresponds to the number of electrons it lost or gained, the sum of which must be equal to 8 and the highest positive valence to the Group (column) number in the Periodic Table. In 1908, J. Stark postulated that chemical properties of an atom are defined by its outer ('valence') electrons, and W. Ramsay in his essay *Electron as the element* already mentioned the electronic nature of the bond between atoms. Finally, in 1913, N. Bohr proposed the model where the majority of the electrons in a molecule are located around the nuclei as in isolated atoms, and only their outer electrons rotate around the axes connecting atoms, forming the chemical bond. In 1916 W. Kossel explained the formation of ions by the transfer of electrons from one atom to another to complete the outer electronic shells of both to the stable 8-electron configurations; he also introduced the important idea that there is a gradual transition from purely polar compounds (e.g., HCl) to typically non-polar ones (e.g., H_2) [1]. In the same year Lewis described the formation of the covalent bond by two identical atoms sharing their electrons to acquire stable octets [2]. Langmuir developed the theory of Lewis, postulating that electrons in the atom are distributed in layers, with the 'cells' for

S. S. Batsanov, A. S. Batsanov, *Introduction to Structural Chemistry,*
DOI 10.1007/978-94-007-4771-5_2, © Springer Science+Business Media Dordrecht 2012

2 electrons in the first layer, 8 in the second, 18 in the third and 32 in the fourth [3, 4, 5]. For a long time, the octet rule was regarded as the norm of chemical bonding, and deviations from it as exceptions. However, later these exceptions became more and more numerous, until their explanation required the introduction of new ideas which will be discussed below. The independent impulse to the development of the electronic theory was given by the Periodic Law (D. I. Mendeleev, 1869) which got its physical explanation in the Bohr-Rutherford model, the quantum theory and, finally, the Pauli exclusion principle, which explained the electronic structure of the atom and thereby the cellular model of Langmuir. The development of these approaches led to the creation of quantum chemistry. Though the discussion of latter is beyond scope of this book, it should be noted that in the fundamental equation of E. Schrödinger (1926), $H\Psi = E\Psi$, where H is the Hamilton operator, E is the total energy of the system, the wavefunction Ψ (or, more exactly, its square) defines the probability of finding an electron in a certain part of space. Because of the uncertainty principle, it is not possible to describe the electron's orbit precisely, but only in terms of probability; hence we speak of the 'electronic cloud'. Schrödinger's equation cannot be solved precisely for any system containing more than one electron, therefore the application of quantum mechanics to chemistry is essentially the quest for suitable approximations.

The region defined by a wavefunction is termed an atomic orbital, which can be defined uniquely by three quantum numbers. The principal quantum number n is the number of the electron shell, the orbital quantum number l defines the sub-shell, and the shape of the orbital. Thus, atomic s-orbitals with the quantum number $l = 0$ are spherically symmetrical, whereas p-orbitals (with $l = 1$) are dumbbell-shaped, are directed along the three Cartesian axes (hence their designation as p_x, p_y and p_z) and tend to form bonds in these directions. The directionality of a (non-spherical) orbital is defined by the magnetic quantum number m_l. Averaging (hybridization) of one *ns* and three *np* orbitals leads to a tetrahedral arrangement of bonds (for instance, in diamond), other combinations of *s, p and d* electrons lead to other types of hybridization and geometrical configurations. The modern state of the calculations and 'experimental measurements' (reconstruction) of orbitals is discussed in the fine essay of Schwartz [6], who points that 'orbitals' are concepts which are useful to approximately describe the structures, properties, and processes of real molecules, crystals, *etc*. Correspondingly, although orbitals are essentially determined by the nature of the molecules, they can be defined in different ways for different purposes. The relation between the wavefunction Ψ and the corresponding orbital Φ is defined by the equation

$$\Psi(X_1, \ldots X_N) \approx \Phi(X_1, \ldots X_N) \tag{2.1}$$

Whether Φ is a satisfactory orbital approximation of Ψ, depends on the type of the molecule, on its state, and also on the nature of the problem. Hence there are no such things as *the* orbitals in a molecule, just as there are no uniquely defined charges of atoms in a molecule. There are many kinds of atomic charges (see below), and similarly, there are many different types of orbitals, appropriate for different

physical phenomena. Firstly, the exact wavefunction Ψ and the exact energy E can be generated from a simple orbital product function Φ by several theoretically well-defined operators. Secondly, the popular density functional approaches of Kohn and Sham (KS) all aim at the calculation of highly *reliable* molecular energies with the help of a product wavefunction of 'KS orbitals' of different kinds. Thirdly, the most famous orbital approach for approximate energies is the first-principles, self-consistent field model of Hartree and Fock. There are also many semi-empirical varieties, such as the iterative extended Hückel, CNDO, AM1, *etc*.

In developing the theory of the chemical bond the great contributions were made by Coulson, Hückel, Hund, Slater, Mulliken (see [7]) and, especially, by Pauling who played the major role in the formation of modern structural chemistry: he has formulated such concepts as the hybridization, the polarity and strength of a bond, the degree of the double-bond character, the principle of the local electro-neutrality of atoms, the effective valence, i.e., has created that language of the given area of science on which experimenters began to speak and think. The valence-bond (VB) theory, developed by Pauling, generally followed the (implicit) idea of nineteenth-century chemists that atoms persist in a molecule as recognisable entities. Later, with the triumph of the theory of molecular orbitals, came the widespread view that in a molecule there are no atoms, only nuclei and electrons (orbitals). However, it is worth noting that the total energy of a benzene molecule, i.e. the energy required to split it into six nuclei of charge + 6, six protons and 42 electrons, all at infinite separations, amounts to 607837 kJ/mol (from MO calculations). The (experimental) atomization energy of benzene, i.e. the energy required to split the molecule into six carbon and six hydrogen atoms, is only 5463(3) kJ/mol, or less than 1 % of the former. For comparison, the sublimation enthalpy of crystalline benzene, which is the measure of intermolecular cohesion, is 44 kJ/mol. Thus, atoms in a molecule are no less "real" than molecules in a crystal. Indeed, later Bader [8] and Parr [9] brought back the concept of atoms in molecules (AIM), now on modern quantum-mechanical basis. Still, notwithstanding all the successes of quantum chemistry, structural chemistry remains a predominantly experimental science.

2.2 Types of Bonds: Covalent, Ionic, Polar, Metallic

The traditional classification of chemical bonds into ionic, covalent, donor-acceptor, metallic and van der Waals corresponds to extreme types, but a real bond is always a combination of some, or even all of these types (Fig. 2.1). Purely covalent bonding can be found only in elemental substances or in homonuclear bonds in symmetric molecules, which comprise a tiny fraction of the substances known. Purely ionic bonds do not exist at all (although alkali metal halides come close) because some degree of covalence is always present. Nevertheless, to understand real chemical bonds it is necessary to begin with the ideal types. In this Section we will consider mainly the experimental characteristics of different chemical bonds and only briefly the theoretical aspects of interatomic interactions.

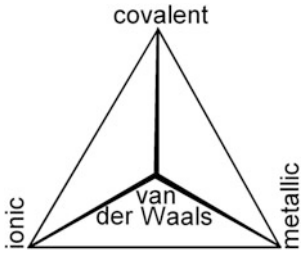

Fig. 2.1 Tetrahedron of chemical bond types. The nature of a given bond can be described by a point within the tetrahedron

2.2.1 Ionic Bond

The ionic bond results from the Coulomb attraction of oppositely charged ions. Its strength is characterised by the electrostatic energy; in MX ionic crystals it is the crystal lattice energy U(MX), which can be determined experimentally from the Born-Haber cycle or calculated theoretically from the known net charges of ions (Z, not to be confused with nuclear charges!) and inter-ionic distances (d), as

$$U = k_M \frac{Z^2}{d}\left(1 - \frac{1}{n}\right) \tag{2.2}$$

where k_M is the Madelung constant and n is the Born repulsion factor (Table 2.1), in good agreement with the experiment. The ionic theory explains many facts of structural inorganic chemistry. Thus, in many ionic structures, larger ions (anions) form a close packing motif while smaller ions (cations) occupy the voids in it. As this motif contains only tetrahedral and octahedral voids, this explains why cations usually have the coordination number, N_c, of 4 or 6. Coulomb interactions being strong, ionic crystals have high fusion (melting) temperatures and high atomization energies, but dissolve in polar liquids (e.g. water) due to high solvation (hydration) heat. The absence of electrons in the inter-ionic space results in low refractive indices and high atomic polarizations, wide band gaps, and insulator properties.

As noted above, Kossel introduced the idea that the transition from ionic to covalent substances is gradual, the covalence increasing with the mutual polarizing influence of ions. This idea was developed by Fajans and his school who defined the polarizabilities of ions and estimated the polarizing action of cations (Z/r^2), but ultimately failed to create a quantitative theory. The reason is obvious [10]: there are no completely ionic substances, only intermediate cases, more or less approaching this type. Hence the parameters of ideal ions are not available experimentally, the more so since ionic radii cannot be uniquely defined from interatomic distances (see Chap. 1). Thus the polarization concept remained only qualitative. However, the contribution in the bond energy of the polarizing effect of atoms can be described in the form that has proven itself for the van der Waals interaction (see Sect. 4.4), where the deviation of the A ⋯ B distance from the mean of A ⋯ A and B ⋯ B distances is a function of the difference of the atomic polarizabilities

$$p_\alpha = \left[\frac{(\alpha_\mathrm{A} - \alpha_\mathrm{B})}{\alpha_\mathrm{A}}\right]^{2/3} \tag{2.3}$$

Table 2.1 Hardness parameters of ions

Electron configuration of ion	He	Ne	Ar (and Cu^+)	Kr (and Ag^+)	Xe (and Au^+)
n	5	7	9	10	12
f_n	1.250	1.167	1.125	1.111	1.091

turning from distances to volumes, this function takes the form

$$p_a = \left[\frac{(\alpha_A - \alpha_B)}{\alpha_A}\right]^2 \tag{2.4}$$

Taking into account the interaction of effective charges of atoms, the total 'energetic' polarizing effect is

$$q = p_a \frac{(Zi)^2}{d} \tag{2.5}$$

Evidently, the smaller the atom the stronger its polarizing effect. If the smaller ion is the cation (as is usually the case) then it reduces the total α of the substance, if the anion then α increases. Such simple approach allows calculating polarizability of inorganic compounds with good accuracy [11].

The ionic model is widely used to predict the coordination numbers, N_c, in crystal structures. Evidently, the higher the r_c/r_a ratio, the more anions can be accommodated around a given cation. The Magnus-Goldschmidt rules, dating back to nineteen-twenties [12], predicted from simple geometrical condiderations the following succession. For $r_c/r_a \leq 0.15$ the stable configuration can only be linear ($N_c = 2$), from 0.15 to 0.22 it should be equilateral triangle ($N_c = 3$), from 0.22 to 0.41 a tetrahedron ($N_c = 4$), from 0.41 to 0.73 an octahedron ($N_c = 6$), above 0.73 a cube ($N_c = 8$). However, even for crystals with essentially ionic bonds these rules often fail. Thus, in $MgAl_2O_4$ the large Mg^{2+} ion has $N_c = 4$ and the smaller Al^{3+} has $N_c = 6$ whereas it should be the other way round [13]. Crystal structures of MX_n also often confound the simple ionic model [14]. Obviously, one would expect the cation to adopt higher N_c with smaller F^- anion than with other, bulkier, halogens (X = Cl, Br, I). In fact, $N_c(MF) \leq N_c(MX)$ and $N_c(MF_2) \approx N_c(MX_2)$, and only for $n = 3$ or 4 it is $N_c(MF_n) \geq N_c(MX_n)$. A striking case is CsF and CsI: their r_c/r_a of 1.25 and 0.76 both predict $N_c = 8$. This is correct for CsI, but CsF with the higher ratio has a NaCl-type (B1) structure with $N_c = 6$!

These failures show that the simple ionic model is a rather imperfect approximation. Firstly, the charges of ions are assumed to equal the formal oxidation states of the corresponding elements. Secondly, the ions are regarded as absolutely hard spheres, whose spatial distribution is governed only by their relative sizes and the quest for the densest possible packing and the nearest possible contacts between oppositely-charged ions. The agreement with the experiment can be improved by assigning to ions more realistic effective charges, e^* (see below, Table 2.2). For alkali halides, for instance, the charges of anions in different compounds with identical cations are related as $(e^*_{MF}/e^*_{MCl})^2 = 1.245$, $(e^*_{MBr}/e^*_{MCl})^2 = 0.923$, $(e^*_{MI}/e^*_{MCl})^2 = 0.826$.

Table 2.2 Effective charges of hydrogen and halogen atoms in molecules

HF	H_2O	H_2S	NH_3	C_2H_2	C_2H_4	CH_4	CH_3I	CH_3Br	CH_3Cl	CH_3F
0.41	0.33	0.11	0.23	0.35	0.16	0.11	0.13	0.33	0.47	0.95
		CS_2	GeH_4	SiH_4	SnH_4	$GeBr_4$	HCl	$ZnBr_2$		
		0	0.09	0.10	0.12	0.17	0.20	0.25		

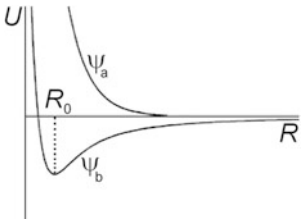

Fig. 2.2 Potential energy (U) of the bonding and antibonding orbitals of a diatomic molecule as functions of the interatomic distance R

Multiplying the ultimate radii of anions from Table 1.17 and assuming $e^*_{MCl} = 1$, by these ratios we obtain the effective, or 'energetic' ionic radii r^* (see Sect. 1.6), viz. F^- 2.30, Cl^- 2.25, Br^- 2.20 and I^- 2.17 Å [11]. It follows that the effective, rather than formal, ratio of the cation and anion radii ($r_c{}^*/r_a{}^*$) in CsF is smaller than in CsI. Hardness of ions is not infinite and varies from ion to ion. In the Born-Landé theory it is defined by the repulsion coefficient n and the rigidity factor $f_n = (n-1)/n$ (see Table 2.1). The product $f_n \times r^*$ then gives the radii of spheres with absolutely identical properties. Their ratio,

$$\overline{R} = \frac{r^*_+}{r^*_-}\frac{f^+_n}{f^-_n} \tag{2.6}$$

which equals 0.68 for CsF, 0.72 for CsCl, 0.745 for CsBr and 0.77 for CsI, now describes the changes of N_c correctly. The agreement with reality can be further improved by taking into account the partly covalent character of the bonding in ionic compounds [14]. The effects of polarization and deformation of ions on ionic crystal structures were surveyed by Madden and Wilson [15] who concluded that the ionic model with formal charges has wider applicability than is often supposed, but covalent anomalies (layered structures, bent bonds, *etc*) can be quantitatively explained by ionic polarization.

2.2.2 Covalent Bond

Usually, a covalent bond between two atoms is formed by two electrons, one from each atom. These electrons tend to be partly localized in the region between the two nuclei. If the orbitals of these electrons are Ψ_1 and Ψ_2, the molecular orbital of the bonded atoms must be their linear combination, symmetric $\Psi_b = \Psi_1 + \Psi_2$ and antisymmetric $\Psi_a = \Psi_1 - \Psi_2$. As illustrated in Fig. 2.2, the former orbital has a minimum of energy at certain distance and generally has lower energy than the

latter, therefore the former orbital is bonding and the latter antibonding. Since an orbital can be occupied by no more than two electrons, this picture was in fact anticipated by the Lewis' model (in 1916—a decade before the beginning of quantum mechanics!) which regarded bonds as shared electron pairs. Lewis also noted that in stable molecules, each atom usually has 8 electrons in its valence shell (except H which has two), counting both the bonding and the unshared electron pairs and taking no account of the bond polarity. This *octet rule* for a long time was regarded as a law of chemistry, apparently resulting from the fact that there are only one *s* and three *p* orbitals in an electron shell, which can accommodate a maximum of 8 electrons between them. Compounds which did not conform to this rule were regarded as special classes of compounds, hypervalent (with >8 electrons) and hypovalent (with <8 electrons). Alternatively, exceptions were explained away by including *d* orbitals into hybridization, or by invoking bond polarity and net atomic charges and assuming that the octet rule applies to the effective number of electrons around each atom (contrary to Lewis' own approach). Today it is clear that this rule, although pedagogically useful, has numerous exceptions which show no extraordinary properties [16]. Particularly, comparison of bonds in hypervalent molecules with those in octet molecules reveals no fundamental difference in their nature. Likewise, saving the octet rule by assigning net charges to atoms, contributes nothing to understanding the structures and properties of molecules. Thus, the nitrogen atom in an a protonated amine or pyridine has a formal charge of $+1$ but shows no corresponding contraction of the bond distances; in fact, this atom has a small negative charge!

It seems that the belief in the octet rule and in *misread* quantum-mechanical concepts helped for a long time to discourage the search for compounds of 'inert' gases, although von Antropoff [17] and Pauling [18] have predicted that these might be chemically awaken by powerful oxidizing agents with high electronegativity. This prediction was confirmed in 1962 when xenon compounds were discovered [19–23]. Since then, over 500 compounds of the 'rare' (formerly 'inert' and later 'noble') gases were synthesized [24] and dozens of them characterized by X-ray diffraction. Finally, solid xenon was converted into metallic state under ultra-high pressure [25, 26]

Another note of caution is necessary. In every modern textbook, the explanation of covalent bonding begins (and sometimes also ends) with the H_2 molecule, because this is the simplest case and historically the first one explored. Unfortunately, it is by no means a typical one—the fact often not appreciated by the students. In fact, H_2 shows many unique properties because it has no non-bonding electrons, so that the bonding pair has also to 'take responsibility' for intermolecular interactions, both attractive and repulsive. As a result, neither job is done properly. The interatomic distance and atomization energy, compressibility and other molecular-physical properties are consistent with the bond order much lower than the conventional 1 [27]. Thus, the covalent radius of hydrogen determined from its bond distances with different atoms (which can compensate the lack of electron density in the bond from their own) is 0.30 Å [28], hence the actual H–H bond length of 0.74 Å in H_2 molecule corresponds to the bond order of only 0.57 (see below, Eq. 2.8). Usually the ionization potentials of A_2 molecules are lower than those of isolated atoms, and the bond dissociation energies of A_2^+ are higher than those of neutral molecules, H_2 shows the

opposite relations in both respects (see Chap. 1). Hydrides of the elements of Groups 15 and 16 violate the general VSEPR rules of molecular geometry (see Sect. 3.2.2): H–A–H angles are smaller than F–A–F, whereas usually the angles widen with the decrease of the ligand electronegativity; this effect was also explained by the electron pair in the A–H bond doubling as the non-bonding pair of the H ligand [29]. The observed van der Waals radius of hydrogen is *ca.* 0.25 Å lower than the value obtained by extrapolating the radii of halogens [27]. This indicates the weakness of the intermolecular repulsion, while the simultaneous weakness of intermolecular attraction can be seen from the large deviation of H_2 from Trouton's law: the enthalpy of evaporation has a constant ratio to the boiling point temperature. For H_2 this ratio is 44.8 J mol^{-1} K^{-1}, compared to the average of 88 J mol^{-1} K^{-1}.

Let us consider the relation between of the dissociation energy and the bond length. Morse [30] introduced the formula which describes well the experimental electronic energy (E) of a diatomic molecule as a function of the inter-nuclear distance near the equilibrium state (d_e)

$$E(d) = D_e\{1 - \exp[-a(d - d_e)]^2\} \tag{2.7}$$

where D_e is the dissociation energy. Assuming that the attractive energy is proportional to the bond order q [31], from Eq. 2.7 it is possible to derive Pauling's equation,

$$d_q = d_1 - b \ln q \tag{2.8}$$

where d_1 and d_q are the lengths of a standard single bond and a bond of the order q, respectively, and b is an (essentially empirical) constant. Pauling himself used the $0.6 \times \log q$ term, which corresponds to $b = 0.26$ if the natural logarithm is used. However, the proportionality between bond energy and bond order is a rather crude simplification: the experimental energies of the C–C and C≡C bonds relate as 1: 2.2, while those of N–N and N≡N bonds as 1: 4.5.

Parr and Borkman [32] have shown that for many diatomic molecules the bond energy at distances (d) near the equilibrium can be described as

$$E = E_o + \frac{E_1}{d} + \frac{E_2}{d^2} \tag{2.9}$$

where the second term reflects the Coulomb interactions, and the third one accounts for the overlap of atomic orbitals. According to the pseudo-potential method, E is proportional to d^{-2} [33], whereas in Phillips' theory it is proportional to $d^{-2.5}$(see Sect. 2.3). The lengths of typical carbon-carbon bonds correlate linearly with bond dissociation energies (E) in the full range of single, double, triple, and highly strained bonds, with E ranging from 16 to 230 kcal mol^{-1}. The equation

$$d = 1.748 - 0.002371E \tag{2.10}$$

(for d in Å, E in kcal/mol) has been tested on 41 typical carbon-carbon bonds, ranging in length from 1.20 to 1.71 Å. This sets a maximum bond length limit of 1.75 Å for carbon-carbon bonds [34].

By far the most-studied type of chemical bonding is known as 'aromatic'. The concept of aromaticity was introduced in the 1860's by Kekulé and Erlenmeyer to describe cyclic molecules (of which benzene is the seminal one) for which the classical theory suggested alternating single and double bonds, but which were much more stable than implied by such a formula, or than their open-chain analogues actually were. In the twentieth century, diffraction methods confirmed Kekulé's insight that benzene ring has sixfold symmetry (D_{6h}) with all six C–C bonds equivalent (1.3983 Å, cf. 1.422 Å in graphite) and intermediate in character between single and double bonds (e.g. in butadiene, 1.467 and 1.349 Å) [35]. At the dawn of quantum chemistry, Pauling [36] introduced the idea of resonance between two or more valence-bond structures as the source of energy gain. For benzene, he estimated the resonance energy (RE) as the difference between the heats of formation or of hydrogenation of benzene and of the (hypothetical) cyclohexatriene. Both comparisons gave essentially the same RE, *ca.* 150 kJ/mol (< 3 % of the atomization energy of benzene). However, other reference reactions would yield different RE; one also must take into account different energies of steric strain (repulsion between non-bonded atoms) in the real and model molecules, which are of the same order of magnitude. Thus, modern estimates of RE of benzene range from 85 to 312.6 kJ/mol [35]. In the MO theory, aromatic molecules were described in terms of circular π-electron delocalization. Hückel [37] postulated that cyclic planar π-electron systems with $(4n+2)$ π-electrons must be stabilized (aromatic) and those with $4n$ π-electrons (e.g. cyclobutadiene) must be destabilized (anti-aromatic) with localized single and double bonds. Hückel's rule was vindicated by the discovery of the aromaticity of cyclopropenyl cation ($n=0$), cyclopentadienyl anion and cycloheptatrienyl cation ($n=1$) and various heterocycles, while Pauling's failure to explain anti-aromaticity [38] in terms of simple VB theory discredited the latter [39]. However, today it is clear that high-precision versions of VB and MO methods (but not the severely simplified versions of the pre-computer era!) give essentially the same results. Furthermore, it is realized that the symmetry of the benzene ring is due to σ-bond equalization: π-bonds 'left to themselves' would have yielded a localized Kekulé structure [40].

Aromatic rings provide the circuits in which circular electric currents can be induced by external magnetic field, hence magnetic susceptibility χ_m of aromatic molecules is (i) highly anisotropic and (ii) higher than the sum of atomic increments χ_a, its 'exhaltation' provides one of the quantitative measures of aromaticity [41]:

$$\Lambda = \chi_m - \sum \chi_a > 0 \tag{2.11}$$

Other aromaticity indices are based on equalization of bond lengths, bond orders or the peculiar proton shifts in NMR spectra (also due to the exhalted magnetism of aromatics) [42].

Today, it is clear that aromaticity is possible in 3-dimensional, as well as planar, systems, such as quasi-spherical cages of fullerenes [43, 44] and polyhedral boranes (e.g. $B_{12}H_{12}^{2-}$) [44, 45], in carbon nanotubes and in some metal clusters (e.g., Au_5Zn^+, Au_{20}) [46]. The $2(n+1)^2$ rule proposed by Hirsch [47] and successfully applied to design various novel aromatic compounds, serves as the 3-dimensional

counterpart of the Hückel's rule for planar systems. However, deviations from this rule are found that indicate the need for further refinement. This vast area has been comprehensively reviewed in two thematic issues of Chemical Reviews [48, 49].

2.2.3 Polar Bond, Effective Charges of Atoms

The term 'ionic substance' is often used in inorganic chemistry, but although the reality of ions is manifest in the ionic conductivity in molten state, and in some cases in the solid state, in fact there are not many compounds which can be regarded even as *practically* ionic, and none with purely ionic bonding. Monoatomic cations are always smaller than anions (except for F^- being smaller than K^+, Rb^+, Cs^+) and tend to polarize the latter, causing a displacement of the anion's electron density towards the cation. The ionization potentials of metals being higher than the electron affinities of nonmetals (see Chap. 1) has similar effect. Thus even in the most ionic crystals the charges must be less then the oxidation numbers. How these can be determined? Dozens of experimental and theoretical methods have been suggested for the determination of atomic charges [50]. For some AX_n or AH_n molecules, the bond polarities and hence the effective charges of ligands are known from IR or XR spectra [51–54]. These values, always <1, are listed in Table 2.2. The most poplular method of estimating the atomic charges in molecules is based on the dipole moments and will be considered in details in Chap. 11 (Table 11.2).

The effective charges of atoms in crystals, rather than molecules, can be determined by Szigeti's spectroscopic method [55], which is also described in details in Chap. 11, using the formula

$$e^* = \frac{3\nu_t}{Ze(n^2+2)}\left[\pi\left(\varepsilon - n^2\right)\overline{m}V\right]^{\frac{1}{2}} \tag{2.12}$$

where ν_t is the transverse vibration frequency of the lattice, n is the refractive index, ε is the dielectric constant, V is the molar volume, Z is the valence of an atom, and $\overline{m}$ is the reduced mass of a vibrating atom. The results are listed in Tables 2.3 and 2.4, in the conventional form e^*/v where v is the formal valence of the atom (i.e. the values are the relative bond ionicities). As we can see, the absolute values of effective charges of O in MO-type oxides are always > 1, whereas in molecules they are < 1. As discussed in Sect. 1.1.2, the $O^- + e^- \rightarrow O^{2-}$ addition requires an expense of energy, but in crystals this is compensated by the Madelung energy, which makes the higher negative charges thermodynamically possible. The charges increase with the coordination number: the phase transition in HgS raises the effective charge from 0.20 to 0.28 as N_c changes from 2 to 4, in MnS a transition with $N_c = 4 \rightarrow 6$ increases e^* from 0.35 to 0.44. An unexpected feature is the greater effective charges in halides of Groups 11 and 12 elements. A study of the band structure of CuX and AgX has revealed that the metals have effective valences exceeding 1, due to participation of d-electrons. Similar increases of the metal valences were observed also in some compounds of the MX_2 type (see below). The problem of the effective valences of

Table 2.3 Effective atomic charges (e^*/v) in MX crystals by Szigeti's method (from [56], except where specified)

M (v = 1)	F	Cl	Br	I
Li	0.81	0.77	0.74	0.54
Na	0.83	0.78	0.75	0.74
K	0.92	0.81	0.77	0.75
Rb	0.97	0.84	0.80	0.77
Cs	0.96	0.85	0.82	0.78
Cu		0.98	0.96	0.91
Ag	0.89	0.71	0.67	0.61
Tl		0.88	0.84	0.83
M (v = 2)	O	S	Se	Te
Cu	0.54			
Be	0.55			0.26[a]
Mg	0.59	0.49	0.39	
Ca	0.62	0.52	0.36	
Sr	0.64	0.54	0.50	
Ba	0.74	0.65	0.52	
Zn	0.60	0.44	0.40	0.39
Cd	0.59	0.45	0.42	0.38
Hg	0.57	0.28[b]	0.27	0.26
Eu	0.67	0.55	0.53	0.50
Sn		0.33	0.28[c]	0.26
Pb	0.58	0.36	0.35	0.28
Mn	0.55	0.44[d]	0.42	0.33
Fe	0.46[e]			
M (v = 3)	N	P	As	Sb
B	0.38	0.25		
Al	0.41	0.26	0.21	0.16
Ga	0.41	0.19	0.17	0.13
In		0.22	0.18	0.14

[a][57], [b]$N_c = 4$, for $N_c = 2$ $e^* = 0.20$, [c][58], [d]$N_c = 6$, for $N_c = 4$ $e^* = 0.35$, [e]$e^* = 0.44$ for CoO and 0.41 for NiO.

the metallic elements of Groups 11–14 will be discussed later; here it is sufficient to note that in MoS_2 and $MoSe_2$ we assume v = 2 for the chalcogen and v = 4 for the metal. Spectroscopic studies of alkali halides [60], MF_2 [61, 62], ZnS and GaAs [63] have shown that their effective charges decrease on heating, signifying that the bond covalency increases.

Another spectroscopic method of measuring bond polarity (or ionicity) f_i in solids was developed by Phillips and Van Vechten (PVV) [64–67], using the equation

$$f_i = \frac{C^2}{{E_g}^2} \tag{2.13}$$

where E_g is the band gap and C is the Coulomb component of the bond energy. Numerical values of f_i according to PVV and charges according to Szigeti do not coincide because of different dimensionality, but can be related thus

$$f_i = \frac{(e^*)^2}{n^2} \tag{2.14}$$

Table 2.4 Effective atomic charges (e^*/v) in M_nX_m crystals, by Szigeti's method

MX_2	$e^*/2$	MX_2	$e^*/2$	MX_2	$e^*/2$	M_nX_m	e^*/v
MgF_2	0.76	$FeCl_2$	0.64	$SnSe_2$	0.25	UO_2	0.60
CaF_2	0.84	$FeBr_2$	0.58	ZrS_2	0.44	CeO_2	0.56
SrF_2	0.85	CoF_2	0.74	HfS_2	0.50	ScF_3	0.76
$SrCl_2$	0.76	$CoCl_2$	0.57	$HfSe_2$	0.45	YF_3	0.76
BaF_2	0.87	$CoBr_2$	0.52	MoS_2	0.06	LaF_3	0.74
ZnF_2	0.76	NiF_2	0.68	$MoSe_2$	0.04	AlF_3	0.60
CdF_2	0.80	$NiCl_2$	0.51	MnS_2	0.42	GaF_3	0.60
$CdCl_2$	0.74	$NiBr_2$	0.46	$MnSe_2$	0.38	InF_3	0.61
$CdBr_2$	0.69	Na_2S	0.58	$MnTe_2$	0.30	YH_3	0.50[a]
CdI_2	0.63	Cu_2O	0.29	FeS_2	0.30	Y_2O_3	0.62
HgI_2	0.38	TiO_2	0.60	RuS_2	0.36	Y_2S_3	0.40
EuF_2	0.84	TiS_2	0.39	$RuSe_2$	0.38	La_2O_3	0.62
PbF_2	0.87	$TiSe_2$	0.18	OsS_2	0.40	La_2S_3	0.40
$PbCl_2$	0.90	SiO_2	0.60	$OsSe_2$	0.38	Al_2O_3	0.59
PbI_2	0.72	GeO_2	0.54	$OsTe_2$	0.38	Cr_2O_3	0.49
MnF_2	0.81	GeS_2	0.18	PtP_2	0.28	Fe_2O_3	0.45
$MnCl_2$	0.69	$GeSe_2$	0.17	$PtAs_2$	0.24	As_2S_3	0.20
$MnBr_2$	0.66	SnO_2	0.57	$PtSb_2$	0.26	As_2Se_3	0.14
FeF_2	0.78	SnS_2	0.32	ThO_2	0.58	$RuTe_2$	0.39

[a] [59]

where n is the refractive index. Originally the PVV theory was applied only to structures of B1 and B3 types, but subsequently, owing to the works of Levin [68–70] and others [71–73], it was expanded to other structural types. The value of f_i is affected only slightly by the nature of the anion, but sharply by a change of N_c. Thus, GeO_2 has $f_i = 0.51$ in its quartz-like modification, but $f_i = 0.73$ in the rutile-like form. Phillips used this as the criterion of polymorphism; taking 0.785 as the critical value of f_i for the B3 → B1 transition. This method revealed the evolution of atomic charges under varying thermodynamic conditions, in particular a reduction of f_i on compression of crystals (see below). It is worth mentioning that PVV were anticipated by Hertz, Link and Bokii [74–77], [523] who calculated the bond ionicity

$$i = \frac{P_a}{P_e} \tag{2.15}$$

as the ratio of atomic (P_a) and electronic (P_e) polarizabilities of substances; this parameter can be related to the PVV polarity through the Mossotti-Clausius formula. Since

$$P_o = P_M - P_e = V\left(\frac{\varepsilon - 1}{\varepsilon + 2} - \frac{n^2 - 1}{n^2 + 2}\right) \tag{2.16}$$

then for low-polarity substances, where $\varepsilon \approx n^2$, we obtain

$$P_a = V\left(\frac{\varepsilon - n^2}{n^2 + 2}\right). \tag{2.17}$$

Combination of Eq. 2.17 with

$$P_e = V\left(\frac{n^2-1}{n^2+2}\right) \tag{2.18}$$

gives

$$i \approx \frac{\varepsilon - n^2}{n^2 - 1} \tag{2.19}$$

apparently similar to the equation:

$$i = \frac{\varepsilon - n^2}{\varepsilon - 1} \tag{2.20}$$

which follows from Eq. 2.13 and the basic formulae of the dielectric theory,

$$n^2 = 1 + \left(\frac{h\nu_\mathrm{p}}{E_\mathrm{g}}\right)^2 \quad \text{and} \quad \varepsilon = 1 + \left(\frac{h\nu_\mathrm{p}}{C}\right)^2 \tag{2.21}$$

X-ray spectroscopy (XRS) gives important information on the bond polarity. Experiments have shown that the binding energy of inner electrons of an atom (E_BIE) depends on the external electronic environment, i.e. on the effective charges of atoms: a positive net charge increases and negative one reduces E_BIE. Therefore, knowing the values of E_BIE in different crystalline compounds, one can define the magnitudes and signs of the atomic charges, and how they vary with the composition and structure changes. Thus, effective atomic charges in MX crystals were found to increase with N_c and $\Delta\chi$ [78], while in the succession MnS, MnO, MnO_2, MnF_2, the MnK_α-edge of the X-ray absorption band shifts to higher energies by 1, 3, and 3.6 eV, respectively [79]. In the succession $Au_2O_3 \rightarrow AuCl_3 \rightarrow AuCN \rightarrow Au \rightarrow CsAu \rightarrow M_3AuO$ the energies of the AuL_I and AuL_III absorption edges consistently decrease, passing through $e^* = 0$ for the pure metal, which indicates that in CsAu and M_3AuO the Au atoms bear negative charges, explicable by exceptionally high electron affinity of gold (2.3 eV) [80]. A study of the electron density distribution in BaAu suggested a $Ba^{2+}\,\bar{e}Au^-$electron structure.

The most reliable charge determinations by XRS [81–85] are compiled in Table 2.5. The effective charges decrease when the valence of the central atom increases or when the electronegativity of the ligands decreases. The effective charges of S, P, Si and Cl atoms in organic compounds were determined by the shifts of the K_α-line in comparison with the same atoms in the elemental solids [86, 87]. The drawback of this method is the smallness of ΔK_α in comparison with the absolute binding energies, but its advantage is that the the volume to which the charge refers is known precisely, as electronic transitions are localized within the atom; the values ΔK_α can be scaled against the effective atomic charges calculated from electronegativities [88].

Most structural methods 'see' either the position of the atomic nucleus (neutron diffraction, NMR spectroscopy), or the atomic center of mass (optical and microwave

Table 2.5 Effective atomic charges from X-ray spectroscopy

M_nX_m	e^*(M)/v	MX_n	e^*(M)/v	M_nX_m	e^*(M)/v
NaF	0.95	SiF_4	0.35	GeSe	0.17
NaCl	0.92	$SiCl_4$	0.25	Y_2O_3	0.54
NaBr	0.83	SiO_2	0.23	Al_2O_3	0.25
NaI	0.75	SiC	0.12	$Al(OH)_3$	0.26
Na_2O	0.90	SnF_2	0.83	AlN	0.21
CuF_2	1.0	$SnCl_2$	0.76	In_2S_3	0.24
CuO	0.51	SnI_2	0.42	In_2Se_3	0.17
Cu_2O	0.39	SnSe	0.36	As_2S_3	0.16
$CdCl_2$	0.70	$SnCl_4$	0.23	As_2Se_3	0.11
$CdBr_2$	0.60	$SnBr_4$	0.20	As_2Te_3	0.09
CdI_2	0.44	SnI_4	0.15	Sb_2S_3	0.30
CdS	0.34	SnS_2	0.33	Sb_2Se_3	0.28
CdSe	0.28	$SnSe_2$	0.24	PF_3	0.27
CdTe	0.22	GeS	0.20	PCl_3	0.14

spectroscopy) or the maximum of the electrostatic potential (electron diffraction) which practically coincide with the nucleus. On the other hand, X-rays are scattered mainly by electrons (with a negligible contribution from the nucleus) and therefore can, in principle, inform about the actual distribution of electrons in crystals. Debye had foreseen such possibility as early as 1915 [89], but its realization took a better part of the twentieth century. The present state of the problem is comprehensively described in books [90, 91] and reviews [92–94].

In principle, a map of the electron density can be calculated by a Fourier series, the amplitudes of which are related in a simple way to the intensities of the diffraction peaks ('reflections'). Unfortunately, we also need to know the *phases* of diffracted beams, which are not measurable and have to be deduced. Secondly, a good-resolution map requires very extensive (ideally — infinite) Fourier series, but the number of measured reflection is of necessity limited. The Fourier map is therefore too crude to extract from it chemically meaningful information. To make X-ray crystallography really informative, the diffraction data is fitted into certain models, which are ultimately rooted in quantum mechanics. The simplest of these is the *spherical-atom approximation*, according to which X-ray scattering of a crystal is the sum of scattering by the spherically-symmetrical, ground-state atoms (usually calculated by Hartree-Fock method). The coordinates of these atoms and the parameters describing their thermal vibrations, are then refined by least-squares technique,

until the difference between the calculated and observed scattering intensities ('R-factor') is minimized. It is then tacitly assumed that the resulting 'atomic' positions are those of the atomic nuclei. In most cases the latter is true within 0.01 Å; the exceptions are triple-bonded C, N and O atoms with their strongly non-spherical electron shells, and especially H, which has no non-bonding electrons. The H atom position determined by X-ray method is usually shifted towards the chemically bonded atom by 0.1 Å or more, especially if the latter atom is electronegative.

Probably, 99.99 % of all X-ray structure determinations to-date have been done on this approximation. Of course, the real distribution of the electron density in an actual crystal/molecule is different from such model (often called pro-crystal/pro-molecule); its topology can be best understood within the framework of the AIM theory, developed by Bader [8]. Electron density is concentrated between atoms which are linked by a covalent bond, and is depleted between atoms which participate in closed-shell interactions (ionic or van der Waals). A good quantitative measure of such effects is the Laplacian of the electron density ($\nabla^2\rho$), equal to the sum of its principal curvatures (second derivatives) at a given point:

$$\nabla^2\rho = \partial^2\rho/\partial x + \partial^2\rho/\partial y + \partial^2\rho/\partial z \tag{2.22}$$

According to the Virial Theorem, the Laplacian of ρ_e is related to the densities of kinetic (G) and potential (V) energies of the electrons,

$$2G + V = \frac{h^2}{16m\pi^2}\nabla^2\rho_e \tag{2.23}$$

where m is the mass of the electron. A positive Laplacian indicates a local depletion of ρ_e and a negative one a local accumulation (this does not imply a local *peak*!). If two atomic nuclei are linked by a line along which ρ_e is enhanced, this gives a clear indication of covalent bonding ('bond path', BP). The one-dimensional minimum of ρ_e on the BCP (bond critical point) signifies the contact between the atoms, while in three dimensions the *atomic basin* of the electron density is enclosed by surfaces of zero flux of ρ_e.

In fact, the difference between ρ_e of a molecule and of its pro-molecule (deformation electron density) is not as big as a Lewis diagram may seem to imply: a bonding electron pair is localized *on* two atoms, not *between* them. Thus, in a H_2 molecule, for which precise *ab initio* calculations are available, the additional accumulation of electron density between the nuclei (compared to the pro-molecule) is only 16 % of the sole electron pair—although the H–H bond in one of the strongest bonds known! In modern X-ray experiments, R-factor usually does not exceed several per cent—another proof of the smallness of the deformation ρ_e. Charge-density studies require much more extensive and accurate sets of experimental data than ordinary, atomic-approximation, studies. Such experiments were practically impossible before 1970s, remained prohibitively long until area detectors and synchrotron radiation came into wide use in 1990's, and even today are far from routine. It is very difficult to distinguish the deformation of the electron density due to a chemical interaction, from the 'smearing' due to thermal motion of atoms; the most sure solution is to eliminate

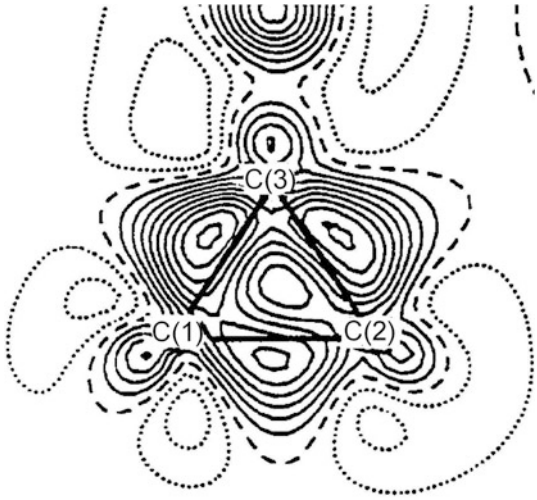

Fig. 2.3 Experimental deformation charge density in the cyclopropane ring of 7-dispiro[2.0.2.1]heptane carboxylic acid. Reproduced with permission from [95], copyright 1996 International Union of Crystallography

thermal motion physically, by collecting the data at liquid-nitrogen, or better still, at liquid-helium temperatures. Nevertheless, today the electron density data is reproducible on a sufficient level of precision, and the main difficulty has shifted to its interpretation. The results depend crucially on the model, and if the latter is inadequate or ambiguous, then the parameters will be biased or indeterminate. The parameterization retains an element of arbitrariness. Worse, often the same data can be fitted equally well (in mathematical sense) to very different sets of variables. More often than is acknowledged, researchers proceed by testing several models and choosing the one that gives the most physically meaningful outcome. And while Laplacian is very efficient in revealing subtle features of the electron density topology, it by the same token magnifies greatly the noise and bias of the original function. Partly for this reason, different tools of topological analysis often give contradictory results.

At present, charge density can be mapped with the precision of 0.05 $e/\text{Å}^3$. The experiments have consistently revealed peaks of the deformation density which can be identified with bonding and non-bonding (lone) electron pairs, as envisaged by Lewis and the VSEPR theory. The charge density at the bond critical point was found to correlate with the strength of the bond, and inversely correlates with bond length. In cyclo-propane rings, the peaks of a (bond) deformation density do not lie on the direct C─C lines, but are shifted outwards (Fig. 2.3). The ellipticity of the bond electron density, i.e. its deviation from cylindrical symmetry, reflects the π-character of the bond. The experimental charge density can serve as the basis of calculating various molecular properties, such as electrostatic potential at the molecular surface (indicating the areas favorable for electrophilic and nucleophilic attacks) or dipole moments. Some polar compounds have their dipole moments much enhanced in the crystal compared to the isolated molecule (e.g. for HCN, 4.4 D *vs* 2.5

Table 2.6 'XRD' effective atomic charges in binary compounds

MX_n	r^*_M	e^*_M/v	MX_n	r^*_M	e^*_M/v	MX	r^*_M	e^*_M/v
LiF		0.88	CaO	1.32	1.00	AlP		0.09
LiH	0.92	0.86	BaO	1.49	1.00	AlAs		0.07
NaCl	1.17	0.88	MnO	1.15	0.62[a]	AlSb		0.05
KCl	1.45	0.97	CoO	1.09	0.74[a]	GaP		0.08
KBr	1.57	0.80	NiO	1.08	0.46	GaAs		0.05
Cu_2O		0.61	Al_2O_3	1.01	0.55	InP		0.06
MgF_2		0.95	Cr_2O_3		0.50	InAs		0.04
MgH_2	0.95	0.95	Sb_2O_3		0.38[b]	InSb		0.02
CaF_2		0.86	SiO_2		0.25[c]	YH_3		0.5[l]
MnF_2		0.90[a]		0.72[d]	0.63[d]	$CaSO_4$		1.0[g]
CoF_2		0.86[a]	TiO_2	0.60	0.75			0.4[h]
MgO	0.93	0.68	BN	0.74	0.15	Fe_3O_4	1.19[e]	0.74[e]
MgS	1.28	0.75	AlN		0.20		1.13[f]	0.64[f]

[a][96], [b][97], [c]quartz, [d]stishovite [81], [e]Fe^{II}, [f]Fe^{III}, [g]Ca, [h]S

D, respectively). On the other hand, estimates of atomic charges proved very model-dependent. Thus, for $NH_4H_2PO_4$ a variety of refinements, fitting the experimental data equally good, yielded the ammonium cation charges varying all the way from 0 to +1 [96]. Observations of 'bond paths', of hydrogen bonds and even weaker intermolecular interactions, attracted criticism [94], since the electron density in intermolecular areas is generally low, close to the level of the experimental error, which makes topological analysis extremely unreliable. Thus, charge-density studies have confirmed many effects which structural chemists suspected for a long time. However, so far they delivered relatively few results which were really unexpected and would have remained unknown without this method.

Many works are devoted to the determination by XRD of charges of atoms in inorganic crystals. Table 2.6 lists the most reliable values of effective charges and atomic radii in binary crystalline compounds, obtained in these studies [97–113]. Similar data for complex compounds can be found in Table S2.1. It is remarkable that in MgH_2 the charge on Mg was estimated as $+1.91\ e$, and on hydrogen as $-0.26\ e$ [114] with 1.4 e per formula unit missing. This charge may be delocalized in interatomic voids, but the material is an insulator with $E_g = 5.6$ eV [115].

Bond polarities in organic carboxylate salts, R-CO_2M (M = H, Be, B, C, N, O, Al, Si, P, Mn^{II}, Fe^{II}, Fe^{III}, Co^{II}, Ni^{II}, Cu^{II}, Zn, Gd) were determined, in good agreement with spectroscopic data and EN-based estimates, by comparing the lengths of the two C-O bonds in the carboxy group, from crystal structures [116]. These bonds must be identical (with the bond order $n = 1.5$) in the fully ionic case but different ($n = 1$ and 2) covalent case:

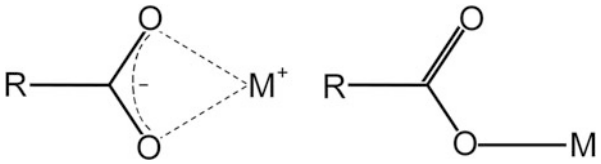

It can be concluded that in the majority of crystalline halides and oxides, a degree of ionicity is between 0.5 and 1.0. The effective sizes (radii) of atoms change with ionization in a non-linear manner (see Sect. 1.5), this translates into $\leq$10 % deviation from the perfectly ionic radii, which explains the efficiency of the ionic radii in inorganic crystal chemistry.

2.2.4 Metallic Bond

The major feature of the electron structure of metals is the availability of freely moving electrons (formerly valence electrons) shared by all atoms. This model was first formulated by Drude who applied the kinetic theory of gases to an 'electron gas' in metals, assuming that there exist charged carriers moving about between the ions with a given velocity and that they collide with one another in the same manner as do molecules in a gas. The metallic bond can be regarded as a non-directional covalent bond. Indeed, a crystal-chemical approach suggests that a transition from covalent to metallic bonding can be linked with the increase of the coordination number, so that valence electrons become increasingly delocalized and finally transfer from the valence into the conduction band. For the metallic bond to form, atoms' valence electrons must be removed from them to move freely in the interatomic voids of the crystal space. This requires the condition $E(\text{A–A}) + I(\text{A}) < E(\text{A}^+ \cdots e^-)$. When the $\text{A}^+ \cdots e^-$ interaction becomes more favourable than the A–A bond, a dielectric $\rightarrow$ metal transition occurs.

In the early theory of metals it was supposed that all valence electrons in atoms become free and the metal structure is a lattice of cations immersed in an 'electron sea'. Now it is known that only a part of the outer electrons of atoms are free, since the metallic radii are larger than those of cations (see Chap. 1). Some studies of electron density distribution in metals estimated the metallic/core radii ratio as 1:0.64 [117, 118]. The effective radii of the atomic cores in metallic structures are close to the bond radii of the same metals in crystalline compounds (see Chap. 1) which correspond to atoms with charges not exceeding $\pm$1. It should be noted that work functions of bulk metals are always smaller than the first ionization potentials of the corresponding atoms (see Sect. 1.1.2) and therefore there is no reason to suppose the ionization of two or more electrons from an atom.

The crystal-chemical mechanism of the metallization in ionic crystals of MX-type was studied under high pressures [119]. Assuming that the metallization of a material under pressure occurs when the chemical bond is destroyed, i.e. the compression energy becomes equal to E(M–X), it was concluded that the interatomic distances

for an ultimately compressed MX crystal are equal to the sum of the *cationic* radius of M^+ and the normal *covalent* radius of X. Thus, metallic binary compounds differ from pure metals in having a sub-lattice of neutral nonmetal atoms X^o. From here it follows that in MX under high pressures the M atom can be the donor of electrons if the bonding is covalent, M°–X°, as $I_M < I_X$. If the substance is ionic, M^+X^-, then X^-anion must be the donor, because $A_X < I_M$. The polar character of the M–X bond prior to pressure-induced metallization can be determined experimentally. The proposed mechanism of metallization implies the availability not only of mobile electrons—for in aromatic molecules they are also mobile to a considerable extent—but also of certain structural voids which these electrons can occupy. Because metallic structures have high N_c (usually, 12), a cluster should have at least 13 metal atoms to acquire metallic properties. Measurements of the photoelectron spectra in clusters of mercury [120, 121] and magnesium [122] showed that their *s-p* band gaps are closed when the number of Hg atoms reaches 18, indicating the onset of the metallic behavior.

It has been shown [123] that the metal sub-lattice in crystal structures of the ZnS, NaCl, NiAs and CsCl types has the same (or similar) N_c of metal and M–M distances (d_{MM}), as the structure of pure metal (d°_{MM}); hence the degree of metallic bonding can be defined as

$$m = c\frac{d^o_{MM}}{d_{MM}} \tag{2.24}$$

As the next logical step, it was suggested [124] to apportion the distribution of the covalent electron density (q) in an MX structure in proportion to the strengths of M–M and M–X bonds,

$$q = \frac{N_{MM}E_{MM}}{N_{MM}E_{MM} + N_{MX}E_{MX}} \tag{2.25}$$

where $N_{MM,MX}$ and $E_{MM,MX}$ are the coordination numbers and energies of the M–M and M–X bonds, respectively. Taking into account the proportionality between the energies and overlap integrals of bonds, we obtain

$$m = uS_{MM}/S^o_{MM} \tag{2.26}$$

here u is the electron concentration (population) in the metal orbitals, S^o and S are the overlap integrals of the M–M bonds at distances d^o_{MM} and d_{MM}. The problem of partitioning of the covalent electron density between M–M and M–X bonds is solved in [11] using a simpler model, viz.

$$q = \frac{\chi_M}{\chi_M + \chi_X} \tag{2.27}$$

where χ_M and χ_X are the electronegativities of the M and X atoms in the MX crystals. If d^o_{MM} and d_{MM} are close, the degree of bond metallicity can be estimated as $m = cq$, otherwise it can be determined from experimental data as

$$m = cq\frac{d^o_{MM}}{d_{MM}} \tag{2.28}$$

In Table S2.2 the values of metallicity calculated by Eqs. 2.25 (m_1) and 2.28 (m_2) are listed. Good agreement of the results prove that for an approximate estimation, it is not necessary to take into account the differences between the metal bond lengths in compounds and elemental solids.

As mentioned above, the metal sub-lattices in the crystal structures of compounds are usually the same, or similar to, the structures of the corresponding pure metals. This problem was considered in depth by Vegas et al. [125] who studied the genesis of structures in metals, alloys and their derivatives. Thus, MBO_4 compounds of the $CrVO_4$ structural type have the metal lattice like the MB structure. The same situation exists in ternary oxides of the MAO_n type, where A = S or Se, and $n = 3$ or 4, and also in $MLnO_3$. This means that the metal skeleton is the basis of the structure of the compound, and atoms of oxygen are simply included into the voids between cations. Such inheriting of the structure of the parent substance by its derivatives can be explained by the minimization of work required to create the new structure on the basis of the metal lattice, although there are also more complex reasons [126].

One more experimental method of characterizing the metallic state is to compare the volumes and refractions (R) of solids. As the refractive indices of metals are very great, the Lorentz-Lorenz function (Eq. 2.18) is close to 1 and $R \approx V$. According to the Goldhammer-Herzfeld [127, 128] criterion, $V \rightarrow R$ when a dielectric converts into a metal. As the measure of bond metallicity, the ratio

$$\frac{R}{V} = \frac{n^2 - 1}{n^2 + 2} \tag{2.29}$$

can be considered [129, 130]. The pressure at which $V = R$, has been often regarded as the pressure of metallization. However, both during isomorphic compression and at phase transitions under high pressures the refractive index also changes (see Chap. 11). Therefore the Goldhammer–Herzfeld criterion is not absolutely correct, although for rough estimations of pressures of metallization it is valid. A more rigorous approach was used in [131, 132] where the changes of $R(CH_4)$ and $R(SiH_4)$ under pressure were studied, revealing a large increase in the R/V ratios at 288 and 109 GPa, respectively, which indicates phase transformations of the insulator–semiconductor type in these materials.

There is one more question to be answered. It is known that phase transition enthalpies (ΔH_{tr}) constitute only a small part of the atomization energy (E_a). Thus, the graphite-diamond transition with change of N_c from 3 to 4 has the $\Delta H_{tr} = 2$ kJ/mol; the transition from 4- to 6-coordinate Sn has 3 kJ/mol, of 6- to 8-coordinate Bi has 0.45 kJ/mol, and that of 8- to 12-coordinate Li has 54 J/mol. In each case, $\Delta H_{tr} \leq 0.01 E_a$, whereas on transition from the Sn_2 molecule ($N_c = 1$) to α-Sn ($N_c = 4$) the E_a increases 3.2 times. Similar transformation for Group 1 or Group 11 metals from $N_c = 1$ to $N_c = 8$ or 12 results in a 3.4-fold increase, and for other metals the changes are even bigger. Note also that the E_a(MX) in crystals exceed those in molecules by a factor of ≈4.3 (see Sect. 2.3), but further increases of N_c in crystals make very little difference, as indicated by small changes in Madelung's constants, from $k_M = 1.748$ at $N_c = 6$ to $k_M = 1.764$ at $N_c = 8$, while some increase in interatomic distances at the B1 → B2 transition, compensates the small increase

of k_M. The reason of this effect consists in the multi-particle interaction of atoms in crystals, in the Coulomb interactions of cations with anions or free electrons.

For a long time the crystal-chemical approach seemed sufficient to describe of the nature of the metallic bond. However, physically more general approach is to consider the band structures of substances, namely that the conduction band containing electrons must be only partly filled [133]. Thus, with a full band the compound $K_2Pt(CN)_4$ is an insulator and the Pt–Pt distance along the chain is 3.48 Å. However, the non-stoichiometric compound $K_2Pt(CN)_4Br_{0.3} \cdot 3H_2O$ is metallic and, since electrons have been removed from the top of the band where maximum anti-bonding interactions are found, it has a much shorter Pt–Pt distance of 2.88 Å. Thus, the partial oxidation of $K_2Pt(CN)_4$, when the band of Pt^{IV} is filled only partly, transforms this compound into a metal. At full oxidation, $K_2Pt(CN)_4Br_2$ is an insulator. The same picture is observed in $La_{2-x}Sr_xCuO_4$ where the metal conductivity is observed at $x > 0.05$.

There is one more way of formation of the metal state in molecular substances without their transition to structures with high coordination numbers. On compression of the condensed molecular H_2, O_2, N_2 and halogens, they acquire metallic properties (see Sect. 5.2 and the review [134]) which result from strengthening of electronic interactions upon shortening of intermolecular distances. These are so-called 'molecular metals'. As the molecules approach one another, three-center A···A–A orbitals or even chain-like structures are formed, where an increase of N_c from 1 (A_2) to 2 (–A–) leads to a linear delocalization of valence electrons.

2.2.5 *Effective Valences of Atoms*

The concept of valence (v) is one of the cornerstones of chemistry. According to IUPAC Compendium of Chemical Terminology, the valence of a chemical element is defined as the number of hydrogen atoms that one atom of this element is able to bind in a compound or to replace in other compounds. However, in solid-state physics and structural chemistry this term usually means the bonding power of atoms and then v may have a non-integer value ('effective valence'), which is derived from physical properties. Thus, there is a widespread opinion [28, 135, 136] that metals of Group 11 (Cu, Ag, and Au) in the solid state have effective valences v^* much higher than 1, which explains the big difference between Group 1 and Group 11 metals of the same period, in physical properties, viz. melting temperatures (T_m), densities (ρ), and bulk moduli B_o (Table 2.7). However, the difference between Groups 1 and 11 goes beyond the solid state, and manifests itself in the structures and properties of gaseous molecules of these elements. Moreover, a certain parallelism is observed in the variation of characteristics of elements in both states. According to spectroscopic data [137], the bonds in molecules Cu_2, Ag_2, and Au_2 are single; i.e. $v = 1$. This agrees with the proximity of the M–M half-distance to the covalent radius of M determined as the length of an M–H bond (definitely single) or an M–CH_3 bond minus the covalent radius of hydrogen or carbon [138]. The same conclusion can

Table 2.7 Properties of Groups 1 and 11 metals in the solid state [138]

M	K	Cu	Rb	Ag	Cs	Au
T_m,°C	63.4	1085	39.3	961	28.4	1064
ρ, g/cm^3	0.86	8.93	1.53	10.5	1.90	19.3
B_o, GPa	3.0	133	2.3	101	1.8	167
v*, Pauling	1	5.5	1	5.5	1	5.5
v*, Brewer	1	4	1	4	1	4
v*, Trömel	1	3	1	3	1	3

be drawn by comparing the ratios between the bond energies and bond lengths in solids and gas-phase molecules, between the atomization energies of solid metals and the dissociation energies of molecules M_2, and between force constants (f) in molecules M_2 and metals M of Groups 1 and 11 elements. Table 2.8 shows that the averaged ratios (k) of these properties for all elements are similar, averaging 1.706 ± 2.2 %, 1.154 ± 1.4 %, and 0.075 ± 5.1 %, respectively. Thus, although the absolute values of physical properties of Groups 1 and 11 elements differ widely, the relative changes (from solid to molecule) are practically identical. Table 2.9 shows the simplest estimation of the electronic energies of isolated atoms, as proportional to $\varepsilon = Z^*/r_o$ where Z^* is the effective nuclear charge (from Table 1.7) and r_o is the orbital radius (from Table 1.8), and the experimental atomization energies (in kJ/mol) of the three pairs of metals. One can see that the energies of isolated atoms are correlated with the energies of atoms in solid metals, e.g. the bond strengths of elements are determined by the properties of isolated atoms. Thus, there are no physical grounds for ascribing the exaggerated 'metallic' valences to Cu, Ag, and Au in the solid state.

Physical properties of the crystalline halides MX of the Groups 1 and 11 metals also strongly differ: the temperatures of melting (T_m) and band gaps (E_g) of alkali halides decrease in the succession MCl → MI, but in halides of Cu, Ag and Tl in the same succession they increase or change little (Table S2.2), although d(M–X) increases in all cases from MCl to MI. Experimental effective charges in alkali halides on average are smaller than in halides of the Group 11 elements (Table 2.3), although the difference of electronegativities $\Delta\chi = \chi(X) - \chi(M)$ is smaller in the case of Cu, Ag and Tl. This fact has been explained [139] by the formation of additional (dative) M → X bonds involving the (n–1)d-electrons of the metals and vacant nd-orbitals of the halogens, resulting in an increase of the atomic valences of Groups 11, 12 and 13 elements on average by 1.5, 2.4 and 3.1, respectively. It should be noted that Lawaetz [140] and Lucovsky and Martin [141] showed that to reconcile the band structure of CuX and AgX with experimental data, one can assume that v^*(Cu, Ag) = 1.5. Robertson [142–145] obtained good results in calculation of the PbI_2 band structure under condition of a 41 % Pb s orbital contribution to the upper valence band state A^+_1. Wakamura and Arai [146] also obtained $v^* = 2.8$, 2.6 and 2.6 for crystalline compounds of divalent Mn, Co and Ni, respectively. The crystal-chemical estimations of v^* for divalent Sn, Pb, Cr, Mn, Fe, Co, Ni give 2.45 ± 0.05.

Liebau and Wang [147, 148] demonstrated that the classical valence term as introduced by Frankland [149] and the term valence as used by solid-state physicists

Table 2.8 Comparison of energies (kJ/mol), distances (Å), and force constants (mdyne/Å) of M−M bonds in solid metals and molecules

M	K	Cu	Rb	Ag	Cs	Au
E_a(M)	89.0	337.4	80.9	284.6	76.5	368.4
E_b(M_2)	53.2	201	48.6	163	43.9	221
k_E	1.673	1.731	1.665	1.746	1.753	1.667
d(M)	4.616	2.556	4.837	2.889	5.235	2.884
d(M_2)	3.924	2.220	4.170	2.530	4.648	2.472
k_d	1.176	1.151	1.160	1.142	1.126	1.167
f(M)	0.007	0.108	0.006	0.093	0.005	0.154
f(M_2)	0.10	1.33	0.08	1.18	0.07	2.12
k_f	0.072	0.081	0.074	0.079	0.071	0.072

Table 2.9 Comparison of energies in Groups 1 and 11 elements for molecular and solid states

M	Z*	r_o	ε	q_ε	E_a	q_E
K	2.2	2.162	1.02		89.0	
Cu	4.4	1.191	3.69	3.62	337.5	3.79
Rb	2.2	2.287	0.96		80.9	
Ag	4.9	1.286	3.81	3.97	284.6	3.52
Cs	2.7	2.518	1.07		76.6	
Au	5.6	1.187	4.72	4.41	368.4	4.81

and crystallographers, are different in nature, and suggested to call them *stoichiometric valence* and *structural valence*, respectively. For the majority of crystalline structures, the difference between these values is <5 %, but for *p*-block atoms with one lone electron pair, the differences of up to 30 % have been reported.

Quantum-chemical estimations show also that the ability to form additional bonds in halides of the Group 11 metals increases from chlorides to iodides. A comparison of the observed ionization potentials and electron affinities of halogens [139] shows that it requires a smaller expense of energy to add the second electron to an I^- ion than to Cl^-. The X^{2-} ions are not found yet, but if they are ever observed in mass spectra, the lifetime of I^{2-} can be predicted to exceed that of F^{2-}.

2.3 Energies of the Chemical Interaction of Atoms

2.3.1 Bond Energies in Molecules and Radicals

Energy characteristics of atoms also define, to a large extent, the strengths of their bonds in molecules, polyatomic ions and radicals. The work required to disrupt a chemical bond, e.g. to separate chemically bonded atoms from the equilibrium distance to a practically infinite one (in the ground state) is called bond energy (E_b). In case of the A_2 and AX molecules, E_b is equal to the dissociation energy of the molecule (D_e) which can be determined by thermochemical, calorimetric, kinetic, mass-spectroscopic and molecular spectroscopic techniques. By definition, D_e characterizes atoms in molecules at the equilibrium state with zero-point energy,

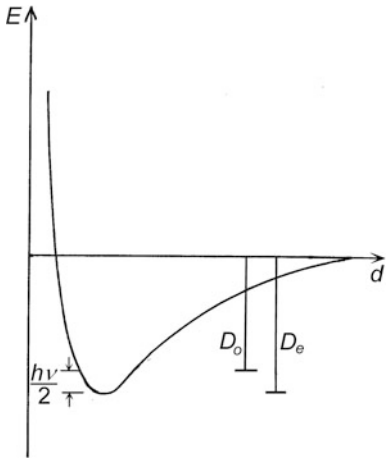

Fig. 2.4 Characteristics of the potential curve

ε (Fig. 2.4). Because $\varepsilon = ½\, h\nu_o > 0$, even at 0 K the measurements give

$$D_o = D_e - \frac{1}{2} h\nu_o \tag{2.30}$$

where D_e is the dissociation energy calculated at the very bottom of the potential energy well. The zero-point energy is highest in H_2 (26 kJ/mol) and somewhat less in molecules with heavier atoms, therefore the difference between D_o and D_e can be ignored for structural-chemistry purposes.

Thermochemical determinations of the bond energy are based on the measurements of the heats of reaction (Q) at constant pressure

$$Q = (E_2 + PV_2) - (E_1 + PV_1) \tag{2.31}$$

where $E_1 + PV_1$ and $E_2 + PV_2$ represent the initial and final states of the system. The enthalpy being $H = E + PV$, it follows that $Q = \Delta H$ at constant P.

Heats of reactions can be measured by the calorimetric and kinetic methods, using photo- and mass-spectrometry. Bond dissociation enthalpy calculated from the thermal effect of the reaction at ambient pressure is close to the bond energy because PV is small, for example for the hydrogen molecule $PV \approx 2.5$ kJ/mol. Finally, the difference between the dissociation energy at 0 K and that at room temperature is also very small; for the hydrogen molecule the difference is $\Delta E \approx 1$ kJ/mol.

Thus measurements of bond energies by different methods usually diverge by several kJ/mol; for this reason the experimental bond energies cited in the present and the next sections, are rounded up to integer kJ/mol, except where independent measurements give better agreement. The bond energies of diatomic molecules and radicals presented here, have been compiled using as the starting-point, such reference books as the NBS Tables of Chemical Thermodynamic Properties (1976–1984), JANAF Thermochemical Tables (1980–1995), Thermochemical Data of Pure Substances (1995), Handbook of Chemistry and Physics (2007–2008), and Thermodynamic Properties of Compounds (electronic version, 2004, in Russian). These data

Table 2.10 Values of n in the Mie equation for molecules MX and M_2

M	n	M	n	M	n	M	n	M	n
Ag	3.7	Cd	4.1	In	3.8	Ni	3.1	Th	2.5
Al	3.3	Cr	4.4	K	2.9	Pb	4.7	Ti	4.2
As	3.8	Co	3.1	La	2.7	Pt	3.6	Tl	3.0
Au	4.2	Cs	3.2	Li	2.2	Rb	2.9	U	3.1
B	2.6	Cu	3.2	Mg	3.7	Sb	3.8	V	3.9
Ba	3.2	Fe	4.0	Mn	3.5	Sc	2.6	W	4.5
Be	3.2	Ga	2.5	Mo	4.1	Sn	3.8	Y	3.5
Bi	4.4	Hg	5.0	Na	2.6	Sr	3.3	Zn	3.9
Ca	3.3	Hf	3.3	Nb	3.4	Ta	3.2	Zr	3.6

have been critically compared, corrected and updated using recent original publications, for which references are given. Where several independent measurements by the same method are available, the preference is given to the more recent works and more authoritative researchers, while results of equal reliability have been averaged.

Bond energies of diatomic molecules are listed in Tables S2.2 and S2.4. Evidently, dissociation energies of hetero-nuclear diatomic molecules increase together with the bond polarity, i.e. from iodides to fluorides and from tellurides to oxides of the same metals. Therefore, $D(\mathrm{M{-}X})$ in halides and chalcogenides are always larger than the additive value, i.e. the half-sum of $D(\mathrm{M{-}M})$ and $D(\mathrm{X{-}X})$. This fact has been first noticed by Pauling, who formulated the dependence of the bond energy on its polarity in terms of electronegativity (see Sect. 2.4). For halides of polyvalent metals, or other elements, e.g. H, B, C, the dissociation energy of a hetero-atomic bond does not necessarily exceed the additive value, because the bonds under comparison may differ not only by polarity, but also by the type of bonding orbitals and the bond order.

Also of paramount importance is the relation between the energy E_b of a bond and its length d. This question has three distinct, but ultimately connected, aspects, viz. (i) the potential curve for a chemical bond of a given order between given types of atoms, (ii) the bond length/bond order relation for a given pair of atoms, and (iii) the correlation between energies and lengths of bonds formed by different elements. However, it is probably impossible to establish a universal dependence $E_b = f(d)$, because the inter-nuclear, nucleus-electron and inter-electron interactions all change with distance in different fashions, and the combined energy curve can be highly specific. The most general form of the potential energy (E) for two interacting atoms is given by the Mie equation:

$$\mathrm{E} = -\frac{a}{d^n} + \frac{b}{d^m} \tag{2.32}$$

where a and b are constants of the substance, d is the bond length, and $m > n$. Here the first term defines the attraction and the second one the repulsion of atoms. The sum of m and n and their product ($m \times n$) can be derived from various physical properties [150], but there is very limited experimental information about the values

of m and n separately. In the equilibrium state Eq. 2.32 transforms into

$$E = \frac{E_e}{n-m}\left[n\left(\frac{d_e}{d}\right)^m - m\left(\frac{d_e}{d}\right)^n\right] \tag{2.33}$$

From here, supposing $m = 2n$ and thereby transforming the Mie equation into the Morse function (see Eq. 2.7) which describes energies of molecules very well, we finally obtain

$$n = d\sqrt{f/2E_e} \tag{2.34}$$

where f is the force constant. The calculations of n from experimental data for molecules at normal thermodynamic conditions [151] are presented in Table 2.10.

As mentioned above, at $m = 2n$ the Mie equation transforms into the Morse function which describes well not only covalent bonds but also van der Waals interactions. This function was used to estimate van der Waals radii [152] and to rationalize the properties of Zn_2, Cd_2 and Hg_2 molecules [153]. Very often E is estimated using the simplified equation

$$E = \frac{a}{d^{\mathrm{n}}} \tag{2.35}$$

i.e. neglecting the repulsion term. Having made this assumption, and using experimental data for transition metals, Wade et al. found that $n \approx 5$ for C–O bond, 3.3 for C–C, and 2–7 for M–O bonds [154–156]. The bond energies and lengths in many molecular and crystalline compounds have been estimated using Eq. 2.35 [157]. The results are briefly as follows. In molecules of univalent elements, Na_2 to Cs_2 and Cl_2 to I_2, $n = 1.2$ and 1.6 while according to Harrison [158] the bond covalent energy depends on the interatomic distance as d^{-2}. In the successions $P_2 \rightarrow Bi_2$ and $S_2 \rightarrow Te_2$, $n = 2.6$ and 1.8, i.e. somewhat less than the canonical factors of 3 and 2, respectively; in molecules of hydrohalides HX, alkali halides, CuX, and SnX or PbX, $n = 1.6$, 2.1, 1.9 and 2.5, respectively. Interestingly, in van der Waals molecules Zn_2, Cd_2, Hg_2, the bond energies vary as $d^{-2.4}$, although according to London's theory of van der Waals interactions, E must be the function of d^{-6}. The values of n in crystalline compounds are smaller than in the corresponding molecules, by 15–30 %. From these n values one can deduce the absence of ideal types of chemical bonds in most molecules and crystals. The bond character in solid metals is especially varied; several authors explain this variability by the fact that the effective and formal valences of atoms are different.

The chemical bond strength usually increases when the bond length decreases. Noteworthy exceptions are the N–N, O–O and F–F single bonds, which are weaker than the longer P–P, S–S and Cl–Cl bonds, respectively. This effect can be explained by the strong repulsion between the bonding and the lone electron pairs at shorter distances, which agree also with lower electron affinities of N, O and F compared with P, S and Cl (see Table 1.3). The dissociation energies of the N–N, O–O and F–F bonds, estimated by extrapolating the D *vs.* X–X curve (derived for larger atoms),

exceed the experimental values by 230, 250 and 210 kJ/mol respectively. This effect should be taken into account at additive thermochemical calculations.

Another example of electron-electron repulsion affecting bond dissociation energies can be observed on monofluorides of certain elements. Thus, M–F bond energies in LiF (573 kJ/mol) and BeF (575 kJ/mol) are almost equal, notwithstanding substantially shorter bond in the latter, due to the repulsion between the nonbonding *s*-electron of Be and the electron pair of the Be–F bond, which compensates for the increased charge on the metal atom. On the contrary, in BF the bond energy is much higher (742 kJ/mol) as the two nonbonding electrons of the boron atom form a closed s^2-pair interacting weakly with the bond electrons. Introduction of another isolated electron in CF, again reduces the dissociation energy down to 548 kJ/mol.

The interaction of isolated electrons of an M atom with the bond electrons obviously would decrease as the latter shift toward the X atom, i.e. as the bond polarity increases. This explains why the increase of bond energy from M–I to M–F is higher for alkali earth metals (which have uncoupled *s*-electrons) than for alkali metals (which don't), on average 285 *vs*. 185 kJ/mol. Note that the bond energies in the MX_2 molecules (where the alkali earth metal has no non-bonding *s*-electrons) of the same series differ from the corresponding energies of alkali halides by only *ca*. 25 kJ/mol. Exceptionally low dissociation energies of M_2 molecules of alkali-earth metals are due to the formation of stable outer s^2-electron configurations that prevent the formation of covalent bonds; the interaction is rather of van der Waals character and its energy is correspondingly small (see below).

Peculiarities of the electron structures of atoms in molecules become particularly conspicuous when the dissociation energies of MX or M_2 molecules are compared with those of positively charged MX^+ or $M_2{}^+$ radicals. In agreement with Hess' law

$$E(\mathrm{M}-\mathrm{M}) + I(\mathrm{M}) = I(\mathrm{M}_2) + E(\mathrm{M}-\mathrm{M}^+) \tag{2.36}$$

Hence, the difference $I(\mathrm{M})-I(\mathrm{M}_2)$ determines the relationship between $E(\mathrm{M}_2)$ and $E(\mathrm{M}_2{}^+)$. Textbooks usually give few examples thereof, and often the single one of H_2 *vs* $H_2{}^+$, where the dissociation energy decreases from 436 to 256 kJ/mol as one electron in this molecule is removed on ionization. However, this example is rather atypical. Tables S2.5 and S2.8 list all the currently known dissociation energies of positively charged diatomic radicals. For halogens, the picture is easy to interpret. An electron is removed from a non-bonding orbital which is destabilized (compared to isolated atom) by electron-electron repulsion in these electron-rich molecules, hence $I(\mathrm{A}) > I(\mathrm{A}_2)$. Ionization reduces this repulsion, hence $E(\mathrm{A}_2) < E(\mathrm{A}_2{}^+)$. Both relationships are reversed for hydrogen, as it has only bonding electrons which are attracted by both nuclei and therefore are bound stronger than in the atom. The loss of one of these electrons, naturally, weakens the bonding.

One might expect Group 1 metals to be similar to hydrogen in this respect, as they have no non-bonding electrons in the outer shell. The closed shells evidently lie too low in energy (the second ionization potential exceeds the first by an order of magnitude), hence ionization in this case also means the loss of a *bonding* electron. Nevertheless, for all these metals $I(\mathrm{A}) > I(\mathrm{A}_2)$ and $E(\mathrm{A}_2) < E(\mathrm{A}_2{}^+)$, i.e. apparently

two nuclei attract an electron weaker than one and a single electron holds the atoms together stronger than a Lewis pair! The one plausible explanation can be derived from the 'magic formula' of Mulliken (see below, Eq. 2.46) although there are more complicated models also [159–162].

In a modified form, Eq. 2.36 can be extended to dications,

$$E(A_2) + 2I(A) = I_1(A_2) + I_2(A_2) + E(A_2{}^{2+}), \tag{2.37}$$

where I_1 and I_2 are the first and the second ionization potentials, or indeed to bulk solids,

$$E_a(A) + I(A) = \Phi(A) + E_a(A^+) \tag{2.38}$$

where $E_a(A)$ and $E_a(A^+)$ are the atomization energies of the neutral and charged solids, respectively, and $\Phi(M)$ is the work function, which is the ionization potential of a bulk solid. Since $I(M) > \Phi(M)$ always, it follows that $E_a(M^+) > E_a(M)$. However, for alkali metals, $E_a(M^+)$ corresponds to the dissociation of an imaginary solid consisting of metal cations without any valence electrons. Surely, such a system must be altogether unbound!?

This paradox can be resolved as follows. The (molar) ionization potential is the energy required to ionize every atom (or molecule) in a mole of a substance, while Φ is the minimum energy required to remove the *first* electron from a neutral solid, whereas subsequent electrons would require ever greater amounts of energy. To estimate this energy, let us assume as the first approximation, that the I_2/I_1 ratio for a molecule is the same as for an atom with the equal number of valence electrons. This assumption seems not unreasonable in view of the recent observation [163] that successive ionization potentials (at least, for the outer electron shell) for atoms of all elements can be described by a single simple function. Thus, Group 1 diatomic molecules can be 'modeled' by Group 2 or Group 12 atoms. As shown in Table S2.6, for these atoms the I_2/I_1 ratio is fairly constant, averaging 1.9. Taking into account that for metals $I(A) \approx I(A_2)$, Eq. 2.37 can be reduced to

$$E(A_2{}^{2+}) \approx E(A_2) - 0.9I(A). \tag{2.39}$$

From the data in Table S2.7 it is obvious that $E(A_2{}^{2+}) \ll 0$, i.e. the $A_2{}^{2+}$ cation is strongly unbound, as indeed could be expected for a molecule completely stripped of valence electrons. This molecule can also serve as a model for a bulk metal deprived of its electron gas (Eq. 2.38), to estimate the ionization potentials for bulk metals. As mentioned above, Φ is the energy required to strip the first electrons from a neutral solid. When each atom in the solid is surrounded by charged atoms, $E_a(M^+)$ can be found by an expression analogous to Eq. 2.39,

$$E_a(A^+) \approx E_a(A) - 0.9\Phi(A). \tag{2.40}$$

As shown in Table S2.7, $E_a(A)$ is always smaller than 0.9 $\Phi(A)$, i.e. the structure is unbound.

Comparison of Tables S2.3 and S2.5 shows that removing an electron from a multiple bond (in N_2, P_2, As_2) reduces the dissociation energy, while removing an electron from the outer shell in molecules of O_2, chalcogens, halogens, alkali metals strengthens the bond by reducing electron-electron repulsion. Removing an electron from diatomic molecules of Groups 2, 12 and 18 elements, which have the closed s^2 or s^2p^6 outer shells, transforms the van der Waals interaction into the normal chemical bond and therefore these cations become more bound than the corresponding neutral molecules. It is interesting that removing an *np*-electron from Tl ($5s^25p$ shell), on the contrary, transforms the normal covalent bond in the Tl_2 molecule into a weak one, similar to van der Waals interaction, in the Tl_2^+ cation.

Ionization of halides of univalent metals, as well as oxides and chalcogenides of divalent metals, drastically weakens their bonds, because the electron is removed from the negatively charged atom, thus eliminating the Coulomb component of the energy. On ionization of a radical which comprises a multivalent atom and a halogen (or chalcogen), the unpaired electron is removed from the electropositive atom or, if none is present there, from the electronegative atom. In the former case the bond is strengthened, in the latter weakened.

During the last decade the information became available concerning the alteration of bond strengths in A_2 molecules on *negative* ionization. Thus, dissociation energies of Sn_2^- (265 kJ/mol) and Pb_2^- (179 kJ/mol) [164] are higher than those of the corresponding neutral molecules (187 and 87 kJ/mol, respectively). Among transition metals, M_2^- anions with M = Ni, Cu, Pt, Ag and Au have lower bond energies than the neutral molecules and only Pd_2^- has a higher one than Pd_2 [165]. The bond in the As_2^- radical is slightly stronger than in the As_2 molecule [166]. These data on the effects of positive and negative ionization on the bond energies and distances comprise excellent material for quantum chemistry, which still has to be fully utilized.

For a diatomic molecule, determining bond energy invokes no ambiguity: it is exactly equal to the dissociation energy. However, for a larger molecule, e.g. MX_n, the experiment can give only the energies of successive dissociations of the bonds $X_{n-1}M{-}X$, $X_{n-2}M{-}X$, *etc*., until the last X atom is eliminated. A difference of the consecutive dissociation energies in a polyatomic molecule may be very significant: thus, D (CH_3–H) = 439, D($CH_2{-}$H) = 462, D(CH−H) = 424 and D(C−H) = 338 kJ/mol. Although the mean bond energy in MX_n cannot be measured directly, it is generally used in structural chemistry, because in most MX_n molecules all M−X bonds are equivalent and should have equal strength. The average of all these dissociation energies gives the mean bond energy E,

$$E(M{-}X) = \frac{\sum D(M{-}X)}{n} \tag{2.41}$$

There is a certain parallel here with the concept of the mean ionization potential; the similarity extends also to some applications of both parameters (see below). In principle, the mean bond energy in polyatomic molecules may be directly determined, if the strong energetic influence atomizes a molecule completely: $MX_n \rightarrow M + nX$, however such experiments are not yet available. The energies of successive dissociations differ because after each atom is eliminated, the electron structure of the

remaining fragment is rearranged, the difference itself being the measure of this reorganization [167]:

$$E_R = D - E \tag{2.42}$$

The reorganization energy E_R, particularly important in quantum chemistry, will not be discussed here. Nevertheless, the effects of electron reorganization accompanying bond rupture in polyatomic molecules have to be taken into account in structural chemistry also, the dissociation energy being substantially affected by the structure and composition of the molecule.

While the total dissociation energy always increases with the bond order, this energy normalized by the number of bonding electron pairs sometimes reveals the opposite trend, e.g. decreasing in the succession E(C─C) in ethane > ½ E(C═C) in ethylene > 1/2 E(C≡C) in acetylene (357, 290, 262 kJ/mol, respectively). This *relative* weakening of the multiple bond is compensated by strengthening of the adjacent σ bond: extracting the first H atom from C_2H_6, C_2H_4 or C_2H_2 requires respectively 423, 459 and 549 kJ/mol, extracting the second one requires 163, 339, 487 kJ/mol [168, 169]. Such complementarity occurs because the effective nuclear charge of a given atom is screened by the constant number of its electrons and an accumulation of electrons in one bond naturally reduces the screening in other directions. Later we shall observe other manifestations of such compensation.

Experimental values of the mean bond energies for some elements are listed in Tables 2.11 and S2.9. The compilation was based on the above mentioned thermodynamics reference books, revised and (where reference are given) updated using new original publications. The energies of similar hetero-polar bonds in di- and polyatomic molecules (compare Tables S2.3 and 2.11) are only slightly different; this fact contradicts the ionic model. Indeed, if the bonds in the BaF_2, LaF_3 and HfF_4 molecules were purely ionic, their (Coulomb) energies would be higher than in the CaF, LaF and HfF radicals by the same factors as the charges of the metal atoms, i.e. 2-, 3- and 4-fold, respectively. In fact, bond energies in mono- and poly-fluorides differ only by ±10 %. Given that the Coulomb attraction certainly gives the major contribution to the bond energy (see below), one has to assume that as the valence (v) of the metal increases, the bond ionicity should decrease proportionally to $1/\sqrt{v}$ [196]. Below it will be shown how this simple rule agrees with the experimental data.

Thus, in polyatomic molecules with different ligands, bonds of the same type have different energies depending on the composition and structure of the molecule. Therefore the values listed in Table 2.9 are strictly applicable only to the molecules for which they have been determined, and only tentatively to other compounds with similar bonds. Table S2.9 illustrates how the environment of a given bond affects its energy. Leroy et al. [197] have also demonstrated that the energies of homo-atomic single bonds, calculated from the heats of formation of organo-element compounds (C─C 357, P─P 211 and S─S 265 kJ/mol), are close to the energies of the corresponding bonds in elemental substances (adjusted for the number of bonds in the structures), viz. diamond (358 kJ/mol), P_4 (201 kJ/mol) and S_8 (264 kJ/mol). The energies of single covalent bonds, determined by this method from the parameters of elemental substances, are included in Table 2.12.

Table 2.11 Average bond energies (kJ/mol) in MX_n-type molecules. (Bond energies of halides and hydrides of Groups 13–15 elements are calculated using the data from [170, 171] and are given without references)

M	F	Cl	Br	I	M	F	Cl	Br	I
Halide molecules MX_2					Halide molecules MX_3				
Cu	383[a]	302	258		Sb	437[b]	313[b]	264[b]	192[b]
Be	629[b]	463[b]	388[b]	299[b]	Bi	380[b]	279[b]	215[b]	170[b]
Mg	518[b]	391[b]	339[b]	262[b]	Cr	476	336	299	
Ca	558[b]	448[b]	395[b]	321[b]	Mo	494			
Sr	542[b]	438[b]	396[b]	321[b]	W	569	420	359	285
Ba	570[b]	460[b]	412[b]	353[b]	S	339[i]			
Zn	393	320	270	205	Mn	435	319		
Cd	328	274	238	192	Fe	462	345	292	222
Hg	257	227	185	145	Th	669[k]	514[k]	427[k]	
B	657	426	349	250	U	611[k]	477[k]	414[k]	
Al	563	387	321	250	Halide molecules MX_4				
Ga	431	308	258	196	C	487	321	258	199
In	398	279	232	174	Si	595[e]	399[e]	331[e]	246
Tl	360	253	203	146	Ge	471[q]	340[q]	273[q]	209[q]
Ti	690	456	436	344[c]	Sn	409	323[h]	261	210
Zr	636[d]	494[d]	423[d]	340[d]	Pb	327	249[h]	199	164
Hf	644	588	567	470	Ti	585[r]	430[r]	360[r]	295[r]
C	530	367	311	255	Zr	647[d]	488[d]	423[d]	346[d]
Si	600[e]	426[e]	365[e]	293	Hf	658[d]	496	447	355[e]
Ge	551[f]	392[f]	341[f]	269[f]	V		382[h]		
Sn	468	386[g]	323	254	Nb	574[s]	426[s]	372[s]	293[s]
Pb	388	304[g]	262	209	Cr	448	333	269	
V		453[h]	445	375	W	552	405	343	270
N	305	223	150	85.8	S	339[i]	204		
P	478	308	249	181	Th	672[k]	511[k]	448[k]	
As	431	288	235	172	U	609[k]	463[k]	398[k]	
Sb	392	264	213	148	Halide molecules MX_5				
Bi	358	231	180	116	P	461[i]	260		
Cr	507	387	340	249	As	387	253		
Mo	492			375	Nb	566[s]	406[s]	344[s]	
W	603	464	403	335	Ta	600	430	365	258
O	192	207			W	530	374	322	247
S	357[i]	271			S	316[i]			
Se	353	256	240		U	571[k]	412[k]	351[k]	

Table 2.11 (continued)

Te	377	284		
Mn	483	397[j]	342	278
Fe	463	398[j]	343	272
Co	477	382[j]	325	268
Ni	457	369[j]	316	252
Ru	433			
Pt	418			
Th	677[k]	517[k]	402[k]	
U	606[k]	460[k]	406[k]	

Halide molecules MX_3				
B	642	442[l]	366	285
Al	588[m]	422[m]	346[m]	284[m]
Ga	475[m]	355[m]	322[m]	245[m]
In	443[m]	322[m]	285[m]	225[m]
Sc	629[n]	470[n]	382[n]	337[n]
Y	643[o]	490[p]	432[p]	353[p]
La	641[o]	513[p]	456[p]	378[p]
C	477	335	273	205
Si	562	374	303	227
Ge	457	351	285	215
Sn	391	293	238	170
Pb	349	258	210	142
Ti	608	445	380	311
V	555	413[h]	369	
N	280	202	179	169
P	504[i]	329	259	177
As	438[b]	307[b]	252[b]	194[b]

Halide molecules MX_6				
S	329	182	117	42
Se	322	182	128	119
Te	343	204	145	87
W	531	364	301	231
AgF_6	AuF_6	MoF_6	TcF_6	
120[v]	176[w]	447[v]	387[v]	
ReF_6	RuF_6	RhF_6	PdF_6	
430[w]	325[v]	174[v]	118[v]	
OsF_6	IrF_6	PtF_6	UF_6	
382[w]	331[w]	259[w]	524	

Hydride and oxide molecules				
H_2O	H_2S	H_2Se	H_2Te	
459[t]	362[t]	320[t]	266[u]	
NH_3	PH_3	AsH_3	SbH_3	BiH_3
391	322	297	258	215
BH_3	AlH_3	GaH_3	InH_3	TlH_3
376	287	255	225	184
CH_3	SiH_3	GeH_3	SnH_3	PbH_3
408	301	268	235	192
CH_4	SiH_4	GeH_4	SnH_4	PbH_4
416	322	288	253	209
CO_2	SO_2	SeO_2	TeO_2	CrO_2
804	536	422	385	494
MoO_2	WO_2	SO_3	SeO_3	TeO_3
582	636	473	364	348
CrO_3	MoO_3	WO_3	RuO_3	OsO_4
479	584	630	492	530

[a][172], [b][173], [c][174], [d][175], [e][176, 177], [f][178], [g][179], [h][180], [i][181], [j][182], [k][183], [l][184], [m][185], [n][186], [o][187], [p][188], [q][189], [r][190], [s][191], [t][192], [u][193], [v][194], [w][195]

Table 2.12 Energies of single covalent homo-atomic bonds M–M (kJ/mol)

M	E	M	E	M	E	M	E	M	E^c
Li	105[a]	Zn	64[c]	Ge	187[d]	O	144[d]	Tc	263
Na	75[a]	Cd	55[c]	Sn	151[d]	S	264[d]	Re	293
K	53[a]	Hg	33[c]	Pb	73[c]	Se	216[d]	Fe	204
Rb	49[a]	B	286[b]	Ti	175[c]	Te	212[d]	Co	210
Cs	44[a]	Al	168[c]	Zr	225[c]	Cr	185[c]	Ni	210
Cu	201[a]	Ga	135[c]	Hf	232[c]	Mo	263[c]	Ru	319
Ag	163[a]	In	103[c]	N	212[b]	W	341[c]	Rh	273
Au	226[a]	Tl	64[c]	P	211[b]	H	436[a]	Pd	182
Be	119[b]	Sc	161[c]	As	176[d]	F	155[a]	Os	387
Mg	102[c]	Y	181[c]	Sb	142[d]	Cl	240[a]	Ir	326
Ca	87[c]	La	184[c]	Bi	98[d]	Br	190[a]	Pt	277
Sr	80[c]	C	358[d]	V	232[c]	I	149[a]	Th	224
Ba	94[c]	Si	225[d]	Nb	325[c]	Mn	121	U	213
				Ta	354[c]				

[a]see Table S2.3, [b]see Table S2.9, [c][198], [d][199]

Multiple bonds in structural chemistry are traditionally described as combinations of σ- and π-bonds, the proof being the two-step ionization of the C=C bond. The π-bond energy is conventionally calculated by simply subtracting the σ-bond energy from the experimental energy of a multiple bond. The π-bond energies obtained in this way are listed in Table S2.10. As one can see, dissociation energies of multiple bonds in the same molecules, reported by different authors, often show discrepancies exceeding the experimental error by an order of magnitude, because different techniques (of both measurement and calculation) involve the products of dissociation in different valence states. Large discrepancies between the results of different authors are caused also by inherent difficulty of determining a small value as the difference of two large ones. In any case, the simple additive scheme is not applicable here, because the standard energy of the C–C σ-bond (357 kJ/mol) refers to its equilibrium length of 1.54 Å, whilst the carbon-carbon distance in the double bond is only 1.34 Å. A rough estimate of how a contraction by 0.2 Å will affect the energy of the C–C bond can be obtained from the experimental compressibility of diamond. The Universal equation of state (see Sect. 10.6),

$$P(x) = 3B_o[(1-x)/x^2]\exp[\eta(1-x)] \tag{2.43}$$

where P is the pressure, B_o is the bulk modulus, $x = (V/V_o)^{1/3}$ (V and V_o are the initial and the final volumes of the body), $\eta = 1.5(B_o'-1)$ and B_o' is the pressure derivative of B_o, permits to calculate the pressure P required to shorten the bond distance in diamond from 1.54 to 1.34 Å. Taking into account that diamond has $B_o = 456$ GPa and $B_o' = 3.8$, we obtain $P = 405.6$ GPa (!). The work of compression is

$$W_c \approx \frac{1}{2} P \Delta V \tag{2.44}$$

Because for diamond, $V_o = 3.417\ \mathrm{cm^3/mol}$, for $x = 0.87$ we obtain $\Delta V = 1.166\ \mathrm{cm^3}$ and $W_c = 236.6$ kJ/mol. A ratio of the atomization energy of diamond (717 kJ/mol)

to its elastic energy ($B_o V_o = 1558$ kJ/mol) allows to calculate the potential part of W_c as $0.46 \times 236.6 = 108.8$ kJ/mol. Since in the diamond structure $N_c = 4$ and every C–C bond involves two atoms, shortening of a C–C bond requires 54 kJ/mol. Hence, the actual energy of the σ-bond must be reduced from 357 to 303 kJ/mol, but the π-component correspondingly increased from the conventional 262 (mean from Table S2.10) to 316 kJ/mol. Thus the σ- and π-bonds in ethylene have in fact simlar energies, rather than $E(\pi) << E(\sigma)$ of the conventional description. Thus the conventional breakdown of the bond energy into σ- and π-components is essentially formal. Nevertheless it is useful, particularly in highlighting *relative* trends. Thus, it is evident that π-bond energies decrease in the succession O > N > C > S > P > Si, both absolutely and relatively to the σ-components, because the overlap of the valence orbitals decreases in the multiple bonds. In the cases of O and N, the π-bond energy is higher than that of the σ-bond, because the formation of a π-bond reduces the repulsion between σ-bonded and lone electron pairs, which is especially strong in electron-rich O and N atoms (see above).

Theoretical calculation of the bond energy is the task of quantum chemistry. So far, satisfactory quantitative solutions have been achieved only for lighter elements. Nevertheless, in principle the problem has been treated more than half a century ago by Mulliken [200] who generalized the results of the molecular-orbital and valence-bonds methods and derived his 'magic formula',

$$E_b = \sum X_{ij} - \frac{1}{2}\sum Y_{kl} + \frac{1}{2}\sum K_{mn} - PE + E_i \tag{2.45}$$

where ΣX_{ij} is the exchange interaction of bonding electrons, ΣY_{kl} is the repulsion of non-bonding electron pairs, ΣK_{mn} is the exchange interaction of lone electron pairs, PE is the promotion energy and E_i is the ionic interaction. Since the exchange integrals are proportional to the products of wave functions (the overlap integrals) and the exchange energy of the bonding electrons is proportional to their ionization potentials, the first term of Eq. 2.45 can be transformed to

$$\Sigma X_{ij} = k\bar{I}_{ij}\frac{S_{ij}}{1 + S_{ij}} \tag{2.46}$$

where k is an empirical coefficient (usually of the order of 1), $\bar{I}_{ij}$ is the geometrical mean of the ionization potentials of the atoms i and j, and S_{ij} is the overlap integral. Taking into account that the overlap integral defines the fraction of the outer electron cloud which belongs to both atoms, it follows from Eq. 2.46 that the covalent bond energy is always less than half the ionization potential of the bonded atom (because $S \leq 1$). The actual E_b/I ratio for A_2 molecules with single bonds is 0.2 ± 0.1, for AB molecules it varies from 0.3 to 0.6, the higher energy shown by polar bonds.

Returning to the problem of positively charged alkali dimers (see above) we can make use of Eq. 2.46. Indeed, a transition from the two-electron bond in M_2-molecules to the M_2^+-cations yields one-half of S, but $\bar{I}$ for M^+–M increases much more. E.g., $I_1(\text{Li}) = 5.39$ but $\bar{I} = 20.20$ eV, for Na respectively 5.14 and 15.59 eV, etc., whereas for Cu, $I_1 = 7.72$ but $\bar{I} = 12.52$ eV and the bond energy in Cu_2 is 201

kJ/mol compared to only 155 kJ/mol in Cu_2^+. Thus, the relation between the first and second ionization potentials governs the change of bond energies at the positive ionization in molecules M_2.

Mulliken [201–205] calculated the overlap integrals as functions of two parameters:

$$p = \frac{d}{a_o}\frac{\mu_A + \mu_B}{2} \text{ and } t = \frac{\mu_A - \mu_B}{\mu_A + \mu_B} \tag{2.47}$$

where $\mu = Z^*/n^*$ and a_o is the Bohr radius. However, calculations have been carried out only for the integer values of n^* and $p \leq 8$. Later, the integrals were calculated for $n^* = 3.7$ and 4.2 up to $p = 8$ [206], or to $p = 20$ [207], which is enough for all the real bond lengths in molecules and crystals.

Other additive descriptions of the energy of a hetero-atomic chemical bond have been suggested, besides Eq. 2.45. The earliest, as mentioned above, was Pauling's equation [18]

$$E\,(\text{M–X}) = E_{\text{cov}} + E_{\text{ion}} \tag{2.48}$$

where $E_{\text{cov}} = ½\,[E(\text{M–M}) + E(\text{X–X})]$ and E_{ion} is the extra ionic energy, equaled to Q, which is the heat of reaction, $½\,M_2 + ½X_2 = MX$. Later Pauling suggested, as an alternative, to calculate E_{cov} as $[E(\text{M–M}) \cdot E(\text{X–X})]^{½}$. Fereira [208] described the energy of a M–X bond as the sum of three components,

$$E(\text{M–X}) = E_{\text{cov}} + E_{\text{ion}} + E_{\text{tr}} \tag{2.49}$$

representing the covalent, ionic and electron-transfer contributions, respectively; components of this equation have been modified in numerous works [209–217]. However, for empirical estimations one can use Eq. 2.48.

2.3.2 Bond Energies in Crystals

Bond energy (E_{cr}) in a crystalline compound MX_n can be calculated from the average bond energy in the corresponding molecule (E_{mol}) and the sublimation energy (ΔH_s, see Tables 9.4–9.6),

$$E_{\text{cr}} = E_{\text{mol}} + \Delta H_s/n \tag{2.50}$$

where n is the number of atoms with the lower valence in the formula unit (i.e. $n = 2$ for SiO_2 or Li_2O). Alternatively, the bond dissociation energy in MX_n crystals can be calculated directly from heats of formation $\Delta H_f(MX_n)$,

$$E_{\text{cr}}(\text{M–X}) = [\Delta H_f(\text{M}) + n\Delta H_f(\text{X}) - \Delta H_f(MX_n)]/n \tag{2.51}$$

Average bond energies for crystalline compounds are listed in Table 2.13.

Table 2.13 Mean bond energies (kJ/mol) in crystalline compounds M_nX_m (v = valence of M). (Bond energies for ZnSe, ZnTe, HgTe, SnSe, SnTe, FeS, CoS are the averaged values from handbooks and original articles)

v_M	M	X							
		F	Cl	Br	I	O	S	Se	Te
I	Li	853	682	614	529	580	519	484	430
	Na	761	642	581	518	438	425	393	365
	K	731	656	595	527	393	418	391	365
	Rb	717	639	584	515	374	398	402	
	Cs	711	648	591	534	374	396	412	
	Cu		596	557	512	546	514	484	460
	Ag	571	545	477	455	423	438	421	408
	Au		526	494	501				
	Tl	582	508	464	425	390	364	343	322
II	Cu	514	412	329		741	668	603	578
	Be	743	530	453	364	1172	824	725	661
	Mg	710	512	452	364	998	739	662	571
	Ca	776	604	544	460	1062	925	776	662
	Sr	764	612	554	467	1002	910	776	660
	Ba	768	639	584	514	984	918	800	707
	Zn	526	395	342	276	727	602	532[a]	456[a]
	Cd	480	372	326	264	618	538	484	402
	Hg	325	267	227	190	400	391	344	295[a]
	Ge	607			334		715[b]	642	589[c]
	Sn	552	453	392	328	833	682	619[d]	568[e]
	Pb	508	397	350	292	662	570	523[d]	465[e]
	V		576	551	492	1195			
	As					481[f]	389[f]	352[f]	312[f]
	Cr	687	518	460	384		824[g]		
	Mn	642	506	447	382	917	773	680	585
	Fe	621	502	447	358	932	792[h]	707	650
	Co	633	495	433	364	937	805[h]	721	
	Ni	616	488	429	359	915	797	728	660
	Pd	501	409	358	282	741	724		626
	Pt	550	462	429	415		921		
III	Sc	754	573	474	415	1137	919	789	704
	Y	790	597	530	445	1167	951		
	La	788	622	556	472	1134	972	822	765
	U	766	537	500	433		918		
	B	650	455	386	306	1040	707		
	Al	688	462	380	317	1027	738	632	541
	Ga	560	382	340	276	794	631	542	489
	In	555	376	333	265	718	554	491	438
	Tl		287			501			
	Ti	690	505	439	328	1068	617		
	V	655	484	432	325	998			
	As	453	325	274	226	669	534	471[f]	425
	Sb	471	336	290	223	666	501	454	407
	Bi	447	318	252	209	580	464	422	377
	Cr	560	411	378	307	891	651	558[i]	
	W	672[j]	525[j]	465[j]	396[j]				

Table 2.13 (continued)

v_M	M	X							
		F	Cl	Br	I	O	S	Se	Te
	Mn	530				758[k]			
	Re		469	429					
	Fe	547	392	339		810			
	Co	485	319						
	Ir		426	394					
	Pt		366	344					
IV	Ti	610	444	377	320	933	715	650	556
	Zr	706	516	452	378	1096	866	737	663[l]
	Hf	720	522	473	384	1131			
	Si	601	410	341	263	930	610	522	
	Ge	479	351	288	231	725	526[b]	454[d]	348
	Sn	445	336	275	230	689	505	438[d]	
	Pb	364	255			484			
	Th	757	573	497	423	1161[m]	890		
	U	689	516	454	369	1057[m]	808		
	V	559	392			863			
	Te		255	212		517			
	Mo	531	407	355		873	742[g]	659[g]	586[g]
	W	595[j]	454[j]	393[j]	323[j]	971	826[g]	743[n]	709
	Ru					727	705	664	
	Os					791	740	640	
	Pt		320	293	268		615		

MX	Sc	Y	La	B	Al	Ga	In	Th	U
N	1290	1197	1205	1299[o]	1113	901[p]	852[q]	1426[r]	1286[r]
P	1062[q]	1051	1050	984	827	697	630	1270[r]	1107[r]
As	945	1043	1039		745	667	606[s]		1046
Sb	774[t]	911[t]	913[t]		652[u]	587	542		930
C	1335[r]							1435[r]	1344

[a][218, 219, 220, 221], [b][222], [c][223], [d][224], [e][225], [f][226], [g][227], [h][228], [i][229], [j][230], [k][231], [l][232], [m][233], [n][234], [o][235], [p][236], [q][237], [r][238], [s][239], [t][240], [u][241]

2.3.3 Crystal Lattice Energies

In Sect. 2.3.1 and 2.3.2 we have considered the dissociation of bonds, molecules and solids into electroneutral atoms. Alternatively, one can imagine them dissociating into oppositely charged ions. Although such process is always less favorable thermodynamically in vacuum (see above), it can occur in a polar solvent. In any case, ionic description of the crystal proved a very fruitful model in structural chemistry, and historically the earliest one. The energy required to convert a solid ionic material into its independent gaseous ions, is known as the crystal lattice energy (U). It can be experimentally determined from the Haber-Born thermodynamic cycle,

$$U_{298} = -\sum \Delta H_{298}\,(\mathrm{M}) + \sum \Delta H_{298}\,(\mathrm{X}) - \Delta H_{298}\,(\mathrm{M_nX_m}) + \sum I\,(\mathrm{M}) - \sum A\,(\mathrm{X}) \tag{2.52}$$

where $\Delta H_{298}(M_nX_m)$ is the heat of formation of a crystalline M_nX_m compound from the elements under standard conditions, $\Sigma\Delta H_{298}(M)$ and $\Sigma\Delta H_{298}(X)$ are the sums of the heats of formation of n isolated atoms of the metal M and m atoms of the nonmetal X from the elements under standard conditions, I is the ionization potential and A is the electron affinity.

All the parameters featuring in Eq. 2.52 can, in principle, be experimentally determined, provided that the ions in question can exist as individual particles. However, no monoatomic anion with a charge exceeding -1 can exist, as they have $A < 0$. Hence, experimental determination of U is possible, in practice, only for metal halides. For compounds with polyvalent anions, like oxides, chalcogenides, nitrides, *etc*., U can be only calculated theoretically. The history and bibliography on this topic can be found in reviews [242, 243]. When it was realized that inorganic compounds do not have purely ionic bonds, the interest in the concept and values of the crystal lattice energies declined, therefore only a brief outline of this field is given here.

The lattice energy can be expressed as the difference of two terms,

$$U = U_a - U_r \tag{2.53}$$

U_a representing the Coulomb attraction between oppositely charged ions and U_r the repulsion between similarly charged ions. The attractive term is determined easily,

$$U_a = K_M \frac{z^2}{d} \tag{2.54}$$

where K_M is the Madelung constant, which depends on the structure type, stoichiometry of the compound and charges of the ions, z is the ionic charge, d is the interionic distance. There are several ways of expressing U_r as a function of d, of which the best are the approaches of Born and Landé [244–246] and Born and Mayer [247], who expressed the lattice energies in the form of Eqs 2.55 and 2.56, respectively.

$$U_{BL} = -K_M \frac{z^2}{d} + \frac{c}{d^n} \tag{2.55}$$

$$U_{BM} = -K_M \frac{z^2}{d} + \frac{C}{e^{d/\rho}}. \tag{2.56}$$

At the equilibrium interatomic distance $\partial^2 U/\partial d^2 = 0$, i.e. the attractive and the repulsive forces are equal. From here we obtain the well known Born-Landé and Born-Mayer equations,

$$U_{BL} = -K_M \frac{z^2}{d_o} / \left(1 - \frac{1}{n}\right) \tag{2.57}$$

$$U_{BM} = -K_M \frac{z^2}{d_o} / \left(1 - \frac{\rho}{d_o}\right). \tag{2.58}$$

Table 2.14 Madelung constants K_M

MX	K_M	MX_n	K_M	MX_n	K_M	M_nO_m	K_M
HgI	1.277	$HgCl_2$	3.958	$AuCl_3$	7.471	Cu_2O	4.442
HgBr	1.290	$BeCl_2$	4.086	$SbBr_3$	7.644	VO_2	17.57
HgCl	1.311	$PdCl_2$	4.109	BiI_3	7.669	SiO_2	
TlF	1.318	$ZnCl_2$	4.268	$MoCl_3$	7.673	β-quartz	17.61
HgF	1.340	$TiCl_2$	4.347	AuF_3	7.954	α-quartz	17.68
CuCl	1.638	$CdCl_2$	4.489	SbF_3	7.985	tridymite	18.07
NaCl	1.748	$CrCl_2$	4.500	AsI_3	8.002	TiO_2	
CsCl	1.763	CrF_2	4.540	$FeCl_3$	8.299	brookite	18.29
AuI	1.988	CuF_2	4.560	$AlCl_3$	8.303	anatase	19.20
ZnO	5.994	FeF_2	4.624	YCl_3	8.312	rutile	19.26
PbO	6.028	$SrBr_2$	4.624	VF_3	8.728	SnO_2	19.22
BeO	6.368	CdI_2	4.710	FeF_3	8.926	PbO_2	19.26
ZnS	6.552	$CaCl_2$	4.731	YF_3	9.276	ZrO_2	20.16
CuO	6.591	$PbCl_2$	4.754	LaF_3	9.335	MoO_2	18.27
MgO	6.990	NiF_2	4.756	BiF_3	9.824	Al_2O_3	25.03
		MgF_2	4.762	SnI_4	12.36	V_2O_5	44.32
		MnF_2	4.766	UCl_4	13.01		
		CoF_2	4.788	$ThBr_4$	13.03		
		α-PbF_2	4.807	$ThCl_4$	13.09		
		CaF_2	5.039	PbF_4	13.24		
		$AlBr_3$	7.196	SnF_4	13.52		
		BCl_3	7.357	SiF_4	14.32		
		BI_3	7.391	ZrF_4	14.36		

Many other expressions for the crystal lattice energy have been proposed, none of which has any real advantage over the abovementioned methods, which therefore remain in general use.

Born's repulsion coefficient n depends on the type of the electron shell (see Table 2.1). For an MX compound, n is calculated as ½ $[n(M^+) + n(X^-)]$. The ρ coefficient is less variable, averaging 0.35(5). For this reason, Eq. 2.58 is more frequently used for calculations. Assuming $n = 9$ and the interatomic distance $d = 3$ Å, the repulsion energy can be estimated as *ca.* 10 % of the crystal lattice energy.

Equation 2.48 can be improved by adding the third term, which accounts for the van der Waals forces,

$$E^W = \left(\frac{T_{cat} + T_{an}}{(r_{cat} + r_{an})^6} \right) \tag{2.59}$$

where r_{cat} and r_{an} are the radii of the cation and the anion, T_{cat} and T_{an} characterizes the van der Waals attractions of the cations and anions, respectively [248]. To recognize the importance of this contribution, compare NaCl and AgCl. They have similar structures and bond distances, but the van der Waals energy of the latter is 6 times greater due to higher polarizability [249].

Madelung constants are important in many other areas of physical chemistry. Their values for the shortest distances in the most common structural types are listed in Table 2.14 [250–252]. Note that these constants vary widely, from 1.28 to 44.3.

Their rigorous theoretical computation is a demanding task: to obtain an accurate result, the contributions of tens of thousands of ions must be taken into account [253–257] (Madelung constants for organic salts are presented in [258]). This stimulated the quest for more economic methods of calculating K_M; the most successful one has been suggested by Kapustinskii [259, 260], who related K_M to the number (m) and valence (Z) of ions which comprise the formula unit of the crystal:

$$k_M = \frac{2K_M}{mz_M z_X} \tag{2.60}$$

where k_M is the new (reduced) Madelung constant, the values of which are listed in Table S2.11. As one can see, k_M has the average value of 1.55 and varies by ±10 %, i.e. much less than K_M. The deviation of k_M from 1 is due to the crystal field, which in energy terms is characterized by the sublimation heat of the solid. Thus, for the halides of univalent metals, the ratio of the bond energies in the crystal and molecular states is equal to this number (1.55). Kapustinskii suggested that crystal lattice energies can be approximately estimated using for all structures the same $k_M = 1.745$ and the bond distances equal to the sums of ionic radii r_M and r_X (calculated for $N_c = 6$). Merging all constant factors into one, he obtained the expression

$$U = 256\frac{mz_M z_X}{r_M + r_X} \tag{2.61}$$

for U in kcal/mol and r in Å [259] which later was modified [260], in accordance with the Born-Mayer equation, to the formula

$$U = 287\frac{mz_M z_X}{r_M + r_X}\left(1 - \frac{0.345}{r_m + r_X}\right). \tag{2.62}$$

This method applies to complexes, as well as to binary compounds. By minimizing the discrepancy between the calculation and the experiment, one can determine the so-called 'thermochemical radii' of complex ions. These radii correspond to the (imaginary) spherical ions, iso-energetically replacing the real complex ions in the crystal structure. This problem has been discussed in great detail by Yatsimirskii [261] and later studied by Jenkins et al. [262–265]. Kapustinskii's equation has been successfully applied to the fluorides of mono- and divalent metals and to solid solutions of the LnF_3–MF_2 type [266]. A comparison of the experimental crystal lattice energies of CH_3COOM (M = alkali metals), XCH_2COOM (M = Li, Na; X = Cl, Br, I) and $ClCH(CH_3)COOM$ (M = Li, Na) with those calculated by Kapustinskii's equation [267] showed small differences in the lattice energies of all these compounds, i.e. M–O bonds define the crystal lattice energies of these compounds and all differences are due only to their bond distances.

The lattice energies for a variety of mineral and syntetic complex compounds that can be classified as double salts, were calculated by summing the lattice energies of the constituent simple salts [268]. A comparison with the lattice energies obtained from the Born-Haber or other thermodynamic cycles using the Madelung constant or

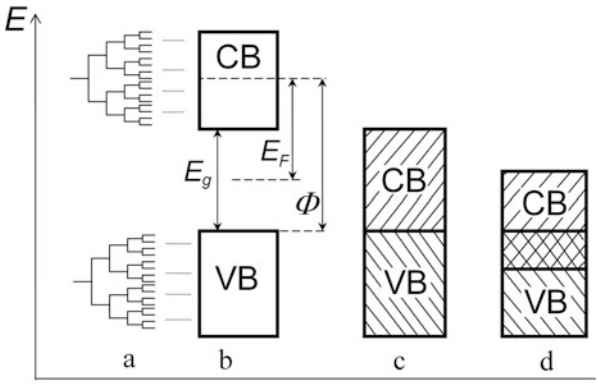

Fig. 2.5 Energy bands in crystals: **a** formation from atomic energy levels; **b** in dielectric, CB—conduction band, VB—valence band, E_g—band gap width, E_F—Fermi energy, Φ—work function; **c** in semiconductor with $E_g \geq 0$ (semi-metal); **d** in metal ($E_g \leq 0$)

more approximately through the Kapustinskii equation shows that this approximation reproduces these values generally to within 1.2 %, even for compounds that have considerable covalent character. Application of this method to the calculation of the lattice energies of silicates, using the sum of the lattice energies of the constituent oxides are, on average, within 0.2 % of the value calculated from the experimental enthalpies of formation.

Glasser and Jenkins [269] have formulated the general (but very simple!) procedures to make thermodynamic prediction for condensed phases, both ionic and organic/covalent, principally via formula unit volumes (or density). Their volume-based approach gives a new thermodynamic tool for such assessments, as it does not require detailed knowledge of crystal structures and is applicable to liquids and amorphous materials, as well as to crystalline solids. The next step was made in the work of Glasser and von Szentpály [270] who used the fundamental principle of electronegativity equalization to calculate the lattice energies for diatomic MY crystals, taking into account ionic and covalent contributions to the chemical bond. This method was applied to Groups 1 and 11 monohalides and hydrides, as well as to alkali metals. A limitation of the model occurs for the coinage metals, Cu, Ag, and Au, where *d* orbitals are strongly involved in the metallic bonding, while the homonuclear molecular bond is dominated by *s* orbitals.

2.3.4 Band Gaps in Solids

The structures of inorganic crystals usually comprise infinite chains, two- and three-dimensional networks of atoms linked by strong ionic or covalent bonds, and the energetic properties of atoms are influenced by all structural units of the crystal. Therefore the narrow electron energy level, characteristic of an isolated atom, is split into as many components as there are bonds in a crystal; each resulting level is also widened due to perturbations from adjacent atoms, the result being a broad band of continuous values of energy in the crystal (Fig. 2.5).

Table 2.15 Band gaps (eV) in MX—type compounds

M	X				M	X			
	F	Cl	Br	I		O	S	Se	Te
Li	12.5	9.4	7.9	6.1	Cu	1.95[a]			
Na	11.0	8.9	7.4	5.9	Be	10.6[b]	5.5	4.2	2.8
K	10.8	8.7	7.4	6.2	Mg	7.3[a]	6.0	5.7[c]	4.2
Rb	10.3	8.3	7.4	6.1	Ca	6.9[d]	5.3[d]	5.0[c]	4.1
Cs	9.9	8.2	7.3	6.2	Sr	5.8[d]	4.8[d]	4.7[c]	3.7
Cu		3.2	2.9	2.95	Ba	4.0[d]	3.9[d]	3.6[d]	3.4
Ag	2.8	3.6	3.05	2.8	Zn	3.4[a]	3.7[e]	2.7[e]	2.2[e]
Tl		3.4	3.0	2.8	Cd	2.3[a]	2.4[e]	1.7[e]	1.5[e]
M	X				Hg	2.8[f]	2.0[g]	0.4[h]	0.1
	N	P	As	Sb	Sn	4.2[i]	1.3[G]	0.9[j]	0.3
Sc	2.26[m]	1.1	0.7		Pb	2.8[a]	0.4[g]	0.3[k]	0.2
Y	1.5[n]	1.0[o]			Mn	3.8[a]	2.8	2.5	1.3
La		1.45[o]		0.8[n]	Fe	2.4[i]			
B	6.1[p]	2.1[q]	1.4[q]		Co	2.7[a]	0.94[s]		
Al	6.23[r]	3.63[r]	3.10[r]	2.39[r]	Ni	3.8[a]	0.5	0.3	0.2
Ga	3.51[r]	2.89[r]	1.52[r]	0.81[r]	Pd	2.4[t]			
In	1.99[r]	1.42[r]	0.42[r]	0.23[r]	Pt	1.3[i]			

[a][271], [b][272], [c][273], [d][274], [e][275], [f][276], [g][277], [G][278], [h][279], [i][280, 281], [j][282], [k][283], [l][284], [m][285], [n][286], [o][287], [p]for c-BN [288, 289], for h-BN $E_g \approx 5.5$ eV [290, 291], [q][292], [r]for w-phases [293], [s][294], [t][295]

Notwithstanding this qualitative difference between the energy spectra of an atom and a crystal, there are also some broad similarities. Just as an atom has certain permitted orbitals and the areas where the presence of electrons is forbidden, so a crystal has bands of permitted states: valence band and conduction band, separated by a band gap (forbidden zones), where no energy states are allowed. In an atom, the outer-shell electrons are chiefly responsible for chemical bonding—in a crystal the same role is played by the valence band. On ionization of an atom, an electron is removed from the valence shell (ideally—to infinity) in a crystal the equivalent process consists in the transfer of an electron from the valence band into the conduction band.

From the viewpoint of the conventional band theory, the band gap is absent in metals and has positive width E_g in dielectrics. The latter can be divided into dielectrics proper, with $E_g > 4$ eV, and semiconductors, with $0 < E_g < 4$ eV. Since E_g defines the energy required to transform a dielectric into a conducting (metallic) state, this parameter is widely used for various physical and chemical purposes and correlations. Tables 2.15, S2.12 and S2.13 comprise the most reliable experimental measurements of E_g.

Theoretical calculations of the band structure of crystals belong to solid state physics and are not discussed here. Quantitative *ab initio* prediction of a band gap is a problem of great complexity. However, empirical and semi-empirical estimates of E_g, using the concepts of structural chemistry, are sufficient for most purposes of physical chemistry and materials science. Indeed, since the valence band of a compound usually involves primary orbitals of the anions (nonmetal atoms), and the conduction band involves primary orbitals of the cations (metal atoms), the energy of the transition between the two (i.e., E_g) must be related to some atomic properties.

The structural-chemical approach has been pioneered by Welkner [296], who observed that E_g depends on the chemical bond energy and the effective atomic charges. The former relation is described by a linear equation [297–300],

$$E_g(\mathrm{MX}) = a\,[E(\mathrm{M}-\mathrm{X}) - b]\,. \tag{2.63}$$

Among structurally similar compounds, E_g increases together with the difference of electronegativities ENs (see next Section) of the bonded atoms ($\Delta\chi$). The form of the correlation is not certain. Thus, for binary compounds Duffy [301, 302] suggested a linear dependence (on the optical EN),

$$E_g = a\Delta\chi \tag{2.64}$$

while Di Quarto et al. [280, 281] have recommended

$$E_g = a\Delta\chi^2 + b \tag{2.65}$$

where the constants a and b are different for the main-group (s, p) and transition (d) elements. On the other hand, the band gap decreases with the increase of the mean principal quantum number of the components, $\overline{n}$, as the interaction of the valence electrons with the nucleus becomes weaker. The dependence of E_g from both $\Delta\chi$ and $\overline{n}$ has been mapped by Mooser and Pearson [303] and later expressed in the analytical form by Makino [304],

$$E_g = a\sqrt{\frac{\Delta\chi}{\overline{n}}} - b \tag{2.66}$$

which gave satisfactory agreement with the experimental data for binary crystalline compounds. Finally, Villars [305, 306] presented a 3D map of E_g, with $\Delta\chi$ and the electron density of atoms as the coordinates. Historical reviews of this approach see in [112, 307].

The resort to graphical representation of the empirical correlations shows the difficulties of the analytical description, due to the multiplicity of factors influencing the electronic structure of crystals. The task can be simplified, making use of the additive character of E_g. Hooge [308, 309] expressed the band gaps of binary compounds as the sums of atomic increments, the increment of each element being constant and depending only on its EN,

$$E_g(\mathrm{MX}) = E_g(\mathrm{M}) + E_g(\mathrm{X}). \tag{2.67}$$

These increments are computational parameters only, but it is also possible to express the band gap of a compound through the sum of the *observed* band gaps of the component elements corrected by two additional terms, accounting for the ionicity and metallicity of the bonds, respectively. The alternative equation has been suggested [310, 311],

$$E_g(\mathrm{MX}) = E_g(\mathrm{M}) + E_g(\mathrm{X}) + a\Delta\chi_{\mathrm{MX}} - b\overline{n} \tag{2.68}$$

where a and b are constants. Band gaps of elements are, of course, different in various allotropic modifications. Therefore in Eq. 2.68 one should use the E_g values of those modifications which are structurally most similar to the compound concerned, e.g. white phosphorus for phosphides, diamond for carbides, *etc*. The development of the additive approach naturally encouraged the measurements of band gaps in elemental solids, which have been carried out for boron, iodine and the elements of the Group 4, 5 and 6. All of them fit the equation

$$E_g = k\frac{I}{n} - c \tag{2.69}$$

where I is the potential ionization, n is the principal quantum number and k and l are structure-related constants. For metals $k = 0.8$, for materials with a continuous covalent network $k = 1.2$, for molecular crystals $k = 1.6$, whilst $c = 1.7$ in all cases.

It is now evident that the conventional view of all metals having the constant $E_g = 0$ is inconsistent both with the above mentioned relations and with the variability of E_g in dielectrics and semiconductors. The difficulties can be resolved on the simple assumption that metals have band gaps of variable *negative* width, equal to the overlap between the valence and the conductivity bands (Fig. 2.5). In fact, a negative E_g has been found experimentally in InN_xSb_{1-x} [313]. Equation 2.69 also gives $E_g < 0$ for metals. Furthermore, in this interpretation the sign of E_g correlates with the thermal dependence of electric conductivity, which in semiconductors increases on heating ($E_g > 0$) and in metals decreases ($E_g < 0$). Table S2.14 lists all the currently available experimental band gap widths for elements, together with the values calculated according to Eq. 2.69.

In another variety of the additive approach, the band gap of a compound is represented by the sum of the covalent and the ionic terms, the former determined by the geometrical properties of the component elements and the latter by $\Delta\chi$ [314]. Phillips [315], by way of quantum-mechanical reasoning, has arrived to a similar additive representation of the band gap,

$$E_g^2 = E_h^2 + C^2 \tag{2.70}$$

where the covalent component E_h depends on the atomic radius and the Coulomb contribution C on $\Delta\chi$. It is noteworthy that Welkner's, Duffy's and the various additive approaches are intrinsically related, because (according to Pauling) the energy of a chemical bond comprises an ionic and a covalent contribution, the latter depending on $\Delta\chi$.

Table 2.16 Band gaps in bulk and nano phases

Substance	E_g, eV		D, nm	Substance	E_g, eV		D, nm
	bulk	nano			bulk	nano	
graphite[a]	0	0.65	0.4	Si[h]	1.1	3.5	1.3
CdS[b]	2.5	3.85	0.7	$Ga_2O_3^i$	4.9	5.9	14
CdSe[c]	1.7	2.2	7	CeO_2^I	3.2	3.45	nano
SnS[C]	1.0	1.8	7	ZrO_2^j	5.2	6.1	7
SnSe[d]	1.3	1.7	19	SnO_2^k	3.6	4.7	3
PbS[e]	0.41	1.0	4.5	WO_3^l	2.6	3.25	9
$Sb_2S_3^f$	2.2	3.8	20	HfO_2^m	5.5	5.5	5
CdI_2^g	3.1	3.6	< 250	diamond[n]	5.5	3.4	4.5

[a][320], [b][321], [c][322], [C][323], [d][324], [e][325], [f][326], [g][327], [h][328], [i][329], [I][330], [j][331], [k][332], [l][333], [m][334], [n][335, 336]

The problem of band gaps has been challenged on completely fresh basis by Nethercot [316] who exploited the similarity between electron transfer from an M to an X atom on formation of a compound, and electric conductivity in a solid. Hence the EN can be a measure of the latter, as well as the former, process. Using the ENs according to Mulliken and assuming the EN of a compound to be the geometrical mean of the elements' ENs (in accordance with Sanderson's theory, see next Section), Nethercot determined the Fermi energy as

$$E^F{}_{MX} = c(\chi_M \chi_X)^{1/2}. \tag{2.71}$$

Then the electron work function can be calculated as

$$\Phi = E^F + \frac{1}{2} E_g. \tag{2.72}$$

The work functions, calculated by Eq. 2.72, agree with the experimental results, the average discrepancy being 3.5 %. For pure metals (for $E_g = 0$) Eqs 2.71 and 2.72 give a linear dependence $\chi = 0.35\Phi$.

Nethercot's approach was based on Sanderson's theory and encouraged more extensive applications of the latter, to determine work functions of metals and compounds [317]. The results are in good agreement with the experiment, e.g. for CaF_2, SrF_2 and BaF_2 the calculated $\Phi = 11.52$, 10.95, 10.48 eV and the observed $\Phi = 11.96$, 10.96, 10.69 eV, respectively. Similar calculations have been repeated later with equal success [318], using the ENs according to Mulliken. Notwithstanding the obvious efficiency of this method [319], it is noteworthy that good results have been obtained for solids with predominantly polar bonds, where bond metallicity could be neglected. No universal rule, linking E_g directly with EN, atomic charges, bond energies, work functions, etc., is currently known. Similar alterations of anions can result in opposite changes of the bang gap with different cations. Thus, for example the band gap in AgCl is wider than in AgF, and in the zinc and cadmium sulfides wider than in the oxides of the same elements (see Table 2.16), although the

bonds are stronger in the latter compounds. A satisfactory agreement with the experiment can be achieved only by taking into account bond polarity and metallicity, as well as *d*-electrons' participation in valence interactions (see above).

Obviously, the above cited values of band gaps correspond to large (ideally, infinite) samples, and can increase substantially for microscopic particles and clusters, which contain a significant fraction of surface atoms with lower coordination number and begin to resemble a molecule, with a correspondingly more covalent character of bonding (cf., k in Eq. 2.69 increasing from 1.2 to 1.6). Measurements of band gaps in clusters of varying diameter (D) confirmed this conclusion.

Polymorphs which do not differ in the coordination number, have similar band gaps, viz. for anatase, rutile and amorphous TiO_2 these are, respectively, 3.5, 3.2 and 3.8 eV for direct, or 3.2, 2.9 and 3.0 eV for indirect transitions. Crystals of ZnS, CdS and CdSe, on transition from wurtzite to cubic forms change band gaps from 3.9 to 3.7 eV, from 2.50 to 2.41 eV, and from 1.70 to 1.74 eV, respectively. At the same time, a transformation of diamond into graphite decreases E_g from 5.5 eV to zero.

2.4 Concept of Electronegativity

Effective charges of atoms are known only for a small minority of polar molecules and crystals, therefore it is important to find a dependence of these values on such characteristics of atoms which allows to estimate the polarity of bonds *a priori*. Such characteristic is the electronegativity of atom (EN) which, according to Pauling who introduced this concept in 1932, is the measure of the power of an atom in a molecule to attract electrons.

2.4.1 Discussion About Electronegativity

For 80 years the concept of electronegativity has been applied and modified in chemistry. This concept is used to explain such chemical properties as acidity of solvents, mechanisms of reactions, electron distributions and bond polarities. The difference of EN ($\Delta\chi$) allows to classify chemical compounds as ionic when $\Delta\chi > 1.7$, or covalent when $\Delta\chi < 1.7$. Metal elements have, as a rule, $\chi \leq 2.0$, nonmetals ≥ 2.0. These aspects are present in all textbooks of general chemistry published in recent decades (e.g. [337]). Thus it may seem amasing today that from the start the EN was a topic of arguments of uncommon intensity. Thus, Fajans ([338] and private communications) pointed that in the succession $HC{\equiv}CCl \rightarrow H_2C{=}CHCl \rightarrow H_3C{-}CH_2Cl$, the charge of the chlorine atom changes sign from $+\delta$ to 0 to $-\delta$, which contradicts the notion of a constant EN of the carbon atom. In fact, χ(C) depends on the state of hybridization, being 2.5 for sp^3, 2.9 for sp^2 and 3.2 for sp. With $\chi(Cl) = 2.9$ or 3.0; this explains the reversion of the charge. In the letter to Fajans in 1959 one of the

authors (S.S.B.) attracted his attention to this fact. Hückel critisized the dimensionality of EN, the square root of energy, as physically meaningless [339], to which it was replied [340] that the parameter used to calculate the bond ionicity, was actually $\Delta\chi^2$ with the dimensionality of energy, just as for the ψ-function the square of its modulus was linked to observables. As early as 1962–1963 it was argued that the idea of EN had run its course and cannot explain new data [341], that it contains actual mistakes [342–345] or that it uses the 'atoms in molecules' approach supposedly contradicting the philosophy of quantum mechanics [346]. The analysis of this critique, exposing its irrational nature, can be found in [347, 348]. Later, more criticism was directed at the problem of dimensionality of EN [349], usually without any account of the earlier discussions. The arguments in favour of EN [350–353] can be summarized thus. The fact that EN is defined through different observed properties and so has a non-unique dimensionality, merely reflects the multi-faceted nature of the chemical bond. Indeed, this can be an asset rather than liability, as EN can serve as nodal point connecting various physical characteristics of a substance, hence its wide usage in chemistry. A certain 'fuzziness' of the concept is in fact typical for chemistry, cf. the notions of metallicity, acidity, etc. Half a century later, it is evident that EN is indispensable in structural chemistry, crystallography, molecular spectroscopy, and various fields of physical and inorganic chemistry; it was even suggested to use EN as the third coordinate of the Periodic Table [354, 355].

2.4.2 Thermochemical Electronegativities

Pauling derived the first quantitative scale of EN using bond energies,

$$\Delta\chi_{MX} = \chi_M - \chi_X = c\Delta E_{MX}{}^{\frac{1}{2}} \tag{2.73}$$

where

$$\Delta E_{MX} = E(M{-}X) - \frac{1}{2}[E(M{-}M) + E(X{-}X)] \tag{2.74}$$

and $c = 0.102$ for E measured in kJ/mol. This formula gives only the differences of ENs, and to obtain the absolute values it was necessary to postulate the EN of one 'key' element. For this role, Pauling chosed hydrogen, initially assigning it $\chi = 0$ and later $\chi = 2.05$, to avoid negative χ for most metals.

Obviously, Eq. 2.73 makes sense only if $\Delta E_{MX} > 0$, which is true for all bonds but a few, such as alkali hydrides which have exceptionally weak M−H bonds, while H−H is the strongest σ-bond known. To overcome this inconsistency, Pauling replaced the geometrical for the arithmetical mean in Eq. 2.74. As $[E(M{-}M)\cdot E(X{-}X)]^{½} < ½\,[E(M{-}M) + E(X{-}X)]$ for purely mathematical reasons, this change restored the condition $\Delta E_{MX} > 0$, albeit at the cost of depriving the formula of the clear physical meaning. This approach gives practically the same values of EN as the previous one, if the factor $c = 0.089$ is used in Eq. 2.73. The geomet-

rical mean for the dependence of the bond energy on electronegativities was later suggested by Matcha [212] and Reddy [215].

Pauling's work initiated numerous determinations of the ENs of elements in various valence states, which were based of more extensive and precise sets of experimental data (for historical reviews see refs. [29, 355, 356]). Most important advances of this 'thermochemical' approach were made in the works of Pauling [28], Allred [357], Reddy et al. [215], Leroy et al. [358–362], Ochterski et al. [363], Murphy et al. [199], Smith [364, 365], Matsunaga et al. [366].

Reddy and Murphy showed that Pauling's equation is valid only for a limited range of molecules where $\Delta\chi$ is small, and substitution of the arithmetical mean by the geometrical mean makes little improvement. A better correlation is found if the 'extra ionic energy' (EIE) is expressed as $k\Delta\chi$ rather than as $k\Delta\chi^2$. The EIE may be represented by a quasi-Coulombic expression based on the Born-Mayer equation, thus Eq. 2.74 transforms into

$$E_{AB} = \frac{1}{2}(E_{AA} + E_{BB}) + a\frac{q_A q_B}{d_{AB}}\left(\frac{1-\rho}{d_{AB}}\right) \tag{2.75}$$

where q is the fractional charge, d is the bond distance, a and ρ are constants. Because according to Bratsch [213, 214]

$$q = \frac{\chi_A - \chi_B}{\chi_A + \chi_B} \tag{2.76}$$

substitution of this expression into Eq. 2.75 gives an expression where EIE is proportional to $\Delta\chi^2$. Pauling's approach requires a qualification: the energy of a bond depends not only on its polarity, but also on its length. Neglecting this in Eq. 2.48 can be justified by the low polarity of the bonds in question, i.e. on the assumption that purely covalent and slightly polar bonds have the same lengths. Allred [357] assumed Eq. 2.73 to be valid if $\Delta\chi \leq 1.8$, but this criterion has not been sufficiently substantiated and any extension of the database by adding the energies for bonds of unspecified polarity can alter both the absolute EN values of elements and the order of their succession. Ionov et al. [367] suggested to remedy this shortcoming by a principal alteration of Eq. 2.73, so as to utilize both thermodynamic and geometrical data. However, the basic correctness of Pauling's insight has been confirmed by other physical methods, hence it is more sensible to account for the geometrical factor by adding a correcting term to Eq. 2.74, rather than by altering its philosophy. This has been achieved by using in this equation a variable parameter c which takes into account the principal quantum numbers, bond distance and valences of atoms, $c = f(n^*, d, v)$ [368]. This correction reflects the fact that (other things being equal) an elongation of a bond lowers its polarity, by reducing the overlap of the valence orbitals, and an increase of valence also reduces the bond polarity. However, the contribution of all these factors is by an order of magnitude smaller than the major (bond-energy) term. In Table S2.15 are compared a few systems of thermochemical ENs, and the averaged results are listed in Table 2.17.

A prominent feature of the thermochemical system is the outstandingly high EN of oxygen, nitrogen and, especially, fluorine, which are often difficult to reconcile with

Table 2.17 Thermochemical electronegativities of atoms in molecules; $\chi(H) = 2.2$

Li	Be	B	C	N	O	F			
1.0	1.5	2.0	2.55	2.9	3.4	3.9			
Na	Mg	Al	Si	P	S	Cl			
0.9	1.3	1.6	1.9	2.15	2.6	3.1			
K	Ca	Sc	Ti	V	Cr	Mn	Fe	Co	Ni
0.75	1.0	1.35	1.6	1.7[a]	1.7[b]	1.7[c]	1.7[d]	1.75[e]	1.8[e]
Cu	Zn	Ga	Ge	As	Se	Br			
1.7[f]	1.6	1.7	2.0	2.1	2.5	2.9			
Rb	Sr	Y	Zr	Nb	Mo	Tc	Ru	Rh	Pd
0.7	0.95	1.2	1.6[g]	1.6[a]	2.2[h]	1.9	2.2	2.2	2.2
Ag	Cd	In	Sn	Sb	Te	I			
1.8	1.7	1.7	1.9[i]	2.0	2.1	2.6			
Cs	Ba	La	Hf	Ta	W	Re	Os	Ir	Pt
0.6	0.85	1.1	1.5[j]	1.5	2.2[k]	1.9	2.2	2.2	2.2
Au	Hg	Tl	Pb	Bi	Th[k]	U[k]			
2.2	1.9	1.3[l]	2.1[m]	2.0	1.5	1.6			

[a] $v = 3$, [b] $v = 3$, for $v = 2$ $\chi = 1.5$, for $v = 4$ $\chi = 2.0$, [c] $v = 3$, for $v = 2$ $\chi = 1.5$, [d] $v = 2$, for $v = 3$ $\chi = 2.0$, [e] $v = 2$, [f] $v = 1$, for $v = 2$, $\chi = 2.0$, [g] $v = 4$, for $v = 2$ $\chi = 1.4$, [h] $v = 4$, for $v = 2$ $\chi = 2.0$, [i] $v = 4$, for $v = 2$ $\chi = 1.6$, [j] $v = 4$, for $v = 2$ $\chi = 1.3$, [k] $v = 4$, [l] $v = 1$, for $v = 3$ $\chi = 1.8$, [m] $v = 4$, for $v = 2$ $\chi = 1.7$

the physical and chemical properties of these atoms in polyatomic molecules and crystals. Thus, fluorine is a surprisingly poor acceptor of hydrogen bonds [369, 370]. However, the apparent dissociation energies of the F–F, O–O and N–N bonds are lower than the intrinsic bond energies because of the electronic destabilization, i.e. the energetically unfavorable effect of the high electron concentration in a small volume (see Sect. 2.3.1). The underestimation of $E(\mathrm{X{-}X})$ in Eq. 2.48 leads to an overestimation of ΔE_{MX} and hence of χ, as Bykov and Dobrotin were the first to notice in the case of fluorine [371]. Later, Batsanov [372] calculated the electron destabilization energies for a number of compounds and re-evaluated the ENs of fluorine, oxygen and nitrogen as 3.7, 3.2 and 2.7, respectively (cf. the conventional values of 4.0, 3.5 and 3.0). The thermochemical method has been significantly improved by Finemann [373], who generalized Eq. 2.74 to cover radicals (R),

$$\Delta E_{M\mathrm{R}} = E(\mathrm{M-R}) - \frac{1}{2}[E(\mathrm{M-M}) + E(\mathrm{R-R})] \tag{2.77}$$

Equation 2.77 was later used to calculate the ENs for radicals of various composition; the averaged values are listed in Table S2.16. It is evident that the presence of multiple bonds in radicals substantially affects the atomic ENs. Equation 2.77 was shown to give the ENs which describe quite accurately the homolytic bond dissociation enthalpies of common covalent bonds (including highly polar ones) with an average

error of *ca.* 5 kJ/mol; by this method the dissociation enthalpies were calculated for more than 250 bonds, including 79 for which experimental values are not available [374]. The weakness of Pauling's approach can be seen in that the electronegativity of hydrogen (unique in this respect of all elements) is not constant but depends substantially on the atom or group (R) connected to it [374]. Thus, $\chi(H) = 1.95$ for R = Me, 2.06 for Et, 2.16 for OH, 2.20 for Cl, 2.26 for F and Ph, 2.27 for ONO_2, and 2.50 for C≡CH. Unique behavior of hydrogen is not uncommon in chemistry and Pauling noted that hydrogen's electronegativity 'misbehaves'. Using an average value of $\chi(H) = 2.2$, as recommended by Pauling, gives generally the correct trends in D(H–A), but the overall accuracy is much lower than that obtained for all other bonds. Therefore Datta and Singh chose $\chi(OH) = 3.500$ as the reference value [374]. They also sugested to use geometrical means of single bond energies in organic compounds for calculating the ENs of radicals.

Note that the energies of single covalent bonds (Table 2.12) change regularly in each subgroup of the Periodic Table. Therefore within each subgroup the ENs of elements are proportional to the square roots of the energies of the corresponding homonuclear bonds. Hence, the entire system of thermochemical ENs can be derived from these energies and the known ENs of the top elements in a group, provided that the F–F, O–O and N–N bond energies are corrected for the electron destabilization by adding 220, 170 and 150 kJ/mol, respectively. Now we can, by comparing the energies of σ- and π-bonds, find out how the EN is affected by the bond order. This problem has been explored for carbon [375] and other elements capable of multiple bonding [376], using Eq. 2.78, which follows the philosophy of Eqs 2.73 and 2.74,

$$(\Delta\chi)^2 = \Delta E = \frac{1}{n}E(\mathrm{A} \sim \mathrm{A}) - E(\mathrm{A} - \mathrm{A}) \tag{2.78}$$

where $\Delta\chi$ is the difference between the ENs displayed by the *same* element A in the directions of the single (A–A) and the multiple (A∼A) bond, n is the order of the latter bond, E is the corresponding energy. Using Eq. 2.78 and the data from Table S2.10, we can find that the ENs of C, Si, P and S in double bonds are *lower* that the standard values, by 0.42, 0.49, 0.43 and 0.34, respectively, but for O and N the 'double-bond' ENs are *higher* that the standard ones, by 0.43 and 0.34. One-third of the energy of the triple C≡C bond (262 kJ/mol) is lower than the energy of one single bond (357 kJ/mol) hence the 'triple-bond' EN is by 0.50 lower than the 'single-bond' EN. The opposite is true for nitrogen: E (N≡N)/3 = 315 kJ/mol > E (N–N) = 212 kJ/mol, hence the formation of a triple bond rises the EN of nitrogen by 0.52. The ENs of elements in the most common multiple bonds are:

(C=) 2.2	(Si=) 1.4	(P=) 1.8	(S=) 2.2	(N=) 3.1	(O=) 3.6
(C≡) 2.1		(P≡) 1.7		(N≡) 3.3	

In a single bonds *adjacent* to a multiple bonds, the EN of the same atom changes in a compensatory manner. Thus, the ENs of carbon, displayed in the central (single) C–C bond in the CH_3CH_2–CH_2CH_3, CH_2 = CH–CH = CH_2, and HC≡C–C≡CH molecules, are 2.6, 3.1 and 3.4, respectively.

Since the change of the bond order usually implies the change of the coordination number, it is useful to consider from this viewpoint the transformation of a molecular structure into a continuous network of covalently bonded atoms in the solid state. Thermodynamically, the depth of the structural rearrangements during gas → crystal transition is characterized by the heat of sublimation ΔH_s (see Chap. 9) from which it is natural to calculate the crystal-state ENs (χ^*) [377]

$$\Delta\chi^* = a\sqrt{\Delta E + \Delta H_s} \tag{2.79}$$

Usually, ΔH_s of nonmetals (which retain the molecular structure in crystal) are small compared to that of metals, where the crystal growth implies the formation of new chemical bonds. Then, assuming the sublimation heat to be additive, almost the entire heat effect of crystallization of a compound can be related to the EN of the metallic component. The same conclusion follows from simple crystallographic reasoning. When molecules assemble into a crystal structure, both the metal and the nonmetal atoms increase their coordination numbers. For the nonmetal this means engaging previously nonbonding electron pairs into chemical bonds, which increases the mean ionization potential and hence the bond energy, according to Eq. 2.46 (see below for details). No such increase of the ionization potentials occurs for the metal, which provides the same number of bonding electrons in the molecular and in the solid state. For both the metal and the nonmetal, the covalent component of the bond (the overlap of the wave functions) is smaller in the crystal, where the bonds are somewhat longer than in the molecules. For the nonmetal the latter effect subtracts from the increase of the bond energy, whilst for the metal, it produces a net decrease. Thus, the ENs of nonmetals in crystalline compounds are close to those in molecules, while those of metals are always lower.

The system of ENs for the crystal state has been developed [378, 379] by comparing the atomization energies of the MX-type compounds with the energies of the M−M and X−X bonds in the solid state, corrected for the difference of the bond distances in the molecules and solids. The crystalline ENs of the same metal, calculated from different halides, practically coincide. Thus the obtained values are reproducible and can be recommended for general use in structural chemistry. Other ENs, tailored for thermodynamic or structural characteristics of crystals, were suggested by Vieillard and Tardy [380] and by Ionov and Sevastianov [381]. For most elements, their results are close to the thermochemical crystalline ENs, they are presented in Table 2.18.

2.4.3 Ionization Electronegativities

Pauling's pioneering paper [18] was soon followed by the work of Mulliken [382, 383], who approached ENs from the viewpoint of quantum mechanics. He proved that ENs can be calculated as

$$\chi = \frac{1}{2}(I_v + A_v) \tag{2.80}$$

Table 2.18 Thermochemical electronegativities of atoms in crystals

Li 0.65	Be 1.15	B 1.4	C 2.5	N 2.7	O 3.2	F 3.7			
Na 0.6	Mg 1.0	Al 1.3	Si 1.9	P 2.1	S 2.5	Cl 3.0			
K 0.5	Ca 0.75	Sc 1.1	Ti 1.55[c]	V 1.4[e]	Cr 1.25[f]	Mn 1.2[f]	Fe 1.4[f]	Co 1.45[f]	Ni 1.5[f]
Cu 1.15[a]	Zn 1.3	Ga 1.4	Ge 2.0	As 2.1	Se 2.5	Br 2.8			
Rb 0.45	Sr 0.7	Y 1. 5	Zr 1.4	Nb 1.6	Mo 1.75	Tc	Ru	Rh	Pd 1.35[f]
Ag 1.3	Cd 1.35	In 1.55	Sn 1.9[d]	Sb 2.0	Te 2.1	I 2.5			
Cs 0.4	Ba 0.65	La 1.0	Hf 1.4	Ta 1.5	W 1.75	Re	Os	Ir	Pt 1.7[f]
Au 1.4	Hg 1.6	Tl 1.1[b]	Pb 2.15[d]	Bi 2.0	Th[g] 1.4	U[g] 1.3			

[a]for Cu^{II} $\chi = 1.6$, [b]for $v = 1$, [c]$v = 4$, for $v = 2$ $\chi = 1.1$, [d]$v = 4$, for $v = 2$ $\chi = 1.4$, [e]for $v = 3$, [f]for $v = 2$, [g]for $v = 4$

where I_v is the valence-state ionization energy and A_v is the electron affinity of the atom. Mulliken's ENs (χ_M) are close to Pauling's values (χ_P) multiplied by a factor of 3 ± 0.2. The most remarkable advantage of Mulliken's method is the opportunity to calculate ENs for various valence states. As *ns* electrons have higher ionization energy than *np* ones, an increase of the *s*-character of an orbital rises the EN of an atom in the succession $sp^3 < sp^2 < sp$ [384], in agreement with the results of the thermochemical method (see above). Pritchard and Skinner [385–388] calculated ENs of atoms in various valence states from spectroscopic data. They obtained good agreement with the thermochemical EN and thus were able, by combining the methods of Pauling and Mulliken, to determine the type of hybridization of the bonds in transition metal compounds. Batsanov [375, 389] calculated the ENs of sp^2 and *sp* hybridized carbon atoms from the experimental values of the ionization potential. The planar-trigonal *olefinic* (sp^2) carbon atom has the EN of 2.3 in the double bond and 2.6 in the single bond, whilst the linear *acetylenic* (*sp*) atom (–C≡) displays the EN of 2.0 in the triple bond and 2.8 in the single bond, also in accordance with thermochemical data.

The theory of EN has been substantially advanced by Iczkowski and Margrave [390], who have shown that within the same shell the ionization energy is a function of the charge q (the number of removed electrons),

$$E(q) = \alpha q + \beta q^2 + \gamma q^3 + \cdots \tag{2.81}$$

where α, β and γ are constants. Neglecting the third and successive members of the series, we obtain for a hydrogen-like atom

$$(\partial E/\partial q)_{q=1} = \frac{1}{2}(I_v + A_v) \tag{2.82}$$

Thus, the assumption that EN is the derivative of the energy by the charge follows Mulliken's formula. Hinze and Jaffe [391–393] regarded EN as the ability of an atom to attract electrons into a given orbital, and therefore introduced the term 'orbital EN' (simultaneously the same term was introduced by Pritchard and Skinner [388]). Having calculated the orbital ENs exhibited by several elements in single and multiple bonds, they obtained for the tetrahedral C (sp^3) $\chi = 2.48$, for the trigonal C (sp^2) $\chi = 2.75$ in the single bond and 1.68 in the double bond, for the linear acetylenic carbon $\chi = 3.29$ in the single and $\chi = 1.69$ in the triple bond.

Mulliken's method, like that of Pauling, tends to overestimate the ENs of fluorine, oxygen and nitrogen, and essentially for the same reason: neglecting the inter-electron repulsion (see above). The quantum-mechanical approach was further developed using the electron density functional theory [394, 395], according to which EN is the negative chemical potential μ,

$$\chi = -\mu = -\left(\frac{\partial E}{\partial N}\right) \tag{2.83}$$

where E is the ground-state energy as a function of the number of electrons (N), for a given potential μ affecting the system. The electron chemical potential has the same tendency towards equalization as the macroscopic (thermodynamic) potential: electrons move from the areas of high potential (μ_h) to those of low potential (μ_l), whereupon μ_l increases and μ_h decreases until they become equal. In the DFT formalism, Mulliken's equation can be derived on the assumption that the energy of the system is a quadric function of the number of electrons [396, 397]. An outline of this approach can be found in the *Structure and Bonding* edition [398], comprising contributions from all the major researchers in this field and in excellent reviews by Allen [399] and Cherkasov et al. [355]. Details of the theoretical calculations are outside the scope of the present book, which is devoted to experimental aspects of structural chemistry. The reader can consult a review by Bergmann and Hinze [400] on the quantum-mechanical calculations of the ENs of elements from the ionization energies. A purely empirical formula linking EN with the ionization potential I and electron affinity A has been suggested by Sacher and Currie [401]. Further development of the Iczkowski-Margrave model is given in [402].

Pearson [403, 404] used the ground-state ionization energy and electron affinity of an atom (I_o and A_o) for calculating 'the absolute electronegativity' by Eq. 2.80. Since I_o and A_o are known for all elements and for all steps of oxidation, Pearson's approach became popular, although it does not conform rigorously to Mulliken's original definition of EN. Pearson's method is now widely used to calculate atomic and molecular electronegativities; selected ENs from this system (normalized by $\chi(H) = 2.2$) are presented in Table S2.16. In general, Pearson's ENs follow the expected

trends in the Periodic Table, increasing from left to right in periods and decreasing from top to bottom in groups. However, there are some strikingly unrealistic values: Cl is assigned higher EN than O and N, Br is on par with O and more electronegative than N, H is as electronegative as N and more so than C or S. The errors disappear if valence-state ionization energies and electron affinities are used. Unfortunately, there is serious ambiguity in specifying the valence state; for instance, for three-coordinate N atom one has to choose from seven possible valence states [406–408].

The ionization energies of ground-state atoms are considerably larger than their electron affinities, hence EN is defined mostly by I_o. Therefore Allen et al. [406–408] introduced the atomic electronegativity scale based upon the spectroscopic (averaged) ionization energies of the valence electrons in a ground-state free atom:

$$\chi = \frac{m\varepsilon_p + n\varepsilon_s}{m+n} \tag{2.84}$$

where m and n are the numbers of p and s valence electrons, ε_p and ε_s are the ionization energies of the p- and s-electrons, determined from atomic spectra. These characterisrics became known as 'spectroscopic electronegativities', SEN. Selected values of SEN, normalized by $\chi(H) = 2.2$, are listed in Table S2.17. SENs are closer to the thermochemical ENs than Pearson's values. According to Allen, SENs characterize the atom's ability to absorb (or to retain, in the case of rare gases) electrons, they do not depend on the valence and coordination number and are specific parameters of elements, which can be regarded as the third dimension of the Periodic Table. SENs correlate with Lewis acidity, defined as $S_a = v/N_c$, where v is the valence and N_c is the average coordination number of an element in its compounds with oxygen [409]. Politzer et al. [405] calculated absolute electronegativities on different levels of MO theory; these magnitudes of ENs are also given in Table S2.17.

All the abovementioned systems of ENs have been normalized to Pauling's thermochemical scale. However, the thermochemical and ionization (except Allen's system) ENs have different dimensionalities, viz. square root of energy and energy, respectively. This reflects the fundamental difference, that Pauling's method uses *mean* bond energies, thus treating all electrons of the central atom as equivalent, while Mulliken's method uses the *first* ionization potentials, thus singling out one electron. To compare the thermochemical and the ionization methods correctly, the energy of valence electrons in the latter should be characterized by the average, rather than the first, ionization potential ($\bar{I}$) of all outer electrons. This gives the simple formula

$$\chi = k\sqrt{\bar{I}} \tag{2.85}$$

where $k = 0.39$ [410]. Significantly, Eq. 2.85 permits to determine ENs for different oxidation states by averaging the corresponding number of successive ionization potentials. This equation gives ENs in accordance with Pauling's scale for *sp*-elements (a-subgroups), but for transition elements the calculated ENs are somewhat lower than the thermochemical values, since *d*-electrons from the previous shell can participate in the bonding. To account for this, in the case of *d*-elements the values of χ

Table 2.19 Ionization electronegativities of elements (for H, $\chi = 2.2$)

Li	Be	B	C	N	O	F			
0.90	1.45	1.90	2.37	2.85	3.31	3.78			
Na	Mg	Al	Si	P	S	Cl			
0.88	1.31	1.64	1.98	2.32	2.65	2.98			
K	Ca	Sc	Ti	V	Cr	Mn	Fe	Co	Ni
0.81	1.17	1.50	1.25[b]	1.60[c]	1.33[b]	1.32[b]	1.35[b]	1.38[b]	1.40[b]
			1.86	1.92[d]	1.63[c]	1.70[c]	1.66[c]	1.72[c]	1.76[c]
				2.22	1.97[d]	2.02[d]			
					2.58	2.93			
Cu	Zn	Ga	Ge	As	Se	Br			
1.48	1.64	1.84	2.09	1.70[c]	2.61	2.88			
1.66[b]				2.35					
Rb	Sr	Y	Zr	Nb	Mo	Tc	Ru	Rh	Pd
0.80	1.13	1.40	1.22[b]	1.52[c]	1.92[d]	1.93[d]	1.35[b]	1.39[b]	1. 45[b]
			1.71	2.02	2.36		1.97[d]	1.99[d]	2.08[d]
Ag	Cd	In	Sn	Sb	Te	I			
1.57	1.65	1.80	1.29[b]	1.60[c]	2.46	2.70			
			2.01	2.24					
Cs	Ba	La	Hf	Ta	W	Re	Os	Ir	Pt
0.77	1.07	1.35	1.28[b]	1.52[c]	1.83[d]	1.83[d]	1.39[b]	1.40[b]	1.45[b]
			1.73	1.94	2.28	2.48	1.85[d]	1.87[d]	1.92[d]
Au	Hg	Tl	Pb	Bi	Po	Th	U		
1.78	1.79	0.96[a]	1.31[b]	1.58[c]	2.50	1.60[d]	1.58[d]		
		1.89	2.07	2.26					

[a] $v = 1$, [b] $v = 2$, [c] $v = 3$, [d] $v = 4$

calculated by Eq. 2.85 must be increased by the term

$$\Delta\chi = 0.1\frac{n}{v} \tag{2.86}$$

where n is the principal quantum number and v is the group or the intermediate valence. The resulting ENs are listed in Table 2.19.

A comparison of the ionization and thermochemical ENs of elements reveals the largest discrepancies for Cu, Ag, Au and smaller ones for Zn, Cd and Hg, due to d-electrons participating in the bonding. For Cu, a comparison of the thermochemical EN with the χ calculated for the s- and d-electrons, revealed a 23 % participation of the 3d-electrons in the Cu–X bonds [387].

It has been proposed [411, 412] to transform Pauling's ENs into Mulliken's, by equalizing their dimensionalities accordingly. However, in these works only the first ionization potentials were used, thus reproducing the shortcoming of Mulliken's original approach. Ionization potentials have also been used in these works and in [413] to determine ENs for groups of atoms (radicals), the mean values of which are listed in Table S2.18.

To calculate EN for crystals, it is sensible to use the work function (Φ), i.e. the energy of removing an electron from a solid, which can be regarded as the ionization potential of the solid (see above). This has been first attempted by Stevenson and Trasatti, who suggested the simple dependence $\chi^* = k\Phi$, where $k = 0.355$ [414] or 0.318 [415, 416]. Eq. 2.87 gives the best agreement with the thermochemical scale of crystalline EN for metals.

$$\chi^* = k\Phi + k\left(\frac{v}{n^*} - 1\right) \tag{2.87}$$

where $k = 0.32$ and other symbols as above. The values of χ^* calculated by this technique using modern values of Φ [417] are listed in Table 2.20; for elements of Groups 1 to 4 and 11 to 14, using the group valences, for other metals the lowest oxidation numbers. It is noteworthy that the heats of formation of inter-metallic compounds can be calculated according to Miedema's theory assuming $\chi^* = \Phi$ [418–420]. However, EN is an atomic property and cannot be adequately derived from bulk properties (see Sect. 1.1.2)

ENs of ions also can be calculated by Mulliken's method in the same way as for neutral atoms, by substituting the ionization potential and electron affinity of the corresponding ion into Eq. 2.80. Thus, to calculate the EN for a cation with the +1 charge, one should use the *second atomic* ionization potential as the first cationic *I*, and the first atomic ionization potential for *A*. For an anion charged –1 the first atomic *A* should be used for *I,* and the second atomic *A* for the electron affinity. The ionic ENs thus calculated [376, 421, 422], are listed in Table S2.19. Bratsch [423] has made a rough estimate that the EN of a neutral atom doubles when it acquires the +1 charge and becomes zero when –1. The latter statement has been since confirmed, whilst the real increase of the EN for cations proved several times, or even an order of magnitude, higher.

2.4.4 Geometrical Electronegativities

Electronegativity being a qualitative property which describes the power of an atom in a molecule to attract the bonding electrons, it can be defined by the ratio of the effective nuclear charge to the covalent radius, Z^*/r^n. Many authors have proposed different values of n in order to reconcile the geometrical and thermochemical systems of EN, see reviews [56, 355, 356, 423]. A brief history of these attempts is presented in Table S2.20. From the Z^* and r, EN can be calculated by the formulae

Table 2.20 Work functions (eV, *upper lines*) and crystal electronegativities (*lower lines*)

Li	Be	B	C						
2.38	3.92	4.5	5.0						
0.60	1.25	1.6	1.92						
Na	Mg	Al	Si						
2.35	3.64	4.25	4.8[a]						
0.54	1.06	1.36	1.64						
K	Ca	Sc	Ti	V	Cr	Mn	Fe	Co	Ni
2.22	2.75	3.3	4.0[b]	4.40	4.58	4.52	4.31	4.41	4.50
0.48	0.73	1.00	1.31	1.35	1.32	1.30	1.23	1.26	1.29
Cu	Zn	Ga	Ge	As	Se				
4.40	4.24	4.19	4.85	5.11	4.72				
1.17	1.21	1.28	1.58	1.75	1.71				
Rb	Sr	Y	Zr	Nb	Mo	Tc	Ru	Rh	Pd
2.16	2.35	3.3	4.0	3.99	4.29	4.4	4.6	4.75	4.8
0.45	0.59	0.98	1.28	1.20	1.37	1.41	1.31	1.36	1.38
Ag	Cd	In	Sn	Sb	Te				
4.30	4.10	3.8	4.38	4.08	4.73				
1.14	1.15	1.14	1.40	1.38	1.67				
Cs	Ba	La	Hf	Ta	W	Re	Os	Ir	Pt
1.81	2.49	3.3	3.20[c]	4.12	4.51	4.99	4.7	4.7	5.32
0.34	0.63	0.96	1.01	1.23	1.40	1.55	1.34	1.34	1.53
Au	Hg	Tl	Pb	Bi	Th	U			
4.53	4.52	3.70	4.0	4.4	3.3	2.2			
1.21	1.28	1.09	1.26	1.47	1.04	0.69			

[a]p-Si, for n-Si $\Phi = 4.8$ eV, [b]α-Ti, for β-Ti $\Phi = 3.65$ eV, [c]α-Hf, for β-Hf $\Phi = 3.53$ eV

of Cottrell and Sutton (Eq. 2.88) [424], Pritchard and Skinner (Eq. 2.89) [425] and Allred and Rochow (Eq. 2.90) [426].

$$\chi_1 = a\left(\frac{Z^*}{r}\right)^{1/2} + b \tag{2.88}$$

$$\chi_2 = c\frac{Z^*}{r} + d \tag{2.89}$$

$$\chi_3 = e\left(\frac{Z^* - f}{r^2}\right) + g. \tag{2.90}$$

where *a, b, c, d, e, f,* and *g* are constants. Most of these constants are composition-dependent and therefore Eqs 2.88–2.90 are of limited utility in structural chemistry.

In view of this, it is expedient to modify these equations, by making the constants universal and including additional terms depending explicitly on the nature of the elements concerned. Thus, Eq. 2.88 was reduced [427] to

$$\chi_1 = \gamma\left(\frac{Z^*}{r}\right)^{\frac{1}{2}} \tag{2.91}$$

where γ is the function of the Group number and the effective principal quantum number. Better agreement between the calculated and thermochemical data can be attained by reducing Eq. 2.90 to

$$\chi_3 = e\frac{Z^*}{(r+\beta)^2} + g \tag{2.92}$$

ENs have been calculated for all elements in different valence states according to Eqs 2.91, 2.89 and 2.92, showing good agreement with the thermochemical characteristics.

Electronegativity can be also calculated by the method proposed by Sanderson [429–431], who has established a correlation between EN and the 'relative electron stability', $S = \rho_a/\rho_{rg}$ of the atom; $\rho_a = N_e/V$, where N_e is the number of electrons in the given atom, V is the its volume, and ρ_{rg} is the same for the iso-electronic atom of the rare-gas type. Sanderson found that the electronic stability, or "compactness", is a good measure of electronegativity:

$$\chi^{1/2} = aS + b. \tag{2.93}$$

Individual values of S have been revised from time to time, and refined data of χ by Sanderson's method, are given in [431, 432]. This method gives only a qualitative agreement with thermochemical values, because the electron densities in the core and valence-shell regions are very different, hence the integral approach cannot give adequate results (see [433]). It makes more sense to calculate χ in terms of the electron density of the outer (valence) shell of the atom, ρ_e. To do this, the number of valence electrons v should be divided by the volume of the outer shell, $V_e = V_a - V_c$ where V_a is the atomic volume, V_c is the core volume, so $\rho_e = v/V_e$. Assuming that the outer electrons in the atom are identical, one can treat them as a Fermi gas. Then the energy of these electrons is $E_e \sim \rho_e{}^{2/3}$. Since χ is proportional to $E^{1/2}$, we obtain

$$\chi_4 = C\rho_e^{1/2} \tag{2.94}$$

[434, 435]. Note, however, that treating the valence electrons as a Fermi gas means that these electrons are similar to those in metals. In any group of elements in the Periodic Table, the metallicity of bonding increases on going down the column to peak in Period 6. Therefore, ρ_e in Eq. 2.94 should be normalized against these elements. For example, the ratio of the effective principal quantum number of a given period to n^* is 4.2. The work equation will then appear as

$$\chi_4{}^* = 2.65\left(\frac{n^*\rho_e}{4.2}\right)^{1/3}. \tag{2.95}$$

Table 2.21 Geometrical electronegativities of atoms in the group valences, in molecules (*upper lines*) and crystals (*lower lines*)

Li	Be	B	C	N	O	F			
1.01	1.54	2.05	2.61	3.08	3.44	3.90			
0.38	0.98	1.71	1.97	2.86	3.15	3.48			
Na	Mg	Al	Si	P	S	Cl			
0.99	1.28	1.57	1.89	2.20	2.58	2.91			
0.37	0.70	1.32	1.47	2.09	2.45	2.69			
K	Ca	Sc	Ti	V	Cr	Mn	Fe[a]	Co[a]	Ni[a]
0.83	1.07	1.36	1.60	1.89	2.10	2.33	1.80	1.86	1.92
0.32	0.58	0.92	1.27	1.06[a]	1.40[b]	1.44[b]	1.17	1.21	1.25
Cu	Zn	Ga	Ge	As	Se	Br			
1.62	1.72	1.89	2.07	2.28	2.53	2.82			
0.71	1.14	1.60	1.64	2.16	2.42	2.63			
Rb	Sr	Y	Zr	Nb	Mo	Tc	Ru[b]	Rh[b]	Pd[b]
0.82	1.01	1.26	1.50	1.80	1.98	2.20	1.86	1.90	1.92
0.32	0.56	0.86	1.16	1.03[a]	1.35[b]	1.38[b]	1.46	1.49	1.51
Ag	Cd	In	Sn	Sb	Te	I			
1.49	1.56	1.65	1.86	1.97	2.15	2.41			
0.55	1.07	1.41	1.47	1.90	2.08	2.28			
Cs	Ba	La	Hf	Ta	W	Re	Os[b]	Ir[b]	Pt[b]
0.75	0.96	1.19	1.54	1.81	1.99	2.26	1.89	1.95	1.96
0.27	0.54	0.81	1.20	1.02	1.37[b]	1.44[b]	1.50	1.54	1.54
Au[c]	Hg	Tl[d]	Pb	Bi	Th[d]	U[d]			
1.55	1.66	1.65	1.81	1.93	1.40	1.44			
1.02	1.12	1.41	1.43	1.84	0.98	1.00			

[a]for $v = 3$, [b]for $v = 4$, [c]for $v = 3$, $\chi = 2.12$ (molecule) and 1.78 (crystal), [d]for $v = 1$, $\chi = 1.47$ (molecule) and 0.56 (crystal)

The satisfactory agreement among χ calculated by the four equations, allows to set up a scale of the averaged geometrical ENs for atoms in molecules in different valences (see [428]) which correspond to σ bonding (upper rows in Table 2.21). To calculate ENs of atoms with π bonds, the covalent radii of atoms for double and triple bonds must be used (Sect. 1.4). From these we obtain $\chi_{C=} = 2.2$, $\chi_{N=} = 4.2$, $\chi_{O=} = 5.2$ and $\chi_{S=} = 2.2$. Hence, formation of π bonds lowers the EN of C or S but increases that of N or O. The dependence of χ(C) on the bond order was established in [436–438].

Strictly speaking, it is incorrect to use the classical (molecular) ENs to interpret the structures and properties of crystalline inorganic compounds. Therefore, systems of ENs were derived specifically for atoms in crystals [428, 439]. Geometrical ENs

in this case should be defined in terms of crystal covalent radii (Sect. 1.4.3). Furthermore, it is necessary to take into account the dependence of χ on the bond order, $q = v/N_c$, which changes as N_c increases on transition from molecules to crystals. Since the bond order figures in the expression for energy, while Pauling's EN is proportional to $\sqrt{E}$, the data calculated by Eqs 2.92, 2.94 and 2.95 should be multiplied by $\sqrt{q}$ to obtain the atomic ENs for crystals. For elements of Groups 14 through 17, which have enough electrons to form four or six bonds in the coordination sphere, this correction is not needed. The lower lines of Table 2.21 list averaged crystalline atomic ENs for the group-number oxidation states, except for metals of Groups 5–10, where ENs refer to their usual oxidation states. For Au and Tl, the ENs also are given for the oxidation states +3 and +1, respectively [428].

Crystalline ENs were also determined by Phillips [440–444]. Assuming that the outer electrons of an atom can be treated as a Fermi gas, he obtained

$$\chi = 3.6\left(\frac{Z}{r}\right) f + 0.5 \tag{2.96}$$

where f is the screening factor according to Thomas−Fermi. Constants 3.6 and 0.5 were chosen for consistency with Pauling's ENs for C and N, while for elements of Groups 11–14 the obtained values were close to the crystalline ENs considered above. Li and Xue [445] calculated crystalline ENs using ionic radii (r_{ion}) for different coordination numbers, as

$$\chi^* = \frac{an^*\sqrt{\bar{I}}}{r_{ion}} + b \tag{2.97}$$

where n^* is the effective quantum number, $\bar{I}$ is the ionization potential of the given ion normalized by $I(\mathrm{H}) = 13.6$ eV, a and b are the constants. ENs calculated by Eq. 2.97 are presented in Table S2.21. Later it was proposed [446] to calculate crystalline ENs using covalent radii of elements in crystals, as

$$\chi^* = \frac{cn_e}{r_{cov}} \tag{2.98}$$

where c is the constant, n_e is the number of the valent electrons and r_{cov} is the crystalline covalent radius of the atom. The authors assumed that in any covalent bond the contributions of the two atoms are inversely proportional to their respective coordination numbers, N_{cA} and N_{cB}. Using the idea of EN equalization on bonding (see Sect. 2.4.6), the bond EN can be defined as the mean of the electron-holding energy of the bonded atoms,

$$\chi^*_{AB} = \left(\frac{\chi_A}{N_{cA}}\frac{\chi_B}{N_{cB}}\right)^{1/2}. \tag{2.99}$$

These ENs were used to rationalize the properties of new superhard materials. They show good agreement with Pettifor's 'chemical scale' of EN [447–449], which

Table 2.22 Recommended values of electronegativities for atoms in molecules

Li 0.95	Be 1.5	B 2.0	C 2.5	N 3.0	O 3.4	F 3.9			
Na 0.90	Mg 1.3	Al 1.6	Si 1.9	P 2.2	S 2.6	Cl 3.0			
K 0.80	Ca 1.05	Sc 1.35	Ti 1.75	V 2.0^{d}	Cr 2.3^{f}	Mn 2.6^{i}	Fe^{II} 1.5	Co^{II} 1.6	Ni^{II} 1.6
Cu 1.6^{a}	Zn 1.7	Ga 1.8	Ge 2.0	As 2.25	Se 2.5	Br 2.85			
Rb 0.75	Sr 1.0	Y 1.3	Zr 1.7	Nb 1.9^{e}	Mo 2.2^{g}	Tc 2.4^{j}	Ru^{IV} 2.0	Rh^{IV} 2.0	Pd^{IV} 2.1
Ag 1.65	Cd 1.6	In 1.7	Sn 1.9^{c}	Sb 2.1	Te 2.2	I 2.6			
Cs 0.70	Ba 0.95	La 1.3	Hf 1.7	Ta 1.9^{e}	W 2.2^{h}	Re 2.2^{j}	Os^{IV} 2.0	Ir^{IV} 2.0	Pt^{IV} 2.05
Au 1.85^{b}	Hg 1.8	Tl^{I} 1.2	Pb 1.9^{c}	Bi 2.1	Th^{IV} 1..5	U^{IV} 1.6			

$^{a}\nu = 1$, for $\nu = 2$ $\chi = 1.9$, $^{b}\nu = 1$, for $\nu = 3$ $\chi = 2.2$, $^{c}\nu = 4$, for $\nu = 2$ $\chi = 1.5$, $^{d}\nu = 5$, for $\nu = 3$ $\chi = 1.6$, $^{e}\nu = 5$, for $\nu = 3$ $\chi = 1.6$, $^{f}\nu = 6$, for $\nu = 3$ $\chi = 1.7$, $^{g}\nu = 6$, for $\nu = 4$ $\chi = 1.9$, $^{h}\nu = 6$, for $\nu = 4$ $\chi = 1.85$, $^{i}\nu = 7$, for $\nu = 3$ $\chi = 1.7$, $^{j}\nu = 7$, for $\nu = 4$ $\chi = 1.9$, $^{k}\nu = 7$, for $\nu = 4$ $\chi = 1.8$

adequately explains the structural properties of crystalline substances. These electronegativity data help to understand the fundamental difference in bonding between inorganic molecules and crystals. In the former, bonds vary widely in polarity; in the latter, bonds are less different and more polar, hence the ionic radii describe the interatomic distances well.

2.4.5 Recommended System of Electronegativities of Atoms and Radicals

As we have seen, values of EN obtained by different methods are consistent, this allows us to recommend the generalized systems of EN for molecules (Table 2.22) and crystals (Table 2.23), taking into account all the available data.

2.4.6 Equalization of Electronegativities and Atomic Charges

The principle of electronegativity equalization (ENE) proposed by Sanderson [211, 429], states that 'when two or more atoms with different electronegativity

Table 2.23 Recommended values of electronegativities for atoms in crystals

Li 0.55	Be 1.1	B 1.5	C 2.0[a]	N 2.9	O 3.2	F 3.5			
Na 0.50	Mg 0.9	Al 1.25	Si 1.5[a]	P 2.1	S 2.5	Cl 2.7			
K 0.40	Ca 0.7	Sc 1.0	Ti 1.3	V^{III} 1.3	Cr^{II} 1.0	Mn^{II} 1.0	Fe^{II} 1.05	Co^{II} 1.1	Ni^{II} 1.1
Cu 1.0	Zn 1.15	Ga 1.3	Ge 1.6[a]	As 2.0	Se 2.4	Br 2.6			
Rb 0.40	Sr 0.6	Y 0.95	Zr 1.2	Nb^{III} 1.2	Mo^{IV} 1.3	Tc^{IV} 1.4	Ru^{IV} 1.4	Rh^{IV} 1.4	Pd^{IV} 1.45
Ag 0.95	Cd 1.1	In 1.25	Sn 1.3	Sb 1.65	Te 1.9	I 2.3			
Cs 0.35	Ba 0.6	La 0.9	Hf 1.2	Ta^{III} 1.1	W^{IV} 1.3	Re^{IV} 1.5	Os^{IV} 1.4	Ir^{IV} 1.45	Pt^{IV} 1.5
Au 1.15	Hg 1.3	Tl 0.8	Pb 1.2	Bi 1.65	Th^{IV} 1.3	U^{IV} 1.4			

combine, they become adjusted to the same intermediate EN within the compound'. This approach became very popular and was applied in numerous empirical [213, 214, 433–435, 450–453] and quantum-chemical [454–472] studies. It allows fast calculation of atomic charges for large series of molecules and crystals, which agree well with *ab initio* calculations and experimental results. According to Parr, the EN of an atom can be treated as the chemical potential (see Eq. 2.83)

$$\chi = -\mu = -\left(\frac{\partial E}{\partial N}\right),$$

so the equalization principle corresponds to equalization of chemical potentials of atoms in a compound. The problem is that in isolated atoms the number of electrons, N, must be integer; hence E is not a continuous function of N. However, if Eq. 2.83 is applied to an individual atom in a molecule, fractional N are acceptable. The mathematics of treating $E(N)$ as being continuous function have been discussed [473].

A method of calculating the molecular electron compactness by Sanderson as

$$EC_{MX} = \sqrt{EC_M EC_X} \tag{2.100}$$

allows us to calculate the atomic charges in molecules by comparing the molecular and atomic EC. Sanderson has postulated (assuming the bond ionicity $q = 0.75$ in NaCl) that one positive or negative charge on atom A will change its EC by the increment $\Delta q = \pm a\sqrt{EC_A}$. The coefficient was estimated as 2.08, later corrected

to 1.56 [472]. Thereby it is possible to calculate *EC* for any cations and anions, and from them to calculate bond ionicities

$$q_A = \frac{EC_{AB} - EC_A}{EC_{A^+} - EC_A}. \tag{2.101}$$

Sanderson has applied this principle indiscriminately, assuming *EC* to equalize for all atoms even in such species as K_2SO_4, where K and S play quite different chemical roles and have different valences. Later it was suggested [474, 475] to equalize *EC* in separate bonded pairs of atoms, rather than throughout the entire molecule. It was also observed that total equalization in organic molecules would give different *EC* for isomers of the same composition, and a novel, rather efficient, method of calculating *EC* for isomers was proposed instead [451–453].

One must keep in mind that different scales of EN have different dimensionality, viz. energy (or potential) in Mulliken's scale, square root of energy in Pauling's scale, relative electron density in Sanderson's, whereas Parr et al. defined the absolute EN as the electronic chemical potential. There is no unique method to calculate EN, for every scale has its own calculation scheme, as it is done by Bratsch for Pauling's scale [213, 214]. ENs of atoms M and X in a M–X bonds can be equalized using the simple rule

$$\chi_M \times f = \frac{\chi_X}{f} \tag{2.102}$$

where f is the equalization factor, $f = \sqrt{\chi_X/\chi_M}$, and χ is the Mulliken electronegativity of atoms (see Eq. 2.80). EN equalization will influence the interatomic distance, decreasing the M size in the M–X separation:

$$r_{q+} = \frac{r_o}{f} \tag{2.103}$$

where r_o is the orbital radius of the electroneutral atom and r_{q+} is the radius of the same atom with a charge of $q+$ [476]. As the first approximation, the atomic radii of the metal atoms in molecules with fractional charges can be calculated by linear interpolation between the radii of neutral atoms and corresponding cations, which gives the bond ionicity (see Table 2.24) [477],

$$i = \frac{r_o - r_{q+}}{r_o - r_{cat}}. \tag{2.104}$$

Bond ionicities in solids can also be calculated in this manner, taking into account the real valence states of atoms. Table 2.25 contains the χ(X) for the tetragonal (te, sp^3) and octahedral (oc, sp^5) hybridization of bonds in structures of the ZnS and NaCl types, together with the standard Mulliken's values of χ(M), and the calculated r_{q+} and i_{cr}, in crystalline compounds MX [477].

Table 2.26 gives the comparison of the bond ionicities in molecules and crystals (i_{mol} and i_{cr}, from Tables 2.24 and 2.25) with the bond polarities calculated as $p = \mu/d$ from the dipole moments (μ) and bond lengths (d), and with the effective charges (e^*)

Table 2.24 Bond ionicities (as fractions of e) in MX molecules

M^I	H	F	Cl	Br	I	M^{II}	O	S	Se	Te
Li	0.40	0.57	0.49	0.46	0.44	Be	0.35	0.24	0.21	0.18
Na	0.44	0.62	0.54	0.51	0.48	Mg	0.43	0.32	0.29	0.25
K	0.58	0.76	0.68	0.65	0.62	Ca	0.61	0.49	0.46	0.42
Rb	0.63	0.83	0.74	0.71	0.68	Sr	0.69	0.57	0.54	0.50
Cs	0.71	0.91	0.82	0.78	0.75	Ba	0.80	0.67	0.64	0.59
Cu	0.29	0.54	0.42	0.38	0.35	Zn	0.40	0.26	0.22	0.17
Ag	0.37	0.68	0.53	0.48	0.44	Cd	0.54	0.37	0.33	0.27
Au	0.22	0.67	0.46	0.39	0.32	Hg	0.50	0.28	0.23	0.15

Table 2.25 Electronegativities (in Mulliken's scale), orbital atomic radii (in Å) and the bond ionicity in MX crystals

M	χ(M)	F_{oc} (15.82)[a]		Cl_{oc} (11.22)		Br_{oc} (10.52)		I_{oc} (9.51)	
		r_{q^+}	i_{cr}	r_{q^+}	i_{cr}	r_{q^+}	i_{cr}	r_{q^+}	i_{cr}
Li	3.005	0.691	0.64	0.821	0.55	0.848	0.53	0.891	0.50
Na	2.844	0.726	0.69	0.862	0.59	0.891	0.57	0.938	0.54
K	2.421	0.846	0.84	1.004	0.74	1.037	0.72	1.091	0.68
Rb	2.332	0.878	0.91	1.043	0.80	1.077	0.78	1.132	0.74
Cs	2.183	0.935	0.99	1.111	0.88	1.147	0.86	1.206	0.82
M	χ	F_{te} (17.63)		Cl_{te} (12.15)		Br_{te} (11.46)		I_{te} (10.26)	
Cu	4.477	0.600	0.68	0.723	0.54	0.744	0.52	0.787	0.47
Ag	4.439	0.645	0.85	0.777	0.68	0.800	0.65	0.846	0.59
Au	5.767	0.679	0.92	0.818	0.67	0.842	0.62	0.890	0.54
M	χ	O_{oc} (12.56)		S_{oc} (9.04)		Se_{oc} (8.64)		Te_{oc} (7.83)	
Mg	4.11	0.732	0.53	0.862	0.404	0.882	0.385	0.927	0.341
Ca	3.29	0.865	0.72	1.019	0.583	1.043	0.562	1.095	0.517
Sr	3.07	0.908	0.81	1.070	0.665	1.094	0.645	1.150	0.596
Ba	2.79	0.971	0.91	1.144	0.769	1.171	0.746	1.230	0.697
M	χ	O_{te} (14.02)		S_{te} (9.84)		Se_{te} (9.48)		Te_{te} (8.52)	
Be	4.65	0.599	0.49	0.715	0.36	0.728	0.35	0.768	0.30
Zn	4.99	0.635	0.57	0.758	0.41	0.773	0.39	0.815	0.33
Cd	4.62	0.680	0.74	0.811	0.55	0.826	0.53	0.872	0.46
Hg	5.55	0.708	0.77	0.846	0.52	0.862	0.49	0.909	0.40

[a] electronegativities of non-metals are given in parentheses

of atoms, determined by Szigeti's method (see Chap. 11). In each case, $i_c > i_{mol}$, in accordance with chemical experience, and the calculated i agrees qualitatively with the empirical values of p and e^*. At the same time, p varies non-monotonically, e.g. for fluorides as LiF < NaF > KF > RbF > CsF, and for iodides as LiI < NaI < KI < RbI > CsI, because of two competing effects: (i) EN of the metal atom decreases with the increase of its size, but (ii) bond ionicity is reduced by the polarizing influence of anions on cations, which increases with the cation size. For this reason, bond ionicity in CsX is always lower than in RbX.

Table 2.26 Calculated and empirical values of the bond ionicity in molecules and crystals MX

MX-type compounds									
M	Property[a]	X = F		X = Cl		X = Br		X = I	
Li	p, i_{mol}	0.84	0.57	0.73	0.49	0.70	0.46	0.65	0.44
	e^*, i_{cr}	0.81	0.64	0.77	0.55	0.74	0.53	0.54	0.50
Na	p, i_{mol}	0.88	0.62	0.79	0.54	0.79	0.51	0.71	0.48
	e^*, i_{cr}	0.83	0.69	0.78	0.59	0.75	0.57	0.74	0.54
K	p, i_{mol}	0.82	0.76	0.80	0.68	0.78	0.65	0.74	0.62
	e^*, i_{cr}	0.92	0.84	0.81	0.74	0.77	0.72	0.75	0.68
Rb	p, i_{mol}	0.78	0.83	0.78	0.74	0.77	0.71	0.75	0.68
	e^*, i_{cr}	0.97	0.91	0.84	0.80	0.80	0.78	0.77	0.74
Cs	p, i_{mol}	0.70	0.91	0.74	0.81	0.73	0.78	0.73	0.75
	e^*, i_{cr}	0.96	0.99	0.85	0.88	0.82	0.86	0.78	0.82
Cu	p, i_{mol}	0.69	0.54	0.53	0.42				
	e^*, i_{cr}		0.68	0.66	0.54	0.64	0.52	0.60	0.47
Ag	p, i_{mol}	0.65	0.68	0.55	0.53				
	e^*, i_{cr}	0.89	0.86	0.71	0.68	0.67	0.65	0.61	0.59
MO-type compounds[b]									
	M	Be	Mg	Ca	Sr	Ba	Zn	Cd	Hg
	i_{mol}	0.35	0.43	0.61	0.69	0.80	0.40	0.54	0.50
	i_{cr}	0.49	0.53	0.72	0.81	0.91	0.57	0.74	0.77
	$e^*/2$	0.55	0.59	0.62	0.64	0.74	0.60	0.59	0.57

[a] p and e^* in the left sub-columns, i_{mol} and i_{cr} in the right ones, [b] p are not given, because for oxides the measurements of μ are few and unreliable

Table 2.27 Electronegativities, empirical atomic radii (Å) and the bond ionicity in molecules MX

M	χ	H (7.176)		F (12.20)		Cl (9.35)		Br (8.63)		I (8.00)	
		r_{q+}	i_{mol}	r_{q+}	i_{mol}	r_{q+}	i_{mol}	r_{q+}	i_{mol}	r_{q+}	i_{mol}
Li	3.005	1.721	0.43	1.320	0.62	1.508	0.53	1.570	0.50	1.630	0.47
Na	2.844	1.907	0.50	1.463	0.69	1.671	0.60	1.739	0.57	1.807	0.54
K	2.421	2.108	0.60	1.617	0.80	1.847	0.70	1.923	0.68	1.997	0.64
Rb	2.332	2.178	0.64	1.670	0.83	1.908	0.74	1.986	0.71	2.062	0.68
Cs	2.183	2.289	0.68	1.755	0.88	2.005	0.79	2.087	0.76	2.168	0.73
Cu	4.477	1.493	0.31	1.145	0.58	1.308	0.46	1.361	0.41	1.414	0.37
Ag	4.439	1.612	0.40	1.236	0.73	1.412	0.58	1.470	0.52	1.527	0.47
Au	5.767	1.766	0.20	1.354	0.59	1.547	0.41	1.610	0.35	1.673	0.29

Since the atomic size is not uniquely defined (see Chap. 1), it is important to assess how much this uncertainty affects the calculations. Table 2.27 illustrates the calculation of the polarities using Pearson's ENs, the empirical radii of neutral isolated atoms [478] and their molecular cations (see Chap. 1). Comparison with the results in Table 2.24 reveals the average variation of 5.6 %, which is acceptable for the purposes of structural chemistry.

In conclusion of this section we should note that the concept of EN has been created by Pauling, first of all, to estimate the bond ionicity (i), i.e. the displacement of valence electrons towards one of the atoms. Experimental values of i(H–X), defined as the ratio of the dipole moment to the bond length, have been approximated by

Table 2.28 Dependence of bond ionicity (%) on differences of electronegativities

$\Delta\chi$	molecule	crystal	$\Delta\chi$	molecule	crystal	$\Delta\chi$	molecule	crystal
0.1	1	4	1.1	23	39	2.1	54	66
0.2	2	8	1.2	26	42	2.2	58	69
0.3	3	12	1.3	29	45	2.3	61	71
0.4	5	16	1.4	32	48	2.4	64	73
0.5	7	20	1.5	35	51	2.6	70	77
0.6	9	23	1.6	38	54	2.8	75	81
0.7	11	26	1.7	41	57	3.0	80	85
0.8	14	29	1.8	44	59	3.2	84	88
0.9	17	32	1.9	47	61	3.4	88	91
1.0	20	36	2.0	51	64	3.6	91	94

Pauling [479] as

$$i = 1 - e^{-A} \tag{2.105}$$

where $A = c\Delta\chi^2$ (in the beginning was accepted $c = 0.25$, and then 0.18). This formula agrees with observations and is often used in the structural and quantum chemistry to estimate bond ionicity in molecules. The change of the bond ionicity upon transition from molecules to a solid (which from the structural viewpoint is principally a change of N_c) can be considered either using 'crystalline EN' or changing an exponent in Eq. 2.105 by $1/N_c$ [18]. The values of i in molecules and crystals as functions of $\Delta\chi$, detrmined by all available experimental methods, are summarized in Table 2.28.

As noted in Chap. 1, a change of the atomic valence has only a slight ($\leq$10 %) effect on the bond energy. Apparently, an increase of the net charge on the metal atom in a polar molecule or in a solid, caused by the increasing valence, should correspondingly enhance the Coulomb component, which is the major part of the bond energy. However this does not occur. There are two alternative explanations of this: either the electric charges on two atoms act only within an orbital and charges of other bonds (accordingly, the total charge on the metal atom) have no effect on the strength of the given bond or, as the valence changes, atomic charges vary so that their product (hence, Coulomb's energy) is invariant. In [313] both alternatives were considered and the latter proved consistent with available experimental data, implying that the effective atomic charge varies in inverse proportion to the oxidation number of the atom. As a first approximation, we assume that as the valence v(M) in MX_n increases in the succession $1 \rightarrow 2 \rightarrow 3 \ldots \rightarrow 8$, the product of the effective charges of atoms M and X remains invariant. Expressing the charge of an atom in a single bond as e^*, we obtain:

$$(e^*)^2 = \frac{(ve^*)_M}{m}\frac{(e^*)_X}{m} \tag{2.106}$$

and, hence, $v = m^2$, where m is the number by which the effective atomic charge (bond ionicity) must be divided for the Coulomb energy to remain constant. Therefore, as

v(M) increases and the ligands remain the same, the effective charge of an atom decreases in proportion to $\sqrt{v}$, i.e. as $\sqrt{1} \rightarrow \sqrt{2} \rightarrow \sqrt{3} \ldots \rightarrow \sqrt{8}$. From here, if we know χ(M) and e^* of the M–X bond for one v (usually for a low-valence state, as these are better studied), we can find the bond ionicities for other valences and, using the dependence $i = f(\Delta\chi)$ and data from Table 2.28, to define χ. Such values, obtained for molecular and crystalline halides, are close to empirical ENs [313].

The values of i calculated from Eq. 2.105 on v(M) in different molecules, give the average (for 700 molecular halides and chalcogenides) of $e^* = \pm 0.5$e, in agreement with Pauling's famous Electroneutrality Rule [480, 481] which states that net charges of atoms in stable molecules and crystals should not exceed ± ½, even though later he softened this limitation to ±1 [475]. This principle later has been proved theoretically, confirmed experimentally and now plays a key role in the description of electronic structure of molecules and crystals.

2.5 Effective Charges of Atoms and Chemical Behavior

In this section we shall consider only the acid-basic properties and redox reactions, as the processes most closely connected with the electronic structure of substances. According to the Brönsted-Lewis theory, the acidity of oxygen-containing molecules depends on the effective charge on the oxygen atom. Sanderson [482] has shown that values of EC of oxides are inversely proportional to the pH of their aqueous solutions. Reed [483] has shown that pK of hydrates and amino-complexes of transition metals also depends on their atomic charges. The EN concept allows also to explain the acid-base properties of organic substances: higher acidity of aromatic compounds in comparison with aliphatic molecules is caused by higher positive charge on the H. For similar reasons, phenols are more acidic than aliphatic alcohols. Apart from the effects of the proximity of multiple bonds, the acidic properties of organic compounds with C–OH bonds depend on other atoms enhancing the EN of the carbon atom and, therefore, the effective positive charge on H. For this reason, Cl_3CCOOH is a stronger acid than H_3CCOOH.

Let us now consider redox reactions from the chemical bonding viewpoint, which is important for physical and structural chemistry. For this purpose we again must return to the concept of atomic charge. This term is used to describe two basically different things: the 'intrinsic charge of atom, q_i' (ICA) and the 'coordination charge of atom, Ω' (CCA). The first type is a deficit (positive charge) or an excess (negative charge) of electrons inside the closed shells of the bonded atoms in comparison with those in the isolated state. This q_i defines the Coulomb energy, is responsible for the IR absorption, causes the atomic polarization bands, and affects the binding energy of the internal electrons in the atom. However, what matters for redox reactions is the electron density in the interatomic space, i.e. the CCA [436]. Suchet, to highlight the same distinction, introduced the terms 'physical' and 'chemical' charges [484, 485]. The CCA of the M and X atoms in a MX crystal are

$$\Omega_M = +Z - cNN_c \text{ and } \Omega_X = -Z + NN_c, \tag{2.107}$$

where Z is the formal charge (valence), c and N are the covalency and the order (multiplicity) of the bonds, N_c is the coordination number. These Ω_M can be compared with the charges determined by X-ray spectroscopy, in which an electron is promoted from an internal shell and into the region of chemical bonding [54]. Table S2.21 contains the Ω_M of several transition metals in complex compounds, experimental and calculated by the EN method. According to these calculations, in crystalline compounds with low bond polarity, Ω_M can even become negative if $N_c > Z$. This prediction has been confirmed by physical methods, e.g. XRD studies of the electron density in PbS, PbSe, and PbTe have shown that within the Pb atom region, limited by $r = 1.66$ Å, there is a negative net charge of -0.4, -0.9, and $-1.1e$, respectively [486]. Gold compounds provide another proof. Thus, CsAu crystallizes in a CsCl-type structure and has $E_g = 2.6$ eV [487], indicating the ionic (rather than inter-metallic) character of the solid, with Au acting as an anion. Note also the structural similarity between K_3BrO and K_3AuO [488]. XRS studies [489] revealed that the AuL_I and AuL_{III} absorption edge energies monotonically decrease in the succession Au_2O_3, $AuCl_3$, AuCN, Au, CsAu and M_3AuO, hence in the last two compounds the charge of Au must be negative. Additional argument in favour of Au^- anion is the dissociation of $M_7Au_5O_2$ compounds into Au^+ and Au^- ions [490]. Besides, ESCA measurements [80, 491] have shown that the electronic structure of BaAu, $BaAu_2$ and $BaAu_{0.5}$ $Pt_{0.5}$ compounds can be formulated as $Ba^{2+}[e^-] \cdot [Au^-]$, $Ba^{2+}(Au^-)_2$ and $[Ba^{2+} \cdot 0.5e^-] \cdot [Au^-{}_{0.5} \cdot Pt^{2-}{}_{0.5}]$, respectively. Such behavior of Au is caused by its having the highest electron affinity of all metals ($A = 2.31$ eV). Platimum takes the second place with $A = 2.12$ eV and, accordingly, Cs_2Pt has the electronic structure $Cs_2{}^+ Pt^{2-}$, i.e. can be considered as an analogue of alkali metal chalcogenides, M_2X [492]. These recent results confirmed negative charges on Pt and Au, predicted from 1959 onwards on the basis of electronegativities [493–495]. This prediction has an important chemical corollary: oxidation of certain compounds of Au and Pt will rise the metal valence (without replacing 'anions') and yield a salt with mixed ligands, e.g.

$$PtI_2 + Cl_2 \rightarrow PtI_2Cl_2$$

For other metals the result will be substitution of the halogeno anions, which does not happen here because the halogen atoms are *not* anions. Similarly, all possible mixed tetra-halides and di-chalcogenides of Pt, tri-halides of Au, and di-halides of Cu were synthesized by Batsanov et al., see reviews in [356, 496]. Similar results were obtained for other high-EN metals, such as Hg, Tl, Sn, Mn, and by other researchers for Fe, Sb, Cr, Re, W, U, with a variety of ligands, such as halogens, chalcogens, SCN, N_3, NO_3, CO_3, SO_4 and methyl. Mixed halides of Pt^{IV} formed different isomers, depending on the order in which of halogens were added, e.g. PtX_2 has the motif of squares with shared vertices, but additional halogens complete these to octahedra in PtX_2Y_2; such compounds were named square-coordinate isomers [493]. TlSeBr also showed different properties depending on the route of the synthesis: Se + TlBr → Se=Tl–Br or 2Tl + Se_2Br_2 → 2 Tl–Se–Br, where Tl had different valences. The

Table 2.29 Change of atomic charges ($-\partial e^*/\partial P$, 10^{-4} GPa^{-1}) in crystals MX under $P = 10$ GPa

M^I	F	Cl	Br	I
Li	5.2	1.5	0	1.9
Na	7.0	2.4	1.5	4.0
K	11.7	5.9	5.4	4.1
Rb	10.6	3.9	2.4	1.7
Cs	10.4	6.7	8.3	7.6
Cu		−8.4	−4.7	6.9
Ag	−3.7	−5.6	−3.4	−6.6
Tl	−12.6	−12.5	−11.6	−10.9
M^{II}	O	S	Se	Te
Be	0	−1.6	1.6	3.7
Mg	0.9	0	0	5.6
Ca	3.7	2.2	3.3	7.5
Sr	7.0	5.9	7.2	9.6
Ba	16.5	16.5	18.0	24.6
Zn	0	−2.2	0	4.4
Cd	0	−2.8	0	5.9
Hg	−5.9	−2.8	0.6	10.0
Sn	−12.2	−2.8	0	0
Pb	−7.8	−3.7	0	4.7
Mn	−0.4	−4.0		1.6
M^{III}	N	P	As	Sb
B	0.6	9.7	4.7	
Al	0.6	5.3	0.6	0
Ga	2.2	9.4	2.5	2.8
In	6.9	10.0	1.9	1.9
La		15.3	14.7	14.4
Th	2.5	7.5		
U	0	3.4		

given structural formulae were confirmed by IR-spectroscopy and these compounds were named the valence isomers [497]. Dehnicke [498] discovered the reactions of 'chemical annihilation of charges'. For example, chloro ligands bear negative charges in $SbCl_5$ but positive in ClF, thus a reaction between these compounds yields $SbFCl_4$ and Cl_2. Similar reactions was carried out with hydrides, viz. $MBH_4 + HX = MBH_{4-n}X_n + H_2$ [499].

2.6 Change of Chemical Bond Character under Pressure

Distribution of the electron density in molecules and crystals depends on thermodynamic parameters. Spectroscopic methods [500–507] show that in crystals under high pressures, e^* usually decreases, although in AgI, TlI, HgTe, AlSb, GaN, InAs, PbF_2 it increases with pressure. High-pressure XRD studies of SiO_2 also indicated an increase of bond ionicity [508]. Studies of Se and GaSe under pressure showed that under compression, bonding electrons are displaced from covalent to intermolecular regions [502, 504] with shortening of the intra- and intermolecular distances.

However, difficulties of measurements of ε, n and Ω under high pressures, increasing anharmonicy of vibrations and deformation of IR absorption bands limits the choice of investigated substances and reduces the precision. Therefore, it is desirable to have independent methods of determining the effective charges of atoms in compressed crystals. It has been proposed [376, 509] to derive atomic charges in crystalline compounds under high pressures from the physical properties of the components of the system. Suppose that a reaction $M + X \rightarrow MX$ has the thermal effect Q at ambient thermodynamic conditions. For such system under pressure, the compression work (W_c) of the initial reagents and the final product can be calculated as

$$W_c = 9V_oB_o/\eta^2\{[\eta(1-x)-1\,]\exp[\,\eta(1-x)]+1\} \tag{2.108}$$

deduced by integrating the 'universal equation of state' (EOS) of Vinet-Ferrante [510]

$$P\,(x) = 3B_o\left[\frac{(1-x)}{x^2}\right]\exp\left[\eta\,(1-x)\right] \tag{2.109}$$

where V_o and V are the starting and final molar volumes, respectively; $x = (V/V_o)^{1/3}$; B_o is the bulk modulus; $\eta = 1.5(B_o'-1)$ and B_o' is the pressure derivative of B_o. Obviously, if W_c (mixture) – W_c (compound) > 0, then ΔW_c should be subtracted from the standard heat effect to yield the Q corresponding to high pressures, and *vice versa*. Usually $\Delta W_c > 0$, hence under pressure Q and $\Delta\chi$ decrease. The results of such approach qualitatively agree with the experiment, except for alkali hydrides, where calculations predict e^* to fall to 0 already at several tens of GPa while in fact no change of electronic structure occurred up to 100 GPa and even beyond [511, 512]. This contradiction can be resolved by taking into account that the compression work only partly goes into changing the chemical bonds [513]. Studies of A_2 molecules and chalcogens in condensed state, revealed that the compression initially (or mainly) results in the contraction of intermolecular distances and only after the bond equalization, i.e., the transformation of the molecular structure into a monatomic one, the covalent bonds begin to shorten. Therefore W_c calculated using Eq. 2.109 must be multiplied by the ratio of vdW energy (ΔH_s) to the A–A bond energy (E_b) in order to obtain the 'efficiency factor', Φ, of high pressure. For metals and semi-metals $\Phi = E_a/B_oV_o$ where E_a is the atomization energy and B_oV_o is the compression energy reduced to $P = 0$, and the product $\Phi \times W_c$ characterizes the compression energy (E_c) spent on altering the chemical bonding.

Thus, a comparison of E_c of mixtures and compounds allows to define a change of Q (and hence of the ENs of atoms) on variation of P, and from Table 2.28 to find the effective charges of atoms. The decrease of Q and the bond polarity under pressure is observed in crystals of AB-type, viz. Group 1– Group 17, Group 2– Group 16, Group 13–Group 15 compounds. Table 2.29 shows that $\partial e^*/\partial P$ for these crystals decrease by 10^{-4} to 10^{-3} GPa^{-1}. Szigeti's method predicts the same signs and similar absolute values, $\partial e^*/\partial P = 1$ to 3.3×10^{-4} GPa^{-1}. Remarkably, the increase of $Q(P)$ in CuX, AgX, and TlX under high pressures indicates an increase of polarity; unfortunately, corresponding data by Szigeti's method are not available.

Chalcogenides of bivalent metals can be divided into two classes: compounds of the Group 2 metals, crystallizing in the B1 structures, become less ionic under compression, while compounds of the Group 12 metals, crystallizing in the B3 structure, become more ionic. On compression of crystalline compounds of the Group 13 and Group 15 elements, the effective charges decrease in agreement with the results of Szigeti's method. Such behavior of substances under pressure can be explained assuming the additive character of compressibility of compounds. If the anion is softer than the cation (e.g. in halides of Cu, Ag and Tl) it will be compressed more strongly. The electronegativity of the anion, being inversely related to the atomic size, will increase and so will $\Delta\chi$, as $\chi_X > \chi_M$. In the case of softer cation (e.g., in alkali halides) χ_M on compression will increase more strongly than χ_X, and ionicity will decrease. However, under stronger compression, as calculated from the experimental EOS, ΔW_c does not change to $P \approx 100$ GPa and on further compression even decreases, as has been shown experimentally by the shock-wave technique [514]. Hence, the situation when $\Delta W_c = Q$, i.e. when the compound must dissociate to neutral atoms (elements), cannot be reached at any pressure. However, metallization of ionic crystals under pressure has been proven experimentally. As noted above, the volumes of MX crystals under P when $\Delta W_c = E_a$, i.e. when chemical bonds are destroyed and valence electrons delocalized, correspond to distances $d(\mathrm{M{-}X}) = r(\mathrm{M}^+) + r(\mathrm{X}^o)$ [515]. It means that if on compression of MX bond polarity decreases, as in alkali halides, ZnO and GaAs [517], then the donor of electrons must be M^o, since $I(\mathrm{M}) < I(\mathrm{X})$. If the bond polarity increases, as in SiC [516], SiO_2 [508], ZnS [63], or remains nearly constant, as in AlN and GaN [507], then X^- must be the donor, since $A(\mathrm{X}) < I(\mathrm{M})$.

The behavior of metals under pressure is remarkable. At ambient conditions, the metal atoms are ionized (by releasing itinerant electrons), but only partly so. Under compression the rest of the outer-shell electrons are 'squeezed out', and the degree of ionization of atoms increases. Ultimately, the atomic cores become cations and the crystal structure of a metal will correspond to a close-packing of cations. Stabilization of such a system requires very high pressures, to counterbalance the repulsion of cations. The parameters of such ultimate states have been calculated [517], see Table S2.22. The internuclear distances are expected to equal the sums of cationic radii.

There have been other attempts to estimate the change of EN and bond polarity under compression. The principal difficulty is that intra- and intermolecular distances change differently. In [518] the increase of covalent radii was calculated as the inverse of the reduction of vdW-radii of elements, and in [519] as being proportional to the ratio of energies of the chemical and vdW-bonds. For the metallic state, the following radii were obtained (Å): F 1.00, Cl 1.25, Br 1.41 and I 1.61, whereas experimental values are Br 1.41 Å [523] and I 1.62 Å [521]; for fluorine and chlorine data are unavailable. Certainly, this approach is not rigorous: it makes no allowance for polymorphic transformations, at which the material changes its properties by a jump. Nevertheless, the obtained values of $\partial e^*/\partial P$, summarized in Table S2.23, are close to experiemental results. The problem of changing bond lengths under pressure has been explored theoretically in terms the bond-valence model [522], yielding for

ionic crystals a quantitative dependence

$$\frac{\Delta d_o}{\Delta P} = 10^{-4}\frac{\Delta d_o^4}{B}, \tag{2.110}$$

where d_o is the initial bond length, $B = 1/b - 2/d_o$ and $b = 0.37$. This relationship allows to compute the effects of pressure on bond lengths and force constants.

2.7 Conclusions

The formation of chemical bonds in molecules or crystals release the energy equal to a few tenths, and more often not exceeding 0.1, of the ionization potentials of the individual (isolated) atoms involved. The ionization potentials of atoms in molecules decrease by similar amounts compared to the free state. Bond energies themselves are determined by the ionization potentials of the isolated atoms, according to Mulliken's theory. Thus the major part of the energy of any chemical system in any aggregate state depends on the nature of the component atoms, and the remaining energy is mostly defined by the immediate atomic environment, or the short-range order in a crystal structure. Inversely the ionization potential, i.e. the electron energy of an atom in molecule or crystal, differs but slightly from that in isolated state. Therefore, in most cases it is a good approximation to regard a molecule as a combination of atoms and to account for all interactions as perturbations. From this viewpoint the geometrical structure of substances will be discussed in the next chapters.

Appendix

Supplementary Tables

Experimental data from the *Handbook of Chemistry and Physics*, 88th edn (2007–2008) are presented without reference, otherwise the references to original papers are given.

Table S2.1 'XRD' effective atomic charges in silicates and complex compounds

± A	Be_2SiO_4	Mg_2SiO_4	Mn_2SiO_4	Fe_2SiO_4	Co_2SiO_4
+ M	0.83	1.75	1.35	1.15	1.57
+ Si	2.57	2.11	2.28	2.43	2.21
– O	1.06	1.40	1.25	1.19	1.29
± A	$MgCaSi_2O_6$	$Mg_2Si_2O_6$	$Fe_2Si_2O_6$	$Co_2Si_2O_6$	$LiAlSi_2O_6$
+ M	1.42	1.82	1.12	0.95	1.0, 1.74
+ Si	2.56	2.28	2.19	2.28	1.8
– O	1.33	1.37	1.10	1.08	1.06
± A	$Al_2SiO_4F_2$	$CaAl_2Si_3O_{10}$	$LiFePO_4$	NaH_2PO_4	
+ M	1.53	2, 1.90	1, 1.35	0.2, 0.6	
+ Si	1.75	1.84	0.77	1.8	
– O	1.00	1.14	0.78	0.8	
± A	K_2NiF_4	Cs_2CoCl_4	K_2PdCl_4	K_2PtCl_4	
+ A	1.82	0.7	0.5	1.0	
– X	0.95	0.7	0.6	0.75	
± A	K_2ReCl_6	K_2PdCl_6	K_2OsCl_6	K_2PtCl_6	
+ A	1.6	1.97	2.5	1.88	
– Cl	0.6	0.66	0.75	0.65	

Complex	A	e^*	Complex	A	e^*
$[Co(NH_3)_6]$	N	–0.62	$[Cr(CN)_6]$	C	+0.22
	H	+0.36		N	–0.54
	Co	–0.49		C	–0.38

Table S2.2 Bond metallicity in crystalline halides MX

M^I	F		Cl		Br		I	
	m_1	m_2	m_1	m_2	m_1	m_2	m_1	m_2
Li	0.06	0.07	0.12	0.10	0.14	0.11	0.17	0.12
Na	0.04	0.05	0.11	0.08	0.10	0.09	0.13	0.11
K	0.03	0.03	0.06	0.07	0.08	0.08	0.10	0.09
Rb	0.02	0.03	0.06	0.06	0.08	0.07	0.10	0.09
Cs	0.02	0.02	0.05	0.05	0.06	0.06	0.08	0.08
Cu			0.12	0.08	0.15	0.09	0.18	0.11
Ag	0.06	0.05	0.12	0.09	0.14	0.10	0.18	0.11
Tl	0.06	0.05	0.12	0.10	0.14	0.12	0.18	0.14
M^{II}	O		S		Se		Te	
Be	0.15	0.12	0.24	0.14	0.27	0.17	0.32	0.18
Mg	0.09	0.10	0.15	0.14	0.19	0.16	0.23	0.17
Ca	0.07	0.09	0.13	0.13	0.15	0.15	0.19	0.17

Table S2.2 (continued)

M^I	F		Cl		Br		I	
	m_1	m_2	m_1	m_2	m_1	m_2	m_1	m_2
Sr	0.06	0.07	0.12	0.12	0.13	0.13	0.17	0.16
Ba	0.06	0.06	0.11	0.11	0.13	0.12	0.16	0.14
Zn	0.13	0.11	0.17	0.15	0.20	0.17	0.26	0.19
Cd	0.12	0.11	0.16	0.15	0.19	0.16	0.25	0.19
Hg	0.15		0.20	0.18	0.26	0.20	0.30	0.23
Sn	0.12	0.10	0.16	0.15	0.19	0.16	0.25	0.19
Pb	0.12	0.11	0.16	0.16	0.19	0.18	0.25	0.21
Cr			0.18	0.14	0.21	0.15	0.26	0.18
Mn	0.11	0.09	0.18	0.12	0.20	0.13	0.25	0.17
Fe	0.13	0.10	0.20	0.15	0.23	0.17	0.29	0.20
Co	0.13	0.11	0.21	0.17	0.24	0.18	0.30	0.21
M^{III}	N		P		As		Sb	
B	0.25	0.18	0.38	0.21	0.44	0.23		
Al	0.20	0.18	0.32	0.24	0.38	0.28	0.40	0.26
Ga	0.21	0.18	0.35	0.24	0.42	0.28	0.44	0.28
In	0.21	0.13	0.34	0.19	0.41	0.23	0.44	0.22
Sc	0.15	0.15	0.26	0.22	0.32	0.26	0.33	0.26
Y	0.13	0.13	0.23	0.21	0.29	0.25	0.31	0.25
La	0.12	0.12	0.22	0.20	0.28	0.24	0.29	0.24
U	0.16	0.14	0.28	0.22	0.33	0.26	0.36	0.26

Table S2.3 Dissociation energies of diatomic molecules (kJ/mol) ($E(M_2)$, kJ/mol: Nb_2 513, Tc_2 330, Re_2 432, Os_2 415, Ir_2 361)

M	Molecules					
	MF	MCl	MBr	MI	MH	M_2
H	570	431	366	298	436	436
Li	577	469	419	345	238	105
Na	477	412	363	304	186	74.8
K	489	433	379	322	174	53.2
Rb	494	428	381	319	173	48.6
Cs	517	446	389	338	175	43.9
Cu	427	375	331	289	255	201
Ag	341	311	278	234	202	163
Au	325	302[a]	286[a]	263[a]	292	226
Be	573	434	316	261	221	11.1[b]
Mg	463	312	250	229	155[A]	4.82[b]
Ca	529	409	339	285	163	13.1b[b]
Sr	538	409	365	301	164	12.94[b]
Ba	581	443	402	323	192	19.5[b]
Zn	364	229	180	153	85.8	3.28[c]
Cd	305	208	159	97.2	69.0	3.84[c]
Hg	180	92.0	74.9	34.7	39.8	4.41[c]
B	732	427	391	361	345	290
Al	675	502	429	370	288	133
Ga	584	463	402	334	276	106

Table S2.3 (continued)

M	Molecules					
	MF	MCl	MBr	MI	MH	M_2
In	516	436	384[d]	307	243	82.0
Tl	439	373	331	285	195	59.4
Sc	599	435[e]	365[e]	300[e]	205	163
Y	685	523	481	423		270
La	659	522	446	412		223[E]
C	514	395	318	253	338	618
Si	576	417	358	243	293	320[f]
Ge	523	391	347	238[g]	263	261[f]
Sn	476	350	337	235	264	187
Pb	355	301	248	184	158[h]	83[f]
Ti	569	405	373	262	205	118
Zr	627	530	420	298[i]	312	298
Hf	650			328[j]		328
N[I]	320	321	254	203	331[k]	945
P[I]	459	342	294	243	293[k]	489
As[I]	463	336	280	240	270[k]	386
Sb[I]	430	292	240	183	260[k]	302
Bi[I]	366	285	181	124	212[k]	204
V	590	477	439		209	269
Ta	573	544				390
O[I]	234	269	241	237	428	498
S[I]	344	264	241	194	351	425
Se[I]	317	227	186	158	300	330
Te[I]	326	209	166	134	256	258
Cr	523	378	328	287	190	152
Mo	464		313		211	436
W	597[m]	458[m]	396[m]	328[m]		666
F	159	261	280	272	570	155
Cl	261	243	219	211	431	240
Br	280	217	193	179	366	190
I	272	211	179	151	298	149
Mn	445	338	314	283	251	61.6
Fe	447	330	298[o]	241[P]	148[q]	118
Co	4315	338	326	285[P]	190[q]	163[n]
Ni	437	377	360	293[P]	243[q]	200[n]
Ru	402				234[q]	193
Rh					247[q]	236
Pd					234[q]	> 136
Pt	582				352[q]	307
Th	652	489	364	336		284
U	648	439	377	299		222

[a][2.1], [A][2.2], [b][2.3], [c][2.4, 2.5], [d][2.6], [e][2.7], [E][2.8], [f][2.9], [g][2.10], [h][2.11], [i][2.12], [I][2.13], [j][2.14], [k][2.15, 2.16], [l][2.17], [m][2.18], [n][2.19], [o][2.20], [P][2.21], [q][2.22]

Table S2.4 Dissociation energies of MZ molecules (kJ/mol)

M	Z						
	O	S	Se	Te	N	P	C
Cu	287	274	255	230			
Ag	357	279	210	196			
Au	233	254	251	237			
Be	440[a]	372					
Mg	338[a]	234					
Ca	383[a]	335					
Sr	415[a]	338	251				
Ba	559[a]	418					
Zn	289[a]	225	171	118			
Cd	231[a]	208	128	100			
Hg	269	217	144	89			
B	809[a]	577	462	354	378	347	448
Al	511[a]	332	318	268	278	217	268
Ga	354[a]			265		230	
In	316[a]	288	245	215		198	
Tl	213[a]					209	
Sc	671	477	385	289	464		444
Y	714	528	435	339	477		418
La	799	573	477	381	519		462
C	1076	713	590	564	750	508	607
Si	800	617	534	429	437		452
Ge	660	534	444[b]	409[b]			456
Sn	528	467	401	338			
Pb	374	343	303	250			
Ti	668	491	381	289	476		423
Zr	766	572			565		496
Hf	790				590		540
N	631	467	370		945	617	754
P	599	442	364	298	617	489	507
As	481[c]	389[c]	352[c]	312[c]	489	433	382
Sb	434	379		277	460	357	
Bi	337	315	280	232		282	
V	637	449	347		523		423
Nb	726						524
Ta	839	670			607	611	
O	498	518	465	376	631	589	1076
S	518	425	371	335	464	444	714
Se	430	371	330	293	370	364	590
Te	377	339	2932	258		298	
Cr	461	331			378	378	
Mn	362	301	239				
Th	877				577	372	453
U	755	528			531	293	455

M	Mo	W	Tc	Re	Fe	Co	Ni
D_{MO}	502	720	548	627	407	384	366

M	Pd	Os	Ir	Pt	Ru	Rh	
D_{MO}	381	575	414	415	528	405	

Table S2.4 (continued)

M	Z						
	O	S	Se	Te	N	P	C
M	Fe	Co	Ni	Pt			
D_{MS}	329	331	318	407[d]			
M	Mo	Tc	Fe	Ni	Ru	Rh	
D_{MC}	482	564	376[e]	337	648	580	
M	Pd	Os	Ir	Pt			
D_{MC}	436	608	631	610			

[a][2.23], [b][2.24], [c][2.25], [d][2.26], [e][2.27]

Table S2.5 Dissociation energies D (kJ/mol) of M_2^+ cations

M	D	M	D	M	D	M	D
Ag	168	Cr	129	Li	132	S	522.5
Al	121	Cu	155	Mg	125	Sb	264
Ar	116	Cs	62.5	Mn	129	Se	413
As	364	F	325.5	Mo	449	Si	334
Au	234.5	Fe	272	N	844	Sn	193
B	187	Ga	126	Na	98.5	Sr	108.5
Be	196.5[a]	Ge	274	Nb	577	Ta	666
Bi	199	H	259.5	Ne	125	Te	278
Br	319	He	230	Ni	208	Ti	229
C	602	Hg	134	O	648	Tl	22
Ca	104	I	263	P	481	V	302
Cd	122.5	In	81	Pb	214	Zr	407
Cl	386	K	80	Pd	197	Xe	99.5
Co	269	Kr	84	Pt	318	Y	281
		La	276[b]	Rb	75.5	Zn	60

[a][2.28], [b][2.8]

Table S2.6 Ionization potentials (eV) for M and M^+ atoms

M	I_1(M)	I_2(M)	I_2/I_1
Be	9.32	18.21	1.95
Mg	7.65	15.04	1.97
Ca	6.11	11.87	1.94
Sr	5.69	11.03	1.94
Ba	5.21	10.00	1.92
Zn	9.39	17.96	1.91
Cd	8.99	16.91	1.88
Hg	10.44	18.76	1.80

Table S2.7 Ionization and dissociation energies (kJ/mol) for metal atoms and molecules

A	I(A)	$I(A_2)$	$E(A_2)$	$E(A_2^+)$	E_a(A)	0.9 Φ(A)
Li	520	493	105	132	159	207
Na	496	472	75	99	107	204
K	419	392	53	80	89	193
Rb	403	376	49	76	81	188
Cs	376	357	44	63	76.5	157

Table S2.8 Dissociation energies D (kJ/mol) of MH^+ and MO^+ cations

MH^+	D	MH^+	D	MO^+	D	MO^+	D
CuH	93	CrH	136	LiO	39	VO	582
AgH	43.5	MoH	176	NaO	37	NbO	688
AuH	144	WH	222	KO	13	TaO	787
BeH	307	OH	488	RbO	29	NO	115
MgH	191	SH	348	CsO	59	PO	791
CaH	284	SeH	304	CuO	134	AsO	495
SrH	209	TeH	305	AgO	123	BiO	174
ZnH	216	MnH	202	BeO	368	CrO	276
HgH	207	TcH	198	MgO	245	MoO	496
ScH	235	ReH	225	CaO	348	WO	695
YH	260	HH	259	SrO	299	SO	524
LaH	243	ClH	453	BaO	441	TeO	339
BH	198	BrH	379	ZnO	161	Re	435
TiH	227	IH	305	ScO	689	FO	335
ZrH	219	FeH	211	YO	698	ClO	468
CH	398	CoH	195	LaO	875	BrO	366
SiH	317	NiH	158	BO	326	IO	316
GeH	377	RuH	160	AlO	146	FeO	343
VH	202	RhH	165	GaO	46	CoO	317
NbH	220	PdH	208	TiO	667	NiO	276
TaH	230	OsH	239	ZrO	753	RuO	372
NH	≥ 436	IrH	306	HfO	685[a]	RhO	295
PH	275	UH	284	CO	811	PdO	145
AsH	291			SiO	478	OsO	418
				GeO	344	IrO	247
				SnO	281	PtO	318
				PbO	247	ThO	848[a]

[a] [2.29]

Table S2.9 Average bond energies (kJ/mol) (Subscripts p, s and t indicate primary, secondary and tertiary carbon atoms; 1 and 2 indicate the number of atoms of a given type, connected to the atom under consideration; superscript indicate the element bonded to the polyvalent atom)

A–B	E(A–B)	A–B	E(A–B)	A–B	E(A–B)
Li—Be	87.4	P=S	441	$^{F}(C—H)_t$	398
Li—B	101	P—F	483	$^{Cl}(C—H)_p$	405
Li—C	126	P—C	331	$^{Cl}(C—H)_s$	403
Li—N	243	O—O	192	$^{Cl}(C—H)_t$	401
Li—O	406	S—S	266	$^{Br}(C—H)_p$	406
Be—Be	119	P=O	643	$^{Br}(C—H)_s$	404
Be—B	186	^{Li}(Be—H)	297	$^{Br}(C—H)_t$	405
Be—C	232	^{BeC}(Be—H)	298	$^{I}(C—H)_p$	409
Be—N	340	$^{CF}(Be—H)_1$	299	$^{I}(C—H)_{s,t}$	406
Be—O	488	^{N}(Be—H)	302	$^{Li}(N—H)_1$	384
Be—F	653	^{O}(Be—H)	311	$^{Li}(N—H)_2$	395
B—B	286	$^{Li}(B—H)_1$	383	$^{Be}(N—H)_1$	400
B—C	323	$^{Li}(B—H)_2$	386	$^{Be}(N—H)_2$	401
B—N	443	$^{Be}(B—H)_1$	375	$^{B}(N—H)_1$	395
B—O	544	$^{Be}(B—H)_2$	378	$^{B}(N—H)_2$	400
B—F	659	$^{B}(B—H)_1$	382	$^{C}(N—H)_1$	380

Table S2.9 (continued)

A–B	E(A–B)	A–B	E(A–B)	A–B	E(A–B)
B—Cl	489	^{B}(B—H)$_2$	381	^{C}(N—H)$_2$	383
B—Br	414	^{C}(B—H)$_1$	376	^{N}(N—H)$_1$	373
B—I	334	^{C}(B—H)$_2$	375	^{N}(N—H)$_2$	378
C—C	357	^{C}(B—H)$_3$	375	^{P}(N—H)$_1$	380
C=C	579	^{N}(B—H)$_1$	379	^{P}(N—H)$_2$	390
C≡C	786	^{N}(B—H)$_2$	386	^{O}(N—H)$_1$	371
C—N	319	^{O}(B—H)$_1$	378	^{O}(N—H)$_2$	375
C=N	571	^{O}(B—H)$_2$	374	^{S}(N—H)$_1$	390
C≡N	872	^{F}(B—H)$_1$	372	^{S}(N—H)$_2$	391
C—P	271	^{Li}(C—H)$_p$	433	^{F}(N—H)$_1$	369
C=P	448	^{Li}(C—H)$_s$	428	^{F}(N—H)$_2$	370
C—O	383	^{Li}(C—H)$_t$	426	^{C}(P—H)$_1$	314
C=O	744	^{Be}(C—H)$_p$	431	^{C}(P—H)$_2$	318
C—S	301	^{Be}(C—H)$_s$	428	^{N}(P—H)$_1$	309
C—F	486	^{Be}(C—H)$_t$	426	^{N}(P—H)$_2$	311
C—Cl	359	^{B}(C—H)$_p$	425	^{P}(P—H)$_1$	320
C—Br	300	^{B}(C—H)$_s$	424	^{P}(P—H)$_2$	317
C—I	234	^{B}(C—H)$_t$	423	^{O}(P—H)$_1$	303
Si—C	295	^{C}(C—H)$_p$	411	^{O}(P—H)$_2$	305
Si—F	606	^{C}(C—H)$_s$	408	^{S}(P—H)$_1$	310
Si—Cl	414	^{C}(C—H)$_t$	405	^{S}(P—H)$_2$	312
Si—Br	343	^{N}(C—H)$_p$	406	^{F}(P—H)$_1$	298
Si—I	262	^{N}(C—H)$_s$	402	^{F}(P—H)$_2$	301
N—N	212	^{N}(C—H)$_t$	402	^{Cl}(P—H)$_1$	303
N=N	515	^{P}(C—H)$_p$	413	^{Cl}(P—H)$_2$	306
N≡N	945	^{P}(C—H)$_s$	411	^{Li}(O—H)	454
N—P	265	^{P}(C—H)$_t$	410	^{Be}(O—H)	471
N=P	450	^{O}(C—H)$_p$	401	^{B}(O—H)	466
N—O	223	^{O}(C—H)$_s$	399	^{C}(O—H)	452
N=O	541	^{O}(C—H)$_t$	397	^{S}(O—H)	458
N—S	224	^{S}(C—H)$_p$	409	^{F}(O—H)	433
N=S	413	^{S}(C—H)$_s$	407	^{N}(S—H)	355
P—P	211	^{S}(C—H)$_t$	404	^{P}(S—H)	362
P=P	360	^{F}(C—H)$_p$	399	^{O}(S—H)	346
P—O	358	^{F}(C—H)$_s$	398	^{S}(S—H)	354

Table S2.10 Additive energies of π-bonds (kJ/mol)

X	Y	*a*	*b*	*c*	X	Y	*a*	*c*
C	C	222	291	272	N	N	303	251
C	Si	57.5	151	159	N	P	185	184
C	N	252	338	264	N	O	317	259
C	P	177	206.5	180	N	S	189	176
C	S	220	233	218	P	P	149	142
Si	Si	36	101	105	P	O	285	222
Si	N	31	155	151	P	S	180	167
Si	P	95	124	121	O	O	306	306
Si	O	240	233.5	209	O	S	249	249
Si	S	168	182.5	209	S	S	159.5	159.5

[a][2.30–2.33], [b][2.34], [c][2.35]

Table S2.11 Reduced Madelung constants

Structure type	k_M	Structure type	k_M	Structure type	k_M
$AlBr_3$	1.199	$BeCl_2$	1.362	MnF_2, TiO_2	1.589
BCl_3	1.226	SiF_4	1.432	PbF_2, SnO_2	1.602
SnI_4	1.236	CdI_2	1.455	CuCl, ZnS	1.638
$AuCl_3$	1.245	SiO_2	1.467	Y_2O_3	1.672
V_2O_5	1.266	Cu_2O	1.481	CaF_2, ZrO_2	1.680
HgI	1.277	$CrCl_2$	1.500	NiAs	1.733
TlF	1.318	BN	1.528	NaCl, MgO	1.748
AsI_3	1.334	BeO	1.560	CsCl	1.763

Table S2.12 Band gaps (eV) in MX_2 type compounds

M	X				M	X			
	F	Cl	Br	I		O	S	Se	Te
Mg	14.5[a]	9.2	8.2		Ti	3.1[c]	2.0	1.6	1.0
Ca	12.5[b]	6.9		6.0	Zr	5.2[d]	2.1		
Sr	11.0[b]	7.5			Hf	5.5[e]	1.9[f]	1.1	0.4[f]
Ba	9.5[b]	7.0			Si	9.0[c]		1.7	1.0
Zn				4.75[g]	Ge	5.4[c]	3.4	2.5	1.2
Cd	8.7[h]	5.7	4.5	3.5	Sn	3.7[c]	2.1[i]	1.02[i]	
Hg		4.4	3.6[j]	2.35[k]	Pb	1.6	1.0		
Sn		3.9	3.4	2.4	Mo		1.9	1.2[l]	0.9
Pb		4.0	3.1[m]	2.3[n]	W		1.8	1.4	0.1
Mn[o]	10.2	8.3	7.7	5.2	Re		1.5[p]	1.35[p]	
Fe[o]		8.3	7.4	6.0	Ru		1.4[p]	0.9[p]	
Co[o]		8.3	7.4	6.0	Pt	≥ 3.5[q]			
Ni[o]	8.8	8.4	7.5	6.0	U	5.5			

[a][2.36], [b][2.37], [c][2.38], [d][2.39], [e][2.40], [f][2.41, 2.42], [g][2.43], [h][2.44], [i][2.45], [j][2.46], [k][2.47, 2.48], [l][2.49], [m][2.50], [n][2.51], [o][2.52], [p][2.53], [q][2.54]

Table S2.13 Band gaps (eV) in M_nX_m type compounds

M_2X_3	E_g	M_2X_3	E_g	M_nX_m	E_g	M_nX_m	E_g
Sc_2O_3	5.7[a]	Tl_2O_3	2.2	Li_3N	2.2[p]	SbI_3	2.3
Sc_2S_3	2.8	Tl_2Te_3	0.7[h]	Li_2O	8.0[q]	$CrCl_3$	9.5[χ]
Y_2O_3	5.6	As_2O_3	4.5	Cu_2O	2.2[r]	$CrBr_3$	8.0[χ]
La_2O_3	5.4	As_2S_3	2.4[i]	Cu_2S	0.34[s]	ZrS_3	2.5[ϕ]
La_2S_3	2.8	As_2Se_3	1.7	Cu_2Se	1.3[t]	$ZrSe_3$	1.85[ϕ]
La_2Se_3	2.3[b]	As_2Te_3	0.8	Cu_2Te	0.67[u]	HfS_3	2.85[ϕ]
La_2Te_3	1.4	Sb_2O_3	3.25[a]	Ag_2S	1.14[v]	$HfSe_3$	2.15[ϕ]
B_2S_3	3.7[c]	Sb_2S_3	1.7[i]	Ag_2Se	1.58[w]	MoO_3	3.8[a]
Al_2O_3	9.5	Sb_2Se_3	1.2	TlS	0.9[x]	WO_3	2.6[λ]
Al_2S_3	4.1	Sb_2Te_3	0.2[j]	Tl_2S_3	1.0[x]	UO_3	2.3[μ]
Al_2Se_3	3.1	Bi_2O_3	2.85[k]	TlS_2	1.4[x]	TeO_2	3.8[a]
Al_2Te_3	2.4	Bi_2S_3	1.6[i]	Tl_2S_5	1.5[x]	MnS_4	3.7[η]
Ga_2O_3	4.9[d]	Bi_2Se_3	0.8[l]	GeS	1.6[y]	$MnSe_4$	3.3[η]
Ga_2S_3	3.2	Bi_2Te_3	0.2[m]	SiC	3.1[z]	$MnTe_4$	3.2[η]

Table S2.13 (continued)

M_2X_3	E_g	M_2X_3	E_g	M_nX_m	E_g	M_nX_m	E_g
Ga_2Se_3	1.75[e]	Cr_2O_3	1.6	GaSe	2.0[α]	$NbCl_5$	2.7[φ]
Ga_2Te_3	1.2[f]	Cr_2S_3	0.9	MgH_2	5.6[β]	$NbBr_5$	2.0[φ]
In_2O_3	3.3[a]	Cr_2Se_3	0.1	YH_3	2.45[γ]	NbI_5	1.0[φ]
In_2S_3	2.6[g]	Fe_2O_3	2.2[n]	LaF_3	9.7[δ]	V_2O_5	2.5[π]
In_2Se_3	1.5	Fe_2Se_3	1.2	GaF_3	9.8[ε]	Nb_2O_5	3.4[a]
In_2Te_3	1.2[f]	Rh_2O_3	3.4[o]	InF_3	8.2[κ]	Ta_2O_5	4.0[a]

[a][2.38, 2.41, 2.42], [b][2.55], [c][2.56], [d][2.57], [e][2.58], [f][2.59], [g][2.60], [h][2.61], [i][2.62], [j][2.63, 2.64], [k]for α-Bi_2O_3 (for β-Bi_2O_3 $E_g = 2.58$ eV) [2.65], [l][2.66], [m][2.67], [n][2.68], [o][2.69], [p][2.70], [q][2.71], [r][2.72, 2.73], [s][2.74], [t][2.75], [u][2.76], [v][2.77], [w]glass [2.78], [x][2.79], [y][2.80, 2.81], [z][2.82], [α][2.83], [β][2.84], [γ][2.85, 2.86], [δ][2.39], [ε][2.87], [κ][2.88], [χ][2.89], [φ][2.90], [λ][2.91], [μ][2.92], [η][2.93], [φ][2.94], [π][2.95]

Table S2.14 Additive band gaps (eV) of elements

Li	Be	B	C	N	O	F			
0.4	0.8	1.3	5.5	7.0	6.5	10			
Na	Mg	Al	Si	P	S	Cl	Ne[a]		
−0.3	+0.3	−0.1	+1.2	2.6	2.6	5.2	21.7		
K	Ca	Sc	Ti	V	Cr	Mn	Fe	Co	Ni
−0.8	−0.5	−0.4	−0.3	−0.3	−0.3	−0.2	−0.1	−0.1	−0.1
Cu	Zn	Ga	Ge	As	Se	Br	Ar[a]		
−0.2	+0.2	−0.5	+0.7	+1.2	+1.8	+1.9	14.2		
Rb	Sr	Y	Zr	Nb	Mo	Tc	Ru	Rh	Pd
−1.0	−0.8	−0.7	−0.6	−0.6	−0.6	−0.5	−0.5	−0.5	−0.4
Ag	Cd	In	Sn	Sb	Te	I	Kr[a]		
−0.5	−0.3	−0.8	+0.1	+0.1	+0.35	+ 1.3	11.6		
Cs	Ba	La	Hf	Ta	W	Re	Os	Ir	Pt
−1.2	−1.0	−0.9	−0.8	−0.7	−0.6	-0.6	−0.5	−0.5	−0.5
Au	Hg	Tl	Pb	Bi	P	At	Xe[a]		
−0.5	−0.3	−0.9	−0.7	−0.2	0	+0.7	9.3		

[a][2.96]

Table S2.15 Thermochemical electronegativities of elements. From top to bottom: Pauling [2.97], Allred [2.98], Batsanov [2.99], Smith [2.100]

Li	Be	B	C	N	O	F			
1.0	1.5	2.0	2.5	3.0	3.5	4.0			
0.98	1.57	2.04	2.55	3.04	3.44	3.98			
1.0	1.4	2.0	2.6	2.7	3.2	3.7			
		1.80	2.59	3.11	3.44	3.84			
Na	Mg	Al	Si	P	S	Cl			
0.9	1.2	1.5	1.8	2.1	2.5	3.0			
0.93	1.31	1.61	1.90	2.19	2.58	3.16			
0.9	1.3	1.6	2.0	2.15	2.6	3.2			
			1.71	1.98	2.50	3.06			
K	Ca	Sc	Ti	V	Cr	Mn	Fe^{II}	Co^{II}	Ni^{II}
0.8	1.0	1.3	1.5	1.6	1.6	1.5	1.8	1.8	1.9
0.82	1.00	1.36	1.54	1.63	1.66	1.55	1.83	1.88	1.91
0.7	1.0	1.35	1.7	1.8	1.9	1.9	1.6	1.65	1.7
Cu	Zn	Ga	Ge	As	Se	Br			
1.8	1.6	1.6	1.8	2.0	2.4	2.8			
1.90	1.65	1.81	2.01	2.18	2.55	2.96			
1.5	1.6	1.75	2.1	2.1	2.5	3.0			
			1.93	2.06	2.37	2.86			
Rb	Sr	Y	Zr	Nb	Mo	Tc	Ru	Rh	Pd
0.8	1.0	1.2	1.6	1.6	1.8	1.9	2.2	2.2	2.2
0.82	0.95	1.22	1.33		2.16			2.28	2.20
0.7	0.95	1.25	1.6	1.6	2.2	1.9	2.2	2.2	2.2
Ag	Cd	In	Sn	Sb	Te	I			
1.9	1.7	1.7	1.8	1.9	2.1	2.5			
1.93	1.69	1.78	1.96	2.05	2.10	2.66			
1.7	1.7	1.7	2.0	2.0	2.2	2.7			
			1.79	1.91	2.14	2.47			
Cs	Ba	La	Hf	Ta	W	Re	Os	Ir	Pt
0.7	0.9	1.1	1.3	1.5	1.7	1.9	2.2	2.2	2.2
0.79	0.89	1.10			2.36			2.20	2.28
0.5	0.8	1.1	1.6	1.5	2.2	1.9	2.2	2.2	2.2
Au	Hg	Tl	Pb	Bi	Th	U			
2.4	1.9	1.8	1.8	1.9	1.3	1.7			
2.54	2.00	2.04	2.33	2.02		1.38			
1.8	1.8	1.8	2.1	2.0	1.5	1.6			

Table S2.16 Average thermochemical electronegativities of radicals R

R	χ	R	χ	R	χ	R	χ
CH_3	2.6	NH_2	3.1	BH_2	1.9	$[HCO_3]$	3.4
CF_3	2.9	NF_2	3.2	PH_2	2.3	$[HPO_4]$	3.4
SiF_3	2.0	NCS	3.2	$SiCH_3$	1.9	$[NO_3]$	3.7
$CHCH_2$	2.7	NNN	3.3	OCH_3	3.4	$[SO_4]$	3.7
CCH	2.8	NC	3.3	OC_6H_5	3.5	O_2	3.5
CHO	2.9	NO_2	3.4	OH	3.5		

Table S2.17 Ionization electronegativities according to Pearson (upper lines), Allen (middle lines), Politzer (lower lines)

Li	Be	B	C	N	O	F
0.92	1.43	1.31	1.92	2.23	2.31	3.19
0.87	1.51	1.96	2.43	2.93	3.45	4.01
0.99	1.64	2.14	2.63	3.18	3.52	4.00
Na	Mg	Al	Si	P	S	Cl
0.87	1.17	0.98	1.46	1.72	1.91	2.54
0.83	1.24	1.54	1.83	2.15	2.47	2.74
0.96	1.36	1.59	1.86	2.25	2.53	2.86
K	Ca	Ga	Ge	As	Se	Br
0.74	0.94	0.98	1.40	1.62	1.80	2.33
0.70	0.99	1.68	1.91	2.11	2.32	2.57
0.98	1.08	1.67	1.82	2.09	2.31	2.60

First transition series

Sc	Ti	V	Cr	Mn	Fe	Co	Ni	Cu	Zn
1.03	1.06	1.11	1.14	1.14	1.23	1.31	1.35	1.37	1.44
1.14	1.32	1.46	1.58	1.67	1.72	1.76	1.80	1.77	1.52
1.15	1.21	1.27	1.17	1.33	1.31	1.28	1.38	1.48	1.57

Table S2.18 Average ionization electronegativities of radicals R

R	χ	R	χ	R	χ	R	χ	R	χ
CF_3	3.3	CCH	3.1	NO_2	4.0	OH	3.5	$[ClO_4]$	4.9
CCl_3	2.9	CO	3.7	NO	3.8	SH	2.3	$[ClO_3]$	4.8
CBr_3	2.6	CN	3.8	NC	3.7	SCN	2.9	$[SO_4]$	4.6
CI_3	2.5	NF_2	3.7	NCS	3.5	SF_5	2.9	$[PO_4]$	4.4
CH_3	2.3	NCl_2	3.2	OF	4.1	SeH	2.2	$[CO_3]$	4.3
$CHCH_2$	2.5	NH_2	2.7	OCl	3.7	TeH	2.1		

Table S2.19 Ionization electronegativities of atoms with charges of ±1

A^+	χ	A^+	χ	A^+	χ	A^+	χ	A^-	χ
Li	16.7	Ba	2.5	C	6.3	Bi	4.2	F	–0.1
Na	10.6	Zn	4.7	Si	4.2	V	3.6	Cl	0.2
K	7.2	Cd	4.4	Ge	4.1	Nb	3.6	Br	0.2
Rb	6.2	Hg	5.0	Sn	3.8	Ta	4.2	I	0.2
Cs	5.7	B	6.2	Pb	3.8	O	9.5		
Cu	5.2	Al	4.6	Ti	3.4	S	6.5		
Ag	5.4	Ga	5.0	Zr	3.3	Se	6.0		
Au	5.5	In	4.6	Hf	3.8	Te	5.3		
Be	4.7	Tl	5.0	N	7.8	F	10.3		
Mg	3.9	Sc	3.2	P	5.2	Cl	7.2		
Ca	3.0	Y	3.1	As	4.9	Br	6.5		
Sr	2.8	La	2.8	Sb	4.3	I	5.7		

Table S2.20 Short history of the development of the geometrical electronegativity concept (pioneering works are shown in **bold**)

Year	Authors	Equation	Notes
1942	**Liu**	$\chi = a(N^* + b)/r^{2/3}$	N^* is the number of e-shells
1946	**Gordy**	$\chi = a\,(n + b)/r + c$	n is the number of electrons
1957	Wilmshurst		≈
1964	Yuan		≈
1966	Chandra		≈
1968	Phillips		applied to semiconductors
1979	Ray, Samuel, Parr		for multiple bonds
1982	Inamoto, Masuda		for polar bonds
1983	Owada		n^* instead of n
1988	Luo, Benson		reduced to Pauling' scale
1951	**Cottrell, Sutton**	$\chi = a(Z^*/r)^{1/2} + b$	dimensionality of $E^{1/2}$
1989	Zhang, Kohen		theoretical $Z^*$and r
1993	Batsanov		for normal and vdW molecules
1952	**Sanderson**	$\chi = a(N/r^3) + b$	$N = \Sigma e$
1980	**Allen, Huheey**		for rare gases
1955	**Pritchard, Skinner**	$\chi = a(Z^*/r) + b$	Z^* according to Slater
1964	Batsanov		corrected Z^*
1971	Batsanov		Z^* for valence states
1975	Batsanov		for crystals
1980	Allen, Huheey		for rare gases
1956	**Williams**	$\chi = a\,(n/r)^b$	n is the number of valence electrons
1958	**Allred, Rochow**	$\chi = a(Z^*–b)\,r^2 + c$	Z* of Slater
1964	Batsanov		corrected Z*
1971	Batsanov		Z^* for valence states
1975	Batsanov		for crystals
1977	Mande		experimental Z^*
1980	Allen, Huhee		for rare gases
1981	Boyd, Marcus		b is calculated by *ab initio*
1982	Zhang		experimental Z^*

Table S2.20 (continued)

Year	Authors	Equation	Notes
1978 **1986**	**Batsanov** **Gorbunov, Kaganyuk**	$\chi = a(N_e^{1/2})/r$	N_e is the number of outer electrons r is calculated by *ab initio*
1990	**Nagle**	$\chi = a(N/\alpha^{1/2}) + b$	α is the polarizability
2006	**Batsanov**	all formulae	Z* and r for valence states

Table S2.21 Crystalline electronegativities according to Li and Xue [2.101, 2.102]

Li	Be	B	C	N	O	F			
1.01	1.27	1.71	2.38	2.94	3.76	4.37			
Na	Mg	Al	Si	P	S	Cl			
1.02	1.23	1.51	1.89	2.14	2.66	3.01			
K	Ca	Sc	Ti	V^{III}	Cr^{III}	Mn^{IV}	Fe^{III}	Co^{III}	Ni^{III}
1.00	1.16	1.41	1.73	1.54	1.59	1.91	1.65	1.69	1.70
Cu	Zn	Ga	Ge	As	Se	Br			
1.16	1.34	1.58	1.85	2.16	2.45	2.74			
Rb	Sr	Y	Zr	Nb^{III}	Mo^{IV}	Tc^{IV}	Ru^{IV}	Rh^{IV}	Pd^{IV}
1.00	1.14	1.34	1.61	1.50	1.81	1.77	1.85	1.86	1.88
Ag	Cd	In	Sn	Sb	Te	I			
1.33	1.28	1.48	1.71	1.97	2.18	2.42			
Cs	Ba	La	Hf	Ta^{III}	W^{IV}	Re^{IV}	Os^{IV}	Ir^{IV}	Pt^{IV}
1.00	1.13	1.33	1.71	1.54	1.78	1.85	1.89	1.88	1.90
Au^{I}	Hg	Tl^{I}	Pb	Bi	Th	U			
1.11	1.33	1.05	1.75	1.90	1.40	1.44			

Table S2.22 Effective coordination charges of metal atoms

Metal	Compounds	Ω_{cal}	Ω_{exp}	Metal	Compounds	Ω_{cal}	Ω_{exp}
Cr	$CrSO_4 \cdot 7H_2O$	1.8	1.9	Co	$Co(NO_3)_3$	0.6	1.2
	$Cr(NO_3)_3$	1.3	1.2		$Co(C_5H_5)_2$	0.7	0.4
	K_2CrO_4	0.5	0.1		$Co(C_5H_5)_2Cl$	0.9	1.0
	$Cr(C_6H_6)_2$	1.4	1.3	Ni	$Ni(C_5H_5)_2$	0.6	0.7
Mn	$Mn(NO_3)_2 \cdot 4H_2O$	1.8	1.8		$Ni(C_5H_5)_2Cl$	0.8	1.0
	$K_3Mn(CN)_6$	0.6	0.9	Os	OsO_2	0.7	0.8
	$Mn(C_5H_5)_2$	1.3	1.5		K_2OsCl_6	0.5	0.8
Fe	$(NH_4)_2Fe(SO_4)_2 \cdot 6H_2O$	1.7	1.9		K_2OsO_4	0.7	0.8
	$K_3Fe(CN)_6$	0.4	1.0		K_2OsNCl_5	0.8	0.7
	$Fe(C_5H_5)_2$	0.7	0.6		$KOsO_3N$	0.9	1.0
	$Fe(C_5H_5)_2Cl$	0.8	0.7				

Table S2.23 Comparison of high pressure radii (r_P) and crystallographic radii (r_c) of cations

Cation	r_p	r_c	Cation	r_p	r_c	Cation	r_p	r_c
Li^+	0.75	0.76	Mg^{2+}	0.70	0.72	Sc^{3+}	0.74	0.74
Na^+	0.98	1.02	Ca^{2+}	1.03	1.00	Y^{3+}	0.88	0.90
K^+	1.37	1.38	Sr^{2+}	1.15	1.18	Cr^{3+}	0.67	0.62
Rb^+	1.52	1.52	Ba^{2+}	1.38	1.35	Mn^{3+}	0.66	0.64
Cs^+	1.63	1.67	Zn^{2+}	0.76	0.74	Fe^{3+}	0.66	0.64
Cu^+	0.78	0.77	Cd^{2+}	0.95	0.95	Th^{4+}	1.07	1.05
Ag^+	1.17	1.15	Pb^{2+}	1.23	1.19	U^{4+}	0.97	1.00
Tl^+	1.44	1.50	B^{3+}	0.38	0.27	Zr^{4+}	1.06	0.84
Be^{2+}	0.47	0.45	Al^{3+}	0.63	0.54	Hf^{4+}	0.90	0.83

Table S2.24 Change of effective atomic charges under pressures, de^*/dP 10^2GPa

M	Cl		Br		I	
	[2.103]	[2.104]	[2.103]	[2.104]	[2.103]	[2.104]
Li	1.22	0.8	2.15	0.95	2.87	
Na	1.26	1.1	2.20	1.3	2.91	1.9
K	1.32	1.8	2.26	2.1	2.94	2.8
Rb	1.33	2.1	2.26	2.6	2.93	3.3
Cs	1.38		2.35		3.01	

Supplementary References

2.1 Reynard LM, Evans CJ, Gerry MCL (2001) J Mol Spectr 205: 344
2.2 Shayesteh A, Bernath PF (2011) J Chem Phys 135: 094308
2.3 Heaven MC, Bondybey VE, Merritt JM, Kaledin AL (2011) Chem.Phys Lett 506: 1
2.4 Czajkowski M, Krause L, Bobkowski R (1994) Phys Rev A49: 775
2.5 Kedzierski W, Supronowicz J, Czajkowski M et al (1995) J Mol Spectr 173: 510
2.6 Girichev GV, Giricheva NI, Titov VA et al (1992) J Struct Chem 33: 362
2.7 Gurvich LV, Ezhov YuS, Osina EL, Shenyavskaya EA (1999) Russ J Phys Chem 73**:** 331
2.8 Liu Y, Zhang C-H, Krasnokutski SA, Yang D-S (2011) J Chem Phys 135: 034309
2.9 Ciccioli A, Gigli G, Meloni G, Testani E (2007) J Chem Phys 127: 054303
2.10 Hillel R, Bouix J, Bernard C (1987) Z anorg allgem Chem 552: 221
2.11 Balasubramanian K (1989) Chem.Rev 89: 1801
2.12 Van der Vis MGM, Cordfunke EHP, Konings RJM (1997) Thermochim Acta 302: 93
2.13 Ponomarev D, Takhistov V, Slayden S, Liebman J (2008) J Molec Struct 876: 34
2.14 Goussis A, Besson J (1986) J Less-Common Met 115: 193
2.15 Berkowitz J (1988) J Chem Phys 89: 7065
2.16 Berkowitz J, Ruscic B, Gibson S et al (1989) J Mol Struct 202: 363
2.17 Nizamov B, Setser DW (2001) J Mol Spectr 206: 53
2.18 Dittmer G, Niemann U (1981) Phil J Res 36: 87
2.19 Gutsev GL, Bauschlicher ChW (2003) J Phys Chem A107: 4755
2.20 Blauschlicher CW (1996) Chem Phys 211: 163
2.21 Han Y-K, Hirao K (2000) J Chem Phys 112: 9353
2.22 Simoes JAM, Beauchamp JL (1990) Chem Rev 90: 629

2.23 Lamoreaux R, Hildenbrand DL, Brewer L (1987) J Phys Chem Refer Data 16: 419
2.24 Giuliano BM, Bizzochi L, Sanchez R et al (2011) J Chem Phys 135: 084303
2.25 O'Hare PAG, Lewis B, Surman S, Volin KJ (1990) J Chem Thermodyn 22: 1191
2.26 Cooke SA, Gerry MCL (2004) J Chem Phys 121: 3486
2.27 Brugh DJ, Morse MD (1997) J Chem Phys 107: 9772
2.28 Antonov IO, Barker BJ, Bondybey VE, Heaven MC (2010) J Chem Phys 133: 074309
2.29 Merritt JM, Bondybey VE, Heaven MC (2009) J Chem Phys 130: 144503
2.30 Leroy G, Sana M, Wilante C, van Zieleghem M-J (1991) J Molec Struct 247: 199
2.31 Leroy G, Temsamani DR, Sana M, Wilante C (1993) J Molec Struct 300: 373
2.32 Leroy G, Temsamani DR, Wilante C (1994) J Molec Struct 306: 21
2.33 Leroy G, Temsamani DR, Wilante C, Dewispelaere J-P (1994) J Molec Struct 309: 113
2.34 von Schleyer PR, Kost D (1988) J Am Chem Soc 110: 2105
2.35 Schmidt M, Truong P, Gordon M (1987) J Am Chem Soc 109: 5217
2.36 Scrocco M (1986) Phys Rev B33: 7228
2.37 Scrocco M (1985) Phys Rev B32: 1301
2.38 Dou Y, Egdell RG, Law DSL et al (1998) J Phys Cond Matter 10: 8447,
2.39 Wiemhofer H-D, Harke S, Vohrer U (1990) Solid State Ionics 40–41: 433
2.40 Cisneros-Morales MC, Aita CR (2010) Appl Phys Lett 96: 191904
2.41 Kliche G (1986) Solid State Commun 59: 587
2.42 Dimitrov V, Sakka S (1996) J Appl Phys 79: 1736
2.43 Tyagi P, Vedeshwar AG (2001) Phys Rev B64: 245406
2.44 Julien C, Eddrief M, Samaras I, Balkanski M (1992) Mater Sci Engin B15: 70
2.45 Roubi L, Carlone C (1988) Canad J Phys 66: 633
2.46 Stanciu GA, Oprica MH, Oud JL et al (1999) J Phys D32: 1928
2.47 da Silva AF, Veissid N, An CY et al (1995) J Appl Phys 78: 5822
2.48 Karmakar S, Sharma SM (2004) Solid State Commun 131: 473
2.49 Anand TJS, Sanjeeviraja C (2001) Vacuum 60: 431
2.50 Ren Q, Liu LQ et al (2000) Mater Res Bull 35: 471
2.51 da Silva AF, Veissid N, An CY et al (1996) Appl Phys Lett 69: 1930
2.52 Thomas J, Polini I (1985) Phys Rev B32: 2522
2.53 Ho CH, Liao PC, Huang YS et al (1997) J Appl Phys 81: 6380
2.54 Gottesfeld S, Maia G, Floriano JB et al (1991) J Electrochem Soc 138: 3219
2.55 Prokofiev AV, Shelykh AI, Golubkov AV, Sharenkova NV (1994) Inorg Mater 30: 326
2.56 Sassaki T, Takizawa H, Uheda K et al (2002) J Solid State Chem 166: 164
2.57 Tu B, Cui Q, Xu P et al (2002) J Phys Cond Matter, 14: 10627
2.58 Adachi S, Ozaki S (1993) Japan J Appl Phys (I) 32: 4446
2.59 Ozaki S, Takada K, Adachi S (1994) Japan J Appl Phys (I) 33: 6213
2.60 Choe S-H, Bang T-H, Kim N-O et al (2001) Semicond Sci Technol 16:98
2.61 Hussein SA, Nassary MM, Gamal GA, Nagat AT (1993) Cryst Res Technol 28: 1021
2.62 Yesugade NS, Lokhande CD, Bhosale CH (1995) Thin Solid Films 263:145
2.63 Lostak P, Novotny R, Kroutil J, Stary Z (1987) Phys Stat Solidi A 104:841
2.64 Lefebre I, Lannoo M, Allan G et al (1987) Phys Rev Lett 59:2471
2.65 Leontie CM, Delibas M, Rusu GI (2001) Mater Res Bull 36:1629
2.66 Torane AP, Bhosale CH (2001) Mater Res Bull 36:1915
2.67 Ismail F, Hanafi Z (1986) Z phys Chem 267:667
2.68 Chernyshova IV, Ponnurangam S, Somasundaran P (2010) Phys Chem Chem Phys 12:14045
2.69 Ghose J, Roy A (1995) Optical studies on Rh_2O_3. In: Schmidt SC, Tao WC (eds) Shock compression of condensed matter. AIP Press, New York
2.70 Fowler P, Tole P, Munn R, Hurst M (1989) Mol Phys 67:141
2.71 Ishii Y, Murakami J-i, Itoh M (1999) J Phys Soc Japan 68:696
2.72 Reimann K, Syassen K (1989) Phys Rev B 39:11113
2.73 Joseph KS, Pradeep B (1994) Pramana 42:41
2.74 Mostafa SN, Mourad MY, Soliman SA (1991) Z phys Chem 171:231

2.75 Haram SK, Santhanam KSV (1994) Thin Solid Films 238:21
2.76 Mostafa SN, Selim SR, Soliman SA, Gadalla EG (1993) Electrochim Acta 38:1699
2.77 Dlala H, Amlouk M, Belgacem S et al (1998) Eur Phys J Appl Phys 2:13
2.78 Kumar MCS, Pradeep B (2002) Semicond Sci Technol 17: 261
2.79 Waki H, Kawamura J, Kamiyama T, Nakamura Y (2002) J Non-Cryst Solids 297:26
2.80 Gauthier M, Polian A, Besson JM, Chevy A (1989) Phys Rev B 40:3837
2.81 Elkorashy A (1990) J Phys Cond Matter 2:6195
2.82 Herve P, Vandamme L (1994) Infrared Phys Technol 35:609
2.83 Gauthier M, Polian A, Besson J, Chevy A (1989) Phys Rev B 40:3837
2.84 Isidorsson J, Giebels IAME, Arwin H, Griessen R (2003) Phys Rev B 68:115112
2.85 Lee MW, Shin WP (1999) J Appl Phys 86:6798
2.86 Wijngaarden RJ, Huiberts JN, Nagengast D et al (2000) J Alloys Compd 308:44
2.87 Varekomp PR, Simpson WC, Shuh DK et al (1994) Phys Rev B 50:14267
2.88 Barrieri A, Counturier G, Elfain A et al (1992) Thin Solid Films 209:38
2.89 Pollini I, Thomas J, Carricarburu B, Mamy R (1989) J Phys Cond Matter 1:7695
2.90 El Ramnani H, Gagnon R, Aubin M (1991) Solid State Commun 77:307
2.91 Kaneko H, Nagao F, Miyake K (1988) J Appl Phys 63:510
2.92 Khila M, Rofail N (1986) Radiochim Acta 40:155
2.93 Goede O, Heimbrodt W, Lamla M, Weinhold V (1988) Phys Stat Solidi B 146:K65
2.94 Hoenle W, Furuseth F, von Schnering HG (1990) Z Naturforsch B 45:952
2.95 Parker JC, Lam DJ, Xu Y-N, Ching WY (1990) Phys Rev B 42:5289
2.96 Sonntag B (1976) Dielectric and optical properties. In: Klein ML, Venables JA (eds) Rare gas solids, vol 1. Acad Press, London
2.97 Pauling L (1960) The nature of the chemical bond, 3rd edn. Cornell Univ Press, Ithaca
2.98 Allred AL (1961) J Inorg Nucl Chem 17:215
2.99 Batsanov SS (2000) Russ J Phys Chem 74:267
2.100 Smith DW (2007) Polyhedron 26:519
2.101 Li K, Xue D (2006) J Phys Chem A110:11332
2.102 Li K, Wang X, Zhang F, Xue D (2008) Phys Rev Lett 100:235504
2.103 Batsanov SS (1997) J Phys Chem Solids 58:527
2.104 Kucharczyk W (1991) J Phys Chem Solids 52:435

References

1. Kossel W (1916) Molecular formation as an issue of the atomic construction. Ann Phys 49:229–362
2. Lewis GN (1916) The atom and the molecule. J Am Chem Soc 38:762–785
3. Langmuir I (1919) The arrangement of electrons in atoms and molecules. J Am Chem Soc 41:868–934
4. Langmuir I (1919) Isomorphism, isosterism and covalence. J Am Chem Soc 41:1543–1559
5. Langmuir I (1920) The octet theory of valence and its applications with special reference to organic nitrogen compounds. J Am Chem Soc 42: 274–292
6. Schwartz WHE (2006) Measuring orbitals: provocation or reality? Angew Chem Int Ed 45:1508–1517
7. Mulliken RS (1978) Chemical bonding. Ann Rev Phys Chem 29:1–30
8. Bader RFW (1990) Atoms in molecules: a quantum theory. Oxford University Press, Oxford
9. Parr RG, Ayers PW, Nalewajski RF (2005) What is an atom in a molecule? J Phys Chem A 109:3957–3959
10. Batsanov SS (1957) On the interrelation between the theory of polarization and the concept of electronegativity. Zh Neorg Khim 2:1482–1487
11. Batsanov SS (2004) Molecular refractions of crystalline inorganic compounds. Russ J Inorg Chem 49:560–568

12. Goldschmidt VM (1954) Geochemistry. Clarendon Press, Oxford
13. O'Keeffe M (1977) On the arrangement of ions in crystals. Acta Cryst A 33:924–927
14. Batsanov SS (1983) On some crystal-chemical peculiarities of inorganic halogenides. Zh Neorg Khim 28:830–836
15. Madden PA, Wilson M (1996) Covalent effects in 'ionic' systems. Chem Soc Rev 25:339–350
16. Gillespie RJ, Silvi B (2002) The octet rule and hypervalence: two misunderstood concepts. Coord Chem Rev 233:53–62
17. von Antropoff A (1924) Die Wertigkeit der Edelgase und ihre Stellung im periodischen System. Angew Chem 37:217–218, 695–696
18. Pauling L (1932) The nature of the chemical bond: the energy of single bonds and the relative electronegativity of atoms. J Am Chem Soc 54:3570–3582
19. Bartlett N (1962) Xenon hexafluoroplatinate Xe^{+} $[PtF6]^{-}$. Proc Chem Soc London 218
20. Bartlett N (1963) New compounds of noble gases: the fluorides of xenon and radon. Amer Scientist 51:114–118
21. Claassen HH, Selig H, Malm JG (1962) Xenon tetrafluoride. J Am Chem Soc 84:3593
22. Chernick CL, Claassen HH, Fields PR et al (1962) Fluorine compounds of xenon and radon. Science 138:136–138.
23. Tramšek M, Žemva B (2006) Synthesis, properties and chemistry of xenon(II) fluoride. Acta Chim Slov 53:105–116
24. Grochala W (2007) Atypical compounds of gases, which have been called 'noble'. Chem Soc Rev 36:1632–1655
25. Goettel KA, Eggert JH, Silvera IF, Moss WC (1989) Optical evidence for the metallization of xenon at 132(5) GPa. Phys Rev Lett 62:665–668
26. Reichlin R, Brister KE, McMahan AK, et al (1989) Evidence for the insulator-metal transition in xenon from optical, X-ray, and band-structure studies to 170 GPa. Phys Rev Lett 62:669–672
27. Batsanov SS (1998) H_2: an archetypal molecule or an odd exception? Struct Chem 9:65–68
28. Pauling L (1960) The nature of the chemical bond, 3rd edn. Cornell Univ Press, Ithaca, New York
29. Gillespie RJ, Robinson EA (1996) Electron domains and the VSEPR model of molecular geometry. Angew Chem Int Ed 35:495–514
30. Morse PM (1929) Diatomic molecules according to the wave mechanics: vibrational levels. Phys Rev 34:57–64
31. Bürgi H-B, Dunitz J (1987) Fractional bonds: relations among their lengths, strengths, and stretching force constants. J Am Chem Soc 109:2924–2926
32. Parr RG, Borkman RF (1968) Simple bond-charge model for potential-energy curves of homonuclear diatomic molecules. J Chem Phys 49:1055–1058
33. Harrison WA (1980) Electronic structure the properties of solids. Freeman, San Francisco
34. Zavitsas AA (2003) The relation between bond lengths and dissociation energies of carbon-carbon bonds. J Phys Chem A 107:897–898
35. Krygowski TM, Cyrański MK (2001) Structural aspects of aromaticity. Chem Rev 101:1385–1420
36. Pauling L, Sherman J (1933) The nature of the chemical bond: the calculation from thermochemlcal data of the energy of resonance of molecules among several electronic structures. J Chem Phys 1:606–617
37. Hückel E (1931) Quantum contributions to the benzene problem. Z Physik 70:204–286
38. Wiberg KB (2001) Aromaticity in monocyclic conjugated carbon rings. Chem Rev 101:1317–1332
39. Hoffmann R, Shaik S, Hiberty PC (2003) A conversation on VB vs MO theory: a never-ending rivalry? Acc Chem Res 36:750–756
40. Pierrefixe SCAH, Bickelhaupt FM (2007) Aromaticity: molecular-orbital picture of an intuitive concept. Chem Eur J 13:6321–6328
41. Gomes JANF, Mallion RB (2001) Aromaticity and ring currents. Chem Rev 101:1349–1384
42. Mitchell RH (2001) Measuring aromaticity by NMR. Chem Rev 101:1301–1316

43. Bühl M, Hirsh A (2001) Spherical aromaticity of fullerenes. Chem Rev 101:1153–1184
44. Chen Z, King RB (2005) Spherical aromaticity: recent work on fullerenes, polyhedral boranes and related structures. Chem Rev 105:3613–3642
45. King RB (2001) Three-dimensional aromaticity in polyhedral boranes and related molecules. Chem Rev 101:1119–1152
46. Boldyrev AI, Wang L-S (2005) All-metal aromaticity and antiaromaticity. Chem Rev 105:3716–3757
47. Hirsh A, Chen Z, Jiao H (2000) Spherical aromaticity in I_h symmetrical fullerenes: the $2(N+1)^2$ rule. Angew Chem Int Ed 39:3915–3917
48. Schleyer P von R (2001) Introduction: aromaticity. Chem Rev 101:1115–1118
49. Schleyer P von R (2005) Introduction: delocalization π and σ. Chem Rev 105:3433–3435
50. Meister J, Schwartz WHE (1994) Principal components of ionicity. J Phys Chem 98:8245–8252
51. Gussoni M, Castiglioni C, Zerbi G (1983) Experimental atomic charges from infrared intensities: comparison with "ab initio" values. Chem Phys Lett 95:483–485
52. Galabov B, Dudev T, Ilieva S (1995) Effective bond charges from experimental IR intensities. Spectrochim Acta A 51:739–754
53. Ilieva S, Galabov B, Dudev T et al (2001) Effective bond charges from infrared intensities in CH_4, SiH_4, GeH_4 and SnH_4. J Mol Struct 565–566:395–398
54. Barinskii RL (1960) Determination of the effective charges of atoms in complexes from the X-ray absorption spectra. J Struct Chem 1:183–190
55. Szigeti B (1949) Polarizability and dielectric constant of ionic crystals. Trans Faraday Soc 45:155–166
56. Batsanov SS (1982) Dielectric methods of studying the chemical bond and the concept of electronegativity. Russ Chem Rev 51:684–697
57. Wagner V, Gundel S, Geurts J et al (1998) Optical and acoustical phonon properties of BeTe. J Cryst Growth 184–185:1067–1071
58. Julien C, Eddrief M, Samaras I, Balkanski M (1992) Optical and electrical characterizations of SnSe, SnS_2 and $SnSe_2$ single crystals. Mater Sci Engin B 15:70–72
59. Schoenes J, Borgschulte A, Carsteanu A-M et al (2003) Structure and bonding in YH_x as derived from elastic and inelastic light scattering. J Alloys Compd 356–357:211–217
60. Jones GO, Martin DH, Mawer PA, Perry CH (1961) Spectroscopy at extreme infra-red wavelengths. II. The lattice resonances of ionic crystals. Proc Roy Soc London A 261:10–27
61. Bosomworth D (1967) Far-infrared optical properties of CaF_2, SrF_2, BaF_2, and CdF_2. Phys Rev 157:709–715
62. Denham P, Field GR, Morse PLR, Wilkinson GR (1970) Optical and dielectric properties and lattice dynamics of some fluorite structure ionic crystals. Proc Roy Soc London A 317:55–77
63. Batana A, Bruno JAO (1990) Volume dependence of the effective charge of zinc-blende-type crystals. J Phys Chem Solids 51:1237–1238
64. Van Vechten J (1969) Quantum dielectric theory of electronegativity in covalent systems. Phys Rev 187:1007–1020
65. Phillips JC, van Vechten J (1970) Spectroscopic analysis of cohesive energies and heats of formation of tetrahedrally coordinated semiconductors. Phys Rev B 2:2147–2160
66. Phillips JC (1970) Ionicity of the chemical bond in crystals. Rev Modern Phys 42:317–356
67. Phillips JC (1974) Electronegativity and tetragonal distortions in $A^{II}B^{IV}C^{V}{}_2$ semiconductors. J Phys Chem Solids 35:1205–1209
68. Levine BF (1973) d-Electron effects on bond susceptibilities and ionicities. Phys Rev B 7:2591–2600
69. Levine BF (1973) Bond-charge calculation of nonlinear optical susceptibilities for various crystal structures. Phys Rev B 7:2600–2626
70. Levine BF (1973) Bond susceptibilities and ionicities in complex crystal structures. J Chem Phys 59:1463–1486
71. Srivastava VK (1984) Ionic and covalent energy gaps of CsCl crystals. Phys Letters A102:127–129

72. Al-Douri Y, Aourag H (2002) The effect of pressure on the ionicity of In–V compounds. Physica B 324:173–178
73. Singth BP, Ojha AK, Tripti S (2004) Analysis of ionicity parameters and photoelastic behaviour of $A^N B^{8-N}$ type crystals. Physica B 350:338–347
74. Hertz W (1927) Dielektrizitätskonstante und Brechungsquotient. Z anorg allgem Chem 161:217–220
75. Linke R (1941) On the refraction exponents of PF_5 and OsO_4 and the dielectric constants of OsO_4, SF_6, SeF_6 and TeF_6. Z phys Chem B 48:193–196
76. Sumbaev OI (1970) The effect of the chemical shift of the X-ray K_α lines in heavy atoms. Sov Phys JETP 30:927–933
77. Batsanov SS, Ovsyannikova IA (1966). X-ray spectroscopy and effective charges of atoms in compounds of Mn. In: Chemical bond in semiconductors thermodynamics. Nauka, Minsk (in Russian)
78. Pantelouris A, Kueper G, Hormes J et al (1995) Anionic gold in Cs_3AuO and Rb_3AuO established by X-ray absorption spectroscopy. J Am Chem Soc 117:11749–11753
79. Saltykov V, Nuss J, Konuma M, Jansen M (2009) Investigation of the quasi binary system BaAu–BaPt. Z allgem anorg Chem 635:70–75
80. Saltykov V, Nuss J, Konuma M, Jansen M (2010) $SrAu_{0.5}Pt_{0.5}$ and $CaAu_{0.5}Pt_{0.5}$, analogues to the respective Ba compounds, but featuring purely intermetallic behaviour. Solid State Sci 12:1615–1619.
81. Nefedov VI, Yarzhemsky VG, Chuvaev AV, Tishkina EM (1988) Determination of effective atomic charge, extra-atomic relaxation and Madelung energy in chemical compounds on the basis of X-ray photoelectron and auger transition energies. J Electron Spectr Relat Phenom 46:381–404
82. Jollet F, Noguera C, Thromat N et al (1990) Electronic structure of yttrium oxide. Phys Rev B 42:7587–7595
83. Larsson R, Folkesson B (1991) Atomic charges in some copper compounds derived from XPS data. Acta Chem Scand 45:567–571
84. Larsson R, Folkesson B (1996) Polarity of Cu_3Si. Acta Chem Scand 50:1060–1061
85. Gutenev MS, Makarov LL (1992) Comparison of the static and dynamic atomic charges in ionic-covalent solids. J Phys Chem Solids 53:137–140
86. Dolenko GN (1993) X-ray determination of effective charges on sulphur, phosphorus, silicon and chlorine atoms. J Molec Struct 291:23–57
87. Dolenko GN, Voronkov MG, Elin VP, Yumatov VD (1993) X-ray investigation of the electron structure of organic compounds containing SiS and SiO bonds. J Molec Struct 295:113–120
88. Jolly WL, Perry WB (1974) Calculation of atomic charges by an electronegativity equalization procedure. Inorg Chem 13:2686–2692
89. Debye P (1915) Zerstreuung von Röntgenstrahlen. Ann Phys 46:809–823
90. Tsirel'son VG, Ozerov RP (1996) Electron density and bonding in crystals. Institute of Physics Publishing, Bristol
91. Coppens P (1997) X-ray charge densities and chemical bonding. Oxford University Press, Oxford
92. Koritsanszky TS, Coppens P (2001) Chemical applications of X-ray charge-density analysis. Chem Rev 101:1583–1628
93. Belokoneva EL (1999) Electron density and traditional structural chemistry of silicates. Russ Chem Rev 68:299–316
94. Dunitz JD, Gavezzotti A (2005) Molecular recognition in organic crystals: directed intermolecular bonds or nonlocalized bonding? Angew Chem Int Ed 44: 1766–1787
95. Yufit DS, Mallinson PR, Muir KW, Kozhushkov SI, De Meijere A (1996) Experimental charge density study of dispiro heptane carboxylic acid. Acta Cryst B 52:668–676
96. Jauch W, Reehuis M, Schultz AJ (2004) γ-Ray and neutron diffraction studies of CoF_2: magnetostriction, electron density and magnetic moments. Acta Cryst A 60:51–57
97. Vidal-Valat G, Vidal J-P, Kurki-Suonio K (1978) X-ray study of the atomic charge densities in MgO, CaO, SrO and BaO. Acta Cryst A 34:594–602

98. Sasaki S, Fujino K, Takeuchi Y, Sadanaga R (1980) On the estimation of atomic charges by the X-ray method for some oxides and silicates. Acta Cryst A 36:904–915
99. Kirfel A, Will G (1981) Charge density in anhydrite, $CaSO_4$. Acta Cryst B 37:525–532
100. Sasaki S, Fujino K, Takeuchi Y, Sadanaga R (1982) On the estimation of atomic charges in $Mg_2Si_2O_6$, $Co_2Si_2O_6$, and $Fe_2Si_2O_6$. Z Krist 158:279–297
101. Gonschorek W (1982) X-ray charge density study of rutile. Z Krist 160:187–203
102. Kirfel A, Josten B, Will G (1984) Formal atomic charges in cubic boron nitride BN. Acta Cryst A 40:C178–C179
103. Will G, Kirfel A, Josten B (1986) Charge density and chemical bonding in cubic boron nitride. J Less-Common Met 117:61–71
104. Zorkii PM, Masunov AE (1990) X-ray diffraction studies on electron density in organic crystals. Russ Chem Rev 59:592–606
105. Vidal-Valat G, Vidal J-P, Kurki-Suonio K, Kurki-Suonio R (1992) Evidence on the breakdown of the Born-Oppenheimer approximation in the charge density of crystalline LiH/D. Acta Cryst A 48:46–60
106. Sasaki S (1997) Radial distribution of electron density in magnetite, Fe_3O_4. Acta Cryst B 53:762–766
107. Hill R, Newton M, Gibbs GV (1998) A crystal chemical study of stishovite. J Solid State Chem 47:185–200
108. Tsirel'son VG, Avilov AS, Abramov YuA et al (1998) X-ray and electron diffraction study of MgO. Acta Cryst B 54:8–17
109. Noritake T, Towata S, Aoki M et al (2003) Charge density measurement in MgH_2 by synchrotron X-ray diffraction. J Alloys Comp 356–357:84–86
110. Schoenes J, Borgschulte A, Carsteanu A-M et al (2003) Structure and bonding in YH_x as derived from elastic and inelastic light scattering. J Alloys Comp 356–357:211–217
111. Belokoneva EL, Shcherbakova YuK (2003) Electron density in synthetic escolaite Cr_2O_3 with a corundum structure and its relation to antiferromagnetic properties. Russ J Inorg Chem 48:861–869
112. Whitten AE, Ditrich B, Spackman MA et al (2004) Charge density analysis of two polymorphs of antimony(III) oxide. Dalton Trans 23–29
113. Saravanan R, Jainulabdeen S, Srinivasan N, Kannan YB (2008) X-ray determination of charge transfer in solar grade GaAs. J Phys Chem Solids 69:83–86
114. Noritake T, Aok M, Towata S et al (2002) Chemical bonding of hydrogen in MgH_2. Appl Phys Lett 81:2008–2010
115. Isidorsson J, Giebels IAME, Arwin H, Griessen R (2003) Optical properties of MgH_2 measured in situ by ellipsometry and spectrophotometry. Phys Rev B 68:115112
116. Ichikawa M, Gustafsson T, Olovsson I (1998) Experimental electron density study of NaH_2PO_4 at 30 K. Acta Cryst B 54:29–34
117. Johnson O (1973) Ionic radii for spherical potential ion. Inorg Chem 12:780–785
118. Johnson O (1981) Electron density and electron redistribution in alloys: electron density in elemental metals. J Phys Chem Solids 42:65–76
119. Batsanov SS (2006) Mechanism of metallization of ionic crystals by pressure. Russ J Phys Chem 80:135–138
120. Brechignac C, Broyer M, Cahuzac Ph et al (1988) Probing the transition from van der Waals to metallic mercury clusters. Phys Rev Letters 60:275–278
121. Pastor GM, Stampell P, Bennemann KH (1988) Theory for the transition from van der Waals to covalent to metallic mercury clusters. Europhys Lett 7:419–424
122. Thomas OC, Zheng W, Xu S, Bowen KH Jr (2002) Onset of metallic behavior in magnesium clusters. Phys Rev Lett 89:213–403
123. Batsanov SS (1971) Quantitative characteristics of bond metallicity in crystals. J Struct Chem 12:809–813
124. Batsanov SS (1979) Band gaps of inorganic compounds of the AB type. Russ J Inorg Chem 24:155–157

125. Vegas A, Jansen M (2002) Structural relationships between cations and alloys; an equivalence between oxidation and pressure. Acta Cryst B 58:38–51
126. Liebau F (1999) Silicates and provskites: two themes with variations. Angew Chem Int Ed 38:1733–1737
127. Goldhammer D (1913) Dispersion und Absorption des Lichtes. Tubner-Ferlag, Leipzig
128. Herzfeld K (1927) On atomic properties which make an element a metal. Phys Rev 29:701–705
129. Duffy JA (1986) Chemical bonding in the oxides of the elements: a new appraisal. J Solid State Chem 62:145–157
130. Dimitrov V, Sakka S (1996) Electronic oxide polarizability and optical basicity of simple oxides. J Appl Phys 79:1736–1740
131. Sun L, Ruoff AL, Zha C-S, Stupian G (2006) Optical properties of methane to 288 GPa at 300 K. J Phys Chem Solids 67:2603–2608
132. Sun L, Ruoff AL, Zha C-S, Stupian G (2006) High pressure studies on silane to 210 GPa at 300 K: optical evidence of an insulator–semiconductor transition. J Phys Cond Matter 18:8573–8580
133. Burdett JK (1997) Chemical bond: a dialog. Wiley, Chichester
134. Hemley RJ, Dera P (2000) Molecular crystals. Rev Mineral Geochem 41:335–419
135. Brewer L (1981) The role and significance of empirical and semiempirical correlations. In: O'Keefe M, Navrotsky A (eds) Structure and bonding in crystals, v 1. Acad Press, San Francisco
136. Trömel M (2000) Metallic radii, ionic radii, and valences of solid metallic elements. Z Naturforsch B 55:243–247
137. Jules JL, Lombardi JR (2003) Transition metal dimer internuclear distance from measured force constant. J Phys Chem A 107:1268–1273
138. Batsanov SS, Batsanov AS (2010) Valent states of Cu, Ag, and Au atoms in molecules and solids are the same. Russ J Inorg Chem 55:913–914
139. Batsanov SS (1980) The features of chemical bonding in b-subgroup metals. Zh Neorg Khim 25:615–623
140. Lawaetz P (1971) Effective charges and ionicity. Phys Rev Letters 26:697–700
141. Lucovsky G, Martin RM, Burstein E (1971) Localized effective charges in diatomic molecules. Phys Rev B 4:1367–1374
142. Robertson J (1978) Tight binding band structure of PbI_2 using scaled parameters. Solid State Commun 26:791–794
143. Robertson J (1979) Electronic structure of SnS_2, $SnSe_2$, CdI_2 and PbI_2. J Phys C 12:4753–4766
144. Robertson J (1979) Electronic structure of SnO_2, GeO_2, PbO_2, TeO_2 and MgF_2. J Phys C 12:4767–4776
145. Robertson J (1979) Electronic structure of GaSe, GaS, InSe and GaTe. J Phys C 12:4777–4790
146. Wakamura K, Arai T (1981) Empirical relationship between effective ionic charges and optical dielectric constants in binary and ternary cubic compounds. Phys Rev B 24:7371–7379
147. Liebau F, Wang X (2005) Stoichiometric valence *versus* structural valence: Conclusions drawn from a study of the influence of polyhedron distortion on bond valence sums. Z Krist 220:589–591
148. Liebau F, Wang X, Liebau W (2009) Stoichiometric valence and structural valence—two different sides of the same coin: "bonding power". Chem Eur J 15:2728–2737
149. Frankland E (1853) Ueber eine neue Reihe organischer Körper, welche Metalle enthalten. Liebigs Ann Chem 85:329–373
150. Moelwyn-Hughes EA (1961) Physical chemistry, 2nd edn. Pergamon Press, London
151. Batsanov SS (2008) Dependence of energies on the bond lengths in molecules and crystals. J Struct Chem 49:296–303
152. Batsanov SS (1998) Estimation of the van der Waals radii of elements with the use of the Morse equation. Russ J General Chem 66:495–500
153. Ceccherini S, Moraldi M (2001) Interatomic potentials of group IIB atoms (ground state). Chem Phys Lett 337:386–390

154. Housecroft CE, Wade K, Smith BC (1978) Bond strengths in metal carbonyl clusters. Chem Commun 765–766
155. Hughes AK, Peat KL, Wade K (1996) Structural and bonding trends in osmium carbonyl cluster chemistry: metal–metal and metal–ligand bond lengths and calculated strengths, relative stabilities and enthalpies of formation of some binary osmium carbonyls. Dalton Trans 4639–4647
156. Hughes AK, Wade K (2000) Metal–metal and metal–ligand bond strengths in metal carbonyl clusters. Coord Chem Rev 197:191–229
157. Batsanov SS (2007) Ionization, atomization, and bond energies as functions of distances in inorganic molecules and crystals. Russ J Inorg Chem 52:1223–1229
158. Harrison WA (1980) Electronic structure and the properties of solids. Freeman, San Francisco
159. Fuentealba P, Preuss H, Stoll H, von Szentpály L (1982) A proper account of core-polarization with pseudopotentials: single valence-electron alkali compounds. Chem Phys Lett 89:418–422
160. Von Szentpály L, Fuentealba P, Preuss H, Stoll H (1982) Pseudopotential calculations on $Rb^+{}_2$, $Cs^+{}_2$, RbH^+, CsH^+ and the mixed alkali dimer ions. Chem Phys Lett 93:555–559
161. Müller W, Meyer W (1984) Ground-state properties of alkali dimers and their cations (including the elements Li, Na, and K) from ab initio calculations with effective core polarization potentials. J Chem Phys 80:3311–3320
162. Szentpály L von (1995) Valence states and a universal potential energy curve for covalent and ionic bonds. Chem Phys Lett 245:209–214
163. Batsanov SS (2010) Simple semi-empirical method for evaluating bond polarity in molecular and crystalline halides. J Mol Struct 980:225–229
164. Ho J, Polak ML, Lineberger WC (1992) Photoelectron spectroscopy of group IV heavy metal dimers: $Sn^-{}_2$, $Pb^-{}_2$, and $SnPb^-$. J Chem Phys 96:144–154
165. Ho J, Polak ML, Ervin KM Lineberger WC (1993) Photoelectron spectroscopy of nickel group dimers: $Ni^-{}_2$, $Pd^-{}_2$, and $Pt^-{}_2$. J Chem Phys 99:8542–8551
166. Lippa TP, Xu S-J, Lyapushina SA et al (1998) Photoelectron spectroscopy of As^-, As^{2-}, As^{3-}, As^{4-}, and As^{5-}. J Chem Phys 109:10727–10731
167. Nau WM (1997) An electronegativity model for polar ground-state effects on bond dissociation energies. J Phys Organ Chem 10:445–455
168. Erwin KM, Gronert S, Barlow SE et al (1990) Bond strengths of ethylene and acetylene. J Am Chem Soc 112:5750–5759
169. Blanksby SJ, Ellison GB (2003) Bond dissociation energies of organic molecules. Acc Chem Res 36:255–263
170. Ponomarev D, Takhistov V, Slayden S, Liebman J (2008) Enthalpies of formation for free radicals of main group elements' halogenides. J Mol Struct 876:15–33
171. Ponomarev D, Takhistov V, Slayden S, Liebman J (2008) Enthalpies of formation for bi- and triradicals of main group elements' halogenides. J Mol Struct 876:34–55
172. Nikitin MI, Kosinova NM, Tsirelnikov VI (1992) Mass-spectrometric study of the thermodynamic properties of gaseous lowest titanium iodides. High Temp Sci 30:564–572
173. Giricheva NI, Lapshin SB, Girichev GV (1996) Structural, vibrational, and energy characteristics of halide molecules of group II–V elements. J Struct Chem 37:733–746
174. Nikitin MI, Tsirelnikov VI (1992) Determination of enthalpy of formation of gaseous uranium pentafluoride. High Temp Sci 30:730–735
175. Van der Vis MGM, Cordfunke EHP, Konings RJM (1997) Thermochemical properties of zirconium halides: a review. Thermochim Acta 302:93–108
176. Hildenbrand DL, Lau KH, Baglio JW, Struck CW (2001) Thermochemistry of gaseous OSiI, $OSiI_2$, SiI, and SiI_2. J Phys Chem A 105:4114–4117
177. Hildenbrand DL, Lau KH, Sanjurjo A (2003) Experimental thermochemistry of the SiCl and SiBr radicals; enthalpies of formation of species in the Si−Cl and Si−Br systems. J Phys Chem A 107:5448–5451
178. Giricheva NI, Girichev GV, Shlykov SA et al (1995) The joint gas electron diffraction and mass spectrometric study of $GeI_4(g) + Ge(s)$ system: molecular structure of germanium diiodide. J Mol Struct 344:127–134

179. Haaland A, Hammel A, Martinsen K-G et al (1992) Molecular structures of monomeric gallium trichloride, indium trichloride and lead tetrachloride by gas electron diffraction. Dalton Trans 2209–2214
180. Hildenbrand DL, Lau KH, Perez-Mariano J, Sanjurjo A (2008) Thermochemistry of the gaseous vanadium chlorides VCl, VCl_2, VCl_3, and VCl_4. J Phys Chem A 112:9978–9982
181. Grant DJ, Matus MH, Switzer JR, Dixon DA (2008) Bond dissociation energies in second-row compounds. J Phys Chem A 112:3145–3156
182. Hildenbrand DL (1995) Dissociation energies of the monochlorides and dichlorides of Cr, Mn, Fe, Co, and Ni. J Chem Phys 103:2634–2641
183. Hildenbrand DL, Lau KH (1992) Trends and anomalies in the thermodynamics of gaseous thorium and uranium halides. Pure Appl Chem 64:87–92
184. Hildenbrand DL (1996) Dissociation energies of the molecules BCl and BCl^-. J Chem Phys 105:10507–10510
185. Ezhov YuS (1992) Force constants and characteristics of the structure of trihalides. Russ J Phys Chem 66:748–751
186. Gurvich LV, Ezhov YuS, Osina EL, Shenyavskaya EA (1999) The structure of molecules and the thermodynamic properties of scandium halides. Russ J Phys Chem 73:331–344
187. Hildenbrand DL, Lau KH (1995) Thermochemical properties of the gaseous scandium, yttrium, and lanthanum fluorides. J Chem Phys 102:3769–3775
188. Struck C, Baglio J (1991) Estimates for the enthalpies of formation of rare-earth solid and gaseous trihalides. High Temp Sci 31:209–237
189. Ezhov YuS (1995) Variations of molecular constants in metal halide series XY_n and estimates for bismuth trihalide constants. Russ J Phys Chem 69:1805–1809
190. Ezhov YuS (1993) Systems of force constants, coriolis coupling constants, and structure peculiarities of XY_4 tetrahalides. Russ J Phys Chem 67:901–904
191. Giricheva NI, Girichev GV (1999) Mean bond dissociation energies in molecules and the enthalpies of formation of gaseous niobium tetrahalides and oxytrihalides. Russ J Phys Chem 73:372–374
192. Berkowitz J, Ruscic B, Gibson S et al (1989) Bonding and structure in the hydrides of groups III-VI deduced from photoionization studies. J Mol Struct Theochem 202:363–373
193. Jones MN, Pilcher G (1987) Thermochemistry. Ann Rep Progr Chem C84:65–104
194. Craciun R, Long RT, Dixon DA, Christe KO (2010) Electron affinities, fluoride affinities, and heats of formation of the second row transition metal hexafluorides: MF_6 (M = Mo, Tc, Ru, Rh, Pd, Ag). J Phys Chem A114;7571–7582
195. Craciun R, Picone D, Long RT et al (2010) Third row transition metal hexafluorides, extraordinary oxidizers, and Lewis acids: electron affinities, fluoride affinities, and heats of formation of WF_6, ReF_6, OsF_6, IrF_6, PtF_6, and AuF_6. Inorg Chem 49:1056–1070
196. Batsanov SS (2002) Bond polarity as a function of the valence of the central atom. Russ J Inorg Chem 47:663–665
197. Leroy G, Temsamani DR, Sana M, Wilante C (1993) Refinement and extension of the table of standard energies for bonds involving hydrogen and various atoms of groups IV to VII of the Periodic Table. J Molec Struct 300:373–383
198. Batsanov SS (1994) Crystal-chemical estimates of bond energies in metals. Inorg Mater 30:926–927
199. Murphy LR, Meek TL, Allred AL, Allen LC (2000) Evaluation and test of Pauling's electronegativity scale. J Phys Chem A 104:5867–5871
200. Mulliken RS (1952) Magic formula, structure of bond energies and isovalent hybridization. J Phys Chem 56:295–311
201. Mulliken RS, Rieke CA, Orloff D, Orloff H (1949) Formulas and numerical tables for overlap integrals. J Chem Phys 17:1248–1267
202. Mulliken RS (1950) Overlap integrals and chemical binding. J Am Chem Soc 72:4493–4503
203. Jaffe HH (1953) Some overlap integrals involving d orbitals. J Chem Phys 21:258–263
204. Jaffe HH (1954) Studies in molecular orbital theory of valence: multiple bonds involving d-orbitals. J Phys Chem 58:185–190

205. Cotton FA, Leto J (1959) Acceptor properties, reorganization energies, and π bonding in the boron and aluminum halides. J Chem Phys 30:993–998
206. Batsanov SS, Zvyagina RA (1966) Overlap integrals and problem of effective charges, vol 1. Nauka, Novosibirsk (in Russian)
207. Batsanov SS, Kozhevina LI (1969) Overlap integrals, vol 2. Nauka, Novosibirsk (in Russian)
208. Ferreira R (1963) Principle of elecronegativity equalization: bond-dissociation energies. Trans Faraday Soc 59:1075–1079
209. Sanderson RT (1975) Interrelation of bond dissociation energies and contributing bond energies. J Am Chem Soc 97:1367–1372
210. Sanderson RT (1983) Electronegativity and bond energy. J Am Chem Soc 105:2259–2261
211. Sanderson RT (1986) The inert-pair effect on electronegativity. Inorg Chem 25:1856–1858
212. Matcha RL (1983) Theory of the chemical bond: accurate relationship between bond energies and electronegativity differences. J Am Chem Soc 105:4859–4862
213. Bratsch SG (1984) Electronegativity equalization with Pauling units. J Chem Educat 61:588–589
214. Bratsch SG (1985) A group electronegativity method with Pauling units. J Chem Educat 62:101–103
215. Reddy RR, Rao TVR, Viswanath R (1989) Correlation between electronegativity differences and bond energies. J Am Chem Soc 111:2914–2915
216. Smith DW (2002) Comment on "Evaluation and test of Pauling's electronegativity rule". J Phys Chem A 106:5951–5952
217. Smith DW (2004) Effects of exchange energy and spin-orbit coupling on bond energies. J Chem Educat 81:886–890
218. Nasar A, Shamsuddin M (1990) Thermodynamic properties of cadmium selenide. J Less-Common Met 158:131–135
219. Nasar A, Shamsuddin M (1990) Thermodynamic investigations of HgTe. J Less-Common Met 161:87–92
220. Nasar A, Shamsuddin M (1990) Thermodynamic properties of ZnTe. J Less-Common Met 161:93–99
221. Nasar A, Shamsuddin M (1992) Investigations of the thermodynamic properties of zinc chalcogenides. Thermochimica Acta 205:157–169
222. O'Hare PAG, Curtis LA (1995) Thermochemistry of (germanium + sulfur): IV. Critical evaluation of the thermodynamic properties of solid and gaseous germanium sulfide GeS and germanium disulfide GeS_2, and digermanium disulfide Ge_2S_2(g). Enthalpies of dissociation of bonds in GeS(g), GeS_2(g), and Ge_2S_2(g). J Chem Thermodyn 27:643–662
223. Tomaszkiewicz P, Hoppe GA, O'Hare PAG (1995) Thermochemistry of (germanium + tellurium): I. Standard molar enthalpy of formation $\Delta^{f}H_{m}^{\circ}$ at the temperature 298.15 K of crystalline germanium monotelluride GeTe by fluorine-bomb calorimetry. A critical assessment of the thermodynamic properties of GeTe(cr and g) and $GeTe_2$(g). J Chem Thermodyn 27:901–919
224. Boone S, Kleppa OJ (1992) Enthalpies of formation for group IV selenides ($GeSe_2$, $GeSe_2$(am), SnSe, $SnSe_2$, PbSe). Thermochim Acta 197:109–121
225. Kotchi A, Gilbert M, Castanet R (1988) Thermodynamic behaviour of the Sn + Te, Pb + Te, Sn + Se and Pb + Se melts according to the associated model. J Less-Common Met 143:L1-L6
226. O'Hare PAG, Lewis BM, Susman S, Volin KJ (1990) Standard molar enthalpies of formation and transition and other thermodynamic properties of the crystalline and vitreous forms of arsenic sesquiselenide (As_2Se_3). Dissociation enthalpies of As-Se bonds. J Chem Thermodyn 22:1191–1206
227. O'Hare PAG (1987) Inorganic chalcogenides: high-tech materials, low-tech thermodynamics. J Chem Thermodyn 19:675–701
228. Cemič L, Kleppa O (1988) High temperature calorimetry of sulfide systems. Phys Chem Miner 16:172–179
229. Goncharuk LV, Lukashenko GM (1986) Thermodynamic properties of chromium selenides, Cr_2Se_3. Russ J Phys Chem 60:1089–1089

230. Dittmer G, Niemann U (1981) Heterogeneous reactions and chemical-transport of tungsten with halogens and oxygen under steady-state conditions of incandescent lamps. Philips J Res 36:87–111
231. Robie RA, Hemingway BS (1985) Low-temperature molar heat capacities and entropies of MnO_2 (pyrolusite), Mn_3O_4 (hausmanite), and Mn_2O_3 (bixbyite). J Chem Thermodyn 17:165–181
232. Johnson GK, Murray WT, Van Deventer EH, Flotow HE (1985) The thermodynamic properties of zirconium ditelluride $ZrTe_2$–1500 K. J Chem Thermodyn 17:751–760
233. Fuger J (1992) Transuranium-element thermochemistry: a look into the past—a glimpse into the future. J Chem Thermodyn 24:337–358
234. O'Hare PAG, Lewis BM, Parkinson BA (1988) Standard molar enthalpy of formation of tungsten diselenide; thermodynamics of the high-temperature vaporization of WSe_2; revised value of the standard molar enthalpy of formation of molybdenite (MoS_2). J Chem Thermodyn 20:681–691
235. Leonidov VYa, Timofeev IV, Lazarev VB, Bozhko AB (1988) Enthalpy of formation of the wurtzite form of boron nitride. Russ J Inorg Chem 33:906–908
236. Ranade MR, Tessier F, Navrotsky A et al (2000) Enthalpy of formation of gallium nitride. J Phys Chem B 104:4060–4063
237. Kulikov IS (1988) Thermodynamics of carbides and nitrides. Metallurgiya, Chelyabinsk (in Russian)
238. Knacke O, Kubaschewski O, Hesselmann K (eds) (1991) Thermochemical properties of inorganic substances, 2nd edn. Springer-Verlag, Berlin
239. Yamaguchi K, Takeda Y, Kameda K, Itagaki K (1994) Measurements of heat of formation of GaP, InP, GaAs, InAs, GaSb and InSb. Materials Transactions JIM 35:596–602
240. Gordienko SP, Fenochka BF, Viksman GSh (1979) Thermodynamics of the lanthanide compounds. Naukova Dumka, Kiev (in Russian)
241. Yamaguchi K, Yoshizawa M, Takeda Y et al (1995) Measurement of thermodynamic properties of Al-Sb system by calorimeters. Materials Transactions JIM 36:432–437
242. Waddington TC (1959) Lattice energies and their significance in inorganic chemistry. Adv Inorg Chem Radiochem 1:157–221
243. Ratkey CD, Harrison BK (1992) Prediction of enthalpies of formation for ionic compounds. Ind Eng Chem Res 31:2362–2369
244. Born M, Lande A (1918) Kristallgitter und bohrsches Atommodell. Verh Dtsch Physik Ges 20:202–209
245. Born M, Lande A (1918) Über Berechnung der Compressibilität regulärer Kristalle aus der Gittertheorie. Verh Dtsch Physik Ges 20:21–216
246. Born M (1919) Eine thermochemischemische Anwendung der Gittertheorie. Verh Dtsch Physik Ges 21:13–24
247. Born M, Mayer JE (1932) Zur Gittertheorie der Ionenkristalle. Z Physik 75:1–18
248. Royer DJ (1968) Bonding theory. McGraw-Hill, New York
249. Bucher M (1990) Cohesive properties of silver halides. J Imaging Sci 34:89–95
250. Johnson QC, Templeton DH (1961) Madelung constants for several structures. J Chem Phys 34:2004–2007
251. Hoppe R (1970) Madelung constants as a new guide in the structural chemistry of solids. Adv Fluorine Chem 6:387–438
252. Alcock NW, Jenkins HDB (1974) Crystal structure and lattice energy of thallium (I) fluoride: inert-pair distortions. Dalton Trans 1907–1911
253. Zucker IJ (1991) Madelung constants and lattice sums for hexagonal crystals. J Phys A 24:873–879
254. Zemann J (1991) Madelung numbers for the theoretical structure type with mutual trigonal prismatic coordination. Acta Cryst A 47:851–852
255. Keshishi A (1996) Calculation of Madelung constant of various ionic structures based on the semisimple Lie algebras. Modern Phys Lett 10:475–485

256. Gaio M, Silvestrelli PL (2009) Efficient calculation of Madelung constants for cubic crystals. Phys Rev B 79:012102
257. Baker AD, Baker MD (2010) Rapid calculation of individual ion Madelung constants and their convergence to bulk value. Am J Phys 78:102–105
258. Izgorodina EI, Bernard UL, Dean PM et al (2009) The Madelung constant of organic salts. Cryst Growth Des 9:4834–4839
259. Kapustinskii A (1933) On the second principle of crystal chemistry. Z Krist 86:359–369
260. Kapustinskii A (1943) Lattice energy of ionic crystals. Acta Physicochim URSS 18:370–377
261. Yatsimirskii KB (1951) Thermochemistry of coordination compounds. Akad Nauk, Moscow (in Russian)
262. Jenkins HDB, Pratt KF (1977) On basic radii of simple and complex ions and repulsion energy of ionic crystals. Proc Roy Soc A 356:115–134
263. Jenkins HDB, Thakur KP (1979) Reappraisal of thermochemical radii for complex ions. J Chem Educat 56:576–577
264. Jenkins HDB, Roobottom HK, Passmore J, Glasser L (1999) Relationships among ionic lattice energies, molecular (formula unit) volumes, and thermochemical radii. Inorg Chem 38:360–3620
265. Glasser L, Jenkins HDB (2000) Lattice energies and unit cell volumes of complex ionic solids. J Am Chem Soc 122:632–638
266. Sorokin NL (2001) Calculations of the lattice energy of fluoride solid solutions with fluorite structure. Russ J Phys Chem 75:1010–1011
267. Aleixo AI, Oliveira PH, Diogo HP, da Piedade MEM (2005) Enthalpies of formation and lattice enthalpies of alkaline metal acetates. Thermochim Acta 428:131–136
268. Yoder CH, Flora NJ (2005) Geochemical applications of the simple salt approximation to the lattice energies of complex materials. Amer Miner 90:488–515
269. Glasser L, Jenkins HDB (2005) Predictive thermodynamics for condensed phases. Chem Soc Rev 34:866–874
270. Glasser L, von Szentpály L (2006) Born-Haber-Fajans cycle generalized: linear energy relation between molecules, crystals and metals. J Am Chem Soc 128:12314–12321
271. Dimitrov V, Sakka S (1996) Electronic oxide polarizability and optical basicity of simple oxides. J Appl Phys 79:1736–1740
272. Xu Y-N, Ching WY (1993) Electronic, optical, and structural properties of some wurtzite crystals. Phys Rev B 48:4335–4351
273. Pandey R, Lepak P, Jaffe JE (1992) Electronic structure of alkaline-earth selenides. Phys Rev B 46:4976–4977
274. KanekoY, Koda T (1988) New developments in IIa–VIb (alkaline-earth chalcogenide) binary semiconductors. J Cryst Growth 86:72–78
275. Rocquefelte X, Whangbo M-H, Jobic S (2005) Structural and electronic factors controlling the refractive indices of the chalcogenides ZnQ and CdQ (Q = O, S, Se, Te). Inorg Chem 44:3594–3598
276. Hanafi ZM, Ismail FM (1988) Colour problem of mercuric oxide photoconductivity and electrical conductivity of mercuric oxide. Z phys Chem 158:8–86
277. Boldish SI, White WB (1998) Optical band gaps of selected ternary sulfide minerals. Amer Miner 83:865–871
278. Sohila S, Rajalakshmi M, Ghosh C et al (2011) Optical and Raman scattering studies on SnS nanoparticles. J Alloys Comp 509:5843–5847
279. Gawlik K-U, Kipp L, Skibowski M et al (1997) HgSe: metal or semiconductor? Phys Rev Lett 78:3165–3168
280. Di Quarto F, Sunseri C, Piazza S, Romano MC (1997) Semiempirical correlation between optical band gap values of oxides and the difference of electronegativity of the elements. J Phys Chem B 101:2519–2525
281. Di Quarto F, Sunseri C, Piazza S, Romano MC (2000) A semiempirical correlation between the optical band gap of hydroxides and the electronegativity of their constituents. Russ J Elektrochem 36:1203–1208

282. Julien C, Eddrief M, Samaras I, Balkanski M (1992) Optical and electrical characterizations of SnSe, SnS_2 and $SnSe_2$ single crystals. Mater Sci Engin B 15:70–72
283. Majumdar A, Xu HZ, Zhao F et al (2004) Bandgap energies and refractive indices of $Pb_{1-x}Sr_xSe$. J Appl Phys 95:939–942
284. Lokhande CD (1992) Chemical deposition of CoS films. Indian J Pure Appl Phys 30:245–247
285. Bai X, Kordesch ME (2001) Structure and optical properties of ScN thin films. Appl Surf Sci 175–176:499–504
286. Hulliger F (1979) Rare earth pnictides. In: Gschneidner KA Jr, Eyring L (eds) Handbook on the physics and chemistry of rare earths, vol 4. Amsterdam: North-Holland
287. Meng J, Ren Y (1991) Investigation of the photoelectronic properties of rare earth monophosphide. Solid State Commun 80: 485–488
288. Miyuata N, Moriki K, Mishima O et al (1989) Optical constants of cubic boron nitride. Phys Rev B 40:12028–12029
289. Onodera A, Nakatani M, Kobayashi M et al (1993) Pressure dependence of the optical-absorption edge of cubic boron nitride. Phys Rev B 48:2777–2780
290. Tarrio C, Schnatterly S (1989) Interband transitions, plasmons, and dispersion in hexagonal boron nitride. Phys Rev B 40:7852–7859
291. Stenzel O, Hahn J, Röder M et al (1996) The optical constants of cubic and hexagonal boron nitride thin films and their relation to the bulk optical constants. Phys Status Solidi 158a:281–287
292. Prasad C, Sahay M (1989) Electronic structure and properties of boron phosphide and boron arsenide. Phys Status Solidi 154b:201–207
293. Vurgaftman I, Meyer JR, Ram-Mohan LR (2001) Band parameters for III–V compound semiconductors and their alloys. J Appl Phys 89:581–5875
294. McBride JR, Hass KC, Weber WH (1991) Resonance-Raman and lattice-dynamics studies of single-crystal PdO. Phys Rev B 44:5016–5028
295. Dey S, Jain VK (2004) Platinum group metal chalcogenides. Platinum Metals Rev 48:16–29
296. Welker H (1952) Uber neue halbleitende Verbindungen. Z Naturforsch 7a:744–749
297. Manca P (1961) A relation between the binding energy and the band-gap energy in semiconductors of diamond or zinc-blende structure. J Phys Chem Solids 20:268–273
298. Vijh AK (1969) Correlation between bond energies and forbidden gaps of inorganic binary compounds. J Phys Chem Solids 30:1999–2005
299. Reddy RR, Ahammed YN (1995) Relationship between refractive index, optical electronegativities and electronic polarizability in alkali halides, III–V, II–VI group semiconductors. Cryst Res Technol 30:263–266
300. Gong X, Gao F, Yamaguchi T et al (1992) Dependence of energy band gap and lattice constant of III-V semiconductors on electronegativity difference of the constituent elements. Cryst Res Technol 27:1087–1096
301. Duffy JA (1977) Variable electronegativity of oxygen in binary oxides: possible relevance to molten fluorides. J Chem Phys 67:2930–2931
302. Duffy JA (1980) Trends in energy gaps of binary compounds: an approach based upon electron transfer parameters from optical spectroscopy. J Phys C 13:2979–2990
303. Mooser E, Pearson WB (1959) On the crystal chemistry of normal valence compounds. Acta Cryst 12:1015–1022
304. Makino Y (1994) Interpretation of band gap, heat of formation and structural mapping for sp-bonded binary compounds on the basis of bond orbital model and orbital electronegativity. Intermetallics 2:55–56
305. Villars P (1983) A three-dimensional structural stability diagram for 998 binary AB intermetallic compounds. J Less-Common Met 92:215–238
306. Villars P (1983) A three-dimensional structural stability diagram for 1011 binary AB_2 intermetallic compounds. J Less-Common Met 99:33–43
307. Phillips JC (1973) Bonds and bands in semiconductors. Academic Press, New York
308. Hooge FN(1960) Relation between electronegativity and energy bandgap. Z phys Chem 24:27–282

309. Shimakawa K (1981) On the compositional dependence of the optical gap in amorphous semiconducting alloys. J Non-Cryst Solids 43:229–244
310. Batsanov SS (1965) A new method of calculating the width of the forbidden zone. J Struct Chem 5:862–864
311. Batsanov SS (1972) Quantitative characteristics of bond metallicity in crystals. J Struct Chem 12:809–813
312. Harrison WA (1980) Electronic structure and properties of solids. Freeman, San Feancisco; Christensen NE, Satpathy S, Pawlowska Z (1987) Bonding and ionicity in semiconductor. Phys Rev 36:1032–1050
313. Veal TD, Mahboob I, McConville CF (2004) Negative band gaps in dilute InN_xSb_{1-x} alloys. Phys Rev Lett 92:136–801
314. Suchet J (1965) Chemical physics of semiconductors. Van Nostrand, Princeton
315. Phillips JC (1970) Ionicity of the chemical bond in crystals. Rev Modern Phys 42:31–356
316. Nethercot AH Jr (1974) Prediction of Fermi energies and photoelectric thresholds based on electronegativity concepts. Phys Rev Lett 33:1088–1091
317. Poole RT, Williams D, Riley J et al (1975) Electronegativity as a unifying concept in the determination of Fermi energies and photoelectric thresholds. Chem Phys Lett 36:401–403
318. Chen ECM, Wentworth WE, Ayala JA (1977) The relationship between the Mulliken electronegativities of the elements and the work functions of metals and nonmetals. J Chem Phys 67:2642–2647
319. Nethercot AH (1981) Electronegativity and a model Hamiltonian for chemical applications. Chem Phys 59:297–313
320. Lonfat M, Marsen B, Sattler K (1999) The energy gap of carbon clusters studied by scanning tunneling spectroscopy. Chem Phys Lett 313:539–543
321. Banerjee R, Jayakrishnan R, Ayub P (2000) Effect of the size-induced structural transformation on the band gap in CdS nanoparticles. J Phys Cond Matt 12:10647–10654
322. Sarangi SN, Sahu SN (2004) CdSe nanocrystalline thin films: composition, structure and optical properties. Physica E 23:159–167
323. Vidal J, Lany S, d'Avezac M et al (2012) Band-structure, optical properties, and defect physics of the photovoltaic semiconductor SnS. Appl Phys Lett 100:032104
324. Franzman MA, Schlenker CW, Thompson ME, Brutchey RL (2010) Solution-phase synthesis of SnSe nanocrystals for use in solar cells. J Am Chem Soc 132:4060–4061
325. Wang Y, Suna A, Mahler W, Kasowski R (1987) PbS in polymers: from molecules to bulk solids. J Chem Phys 87:7315–7322
326. Salem AM, Selim MS, Salem AM (2001) Structure and optical properties of chemically deposited Sb_2S_3 thin film. J Phys D 34:12–17
327. Tyagi P, Vedeshwar AG (2001) Thickness dependent optical properties of CdI_2 films. Physica B 304:166–174
328. Ma DDD, Leo CS, Au FCK et al (2003) Small-diameter silicon nanowire surface. Science 299:1874–1877
329. Wang H, He Y, Chen W et al (2010) High-pressure behavior of β-Ga_2O_3 nanocrystal. J Appl Phys 107:033520
330. Liu B, Li Q, Du X et al (2011) Facile hydrothermal synthesis of CeO_2 nanosheets with high reactive exposure surface. J Alloys Comp 509:6720–6724
331. Ramana CV, Vemuri RS, Fernandez I, Campbell AL (2009) Size-effect on the optical properties of zirconium oxide thin films. Appl Phys Lett 95:231905
332. He Y, Liu JF, Chen W et al (2005) High-pressure behavior of SnO_2 nanocrystals. Phys Rev B 72:212102
333. Gullapalli SK, Vemuri RS, Ramana CV (2010) Structural transformation induced changes in the optical properties of nanocrystalline tungsten oxide thin films. Appl Phys Lett 96:171903
334. Cisneros-Morales MC, Aita CR (2010) The effect of nanocrystallite size in monoclinic HfO_2 films on lattice expansion and near-edge optical absorption. Appl Phys Lett 96:191904
335. Hirai H, Terauchi V, Tanaka M, Kondo K (1999) Band gap of essentially fourfold-coordinated amorphous diamond synthesized from C_{60} fullerene. Phys Rev B 60:6357–6361

336. Alexenskii AE, Osipov VYu, Vul' AYa et al (2001) Optical properties of nanodiamond layers. Phys Solid State 43:14–150
337. Housecroft CE, Constable EC (2010) Chemistry, 4th edn. Pearson, Edinburgh
338. Fajans K (1951) General Chemistry by Linus Pauling. J Phys Chem 55:1107–1108
339. Hückel W (1957) Die chemische Bindung. Kritische Betrachtung der Systematik, der Ausdrucksweisen und der formelmäßigen Darstellung. J prakt Chem 5:105–174
340. Batsanov SS (1960) Comments on Hückel's book. Zh Fiz Khim 34:937–938 (in Russian)
341. Syrkin YaK (1962) Effective charges and electronegativity. Russ Chem Rev 31:197–207
342. Spiridonov VP, Tatevskii VM (1963) On the concept of electronegativity of atoms: content and definitions of electronegativity used by various authors. Zh Fiz Khim 37:994–1000 (in Russian)
343. Spiridonov VP, Tatevskii VM (1963) Analysis of Pauling's scale of electronegativity. Zh Fiz Khim 37:1236–1242 (in Russian)
344. Spiridonov VP, Tatevskii VM (1963) A review of empirical methods of calculating electronegativity by various authors. Zh Fiz Khim 37:1583–1586 (in Russian)
345. Spiridonov VP, Tatevskii VM (1963) A review of semi-empirical and theoretical methods of calculating electronegativities. Zh Fiz Khim 37:1973–1978 (in Russian)
346. Bykov GV (1965) On the electronegativity of atoms (atomic cores) in molecules. Zh Fiz Khim 39:1289–1291 (in Russian)
347. Batsanov SS (1963) On the article "Effective charges and electronegativites" by Ya.K. Syrkin. Zh Fiz Khim 37:1418–1422 (in Russian)
348. Bratsch G (1988) Revised Mulliken electronegativities: calculation and conversion to Pauling units. J Chem Educat 65:34–41
349. Bratsch G (1988) Revised Mulliken electronegativities: applications and limitations. J Chem Educat 65:223–227
350. Batsanov SS (1967) On the articles by V.P. Spiridonov and V.M. Tatevskii criticizing the concept of electronegativity. Zh Fiz Khim 41:2402–2406 (in Russian)
351. Hinze J (1968) Elektronegativität der Valenzzustände. Fortschr chem Forschung 9:448–485
352. Komorowski L (1987) Chemical hardness and Pauling's scale of electronegativities. Z Naturforsch A 42:767–773
353. Komorowski L, Lipinski J (1991) Quantumchemical electronegativity and hardness indices for bonded atoms. Chem Phys 157:45–60
354. Allen LC (1989) Electronegativity is the average one-electron energy of the valence-shell electrons in ground-state free atoms. J Am Chem Soc 111:9003–9014
355. Cherkasov AR, Galkin VI, Zueva EM, Cherkasov RA (1998) The concept of electronegativity: the current state of the problem. Russ Chem Rev 67:375–392
356. Batsanov SS (1968) The concept of electronegativity: conclusions and prospects. Russ Chem Rev 37:332–350
357. Allred AL (1961) Electronegativity values from thermochemical data. J Inorg Nucl Chem 17:215–221
358. Leroy G (1983) Stability of chemical species. Int J Quantum Chem 23:271–308
359. Leroy G, Sana M, Wilante C, van Zieleghem M-J (1991) Revaluation of the bond energy terms for bonds between atoms of the first rows of the Periodic Table, including lithium, beryllium and boron. J Molec Struct 247:199–215
360. Leroy G, Temsamani DR, Wilante C (1994) Refinement and extension of the table of standard energies for bonds containing atoms of the fourth group of the Periodic Table. J Molec Struct 306:21–39
361. Leroy G, Temsamani DR, Wilante C, Dewispelaere J-P (1994) Determination of bond energy terms in phosphorus containing compounds. J Molec Struct 309:113–119
362. Leroy G, Dewispelaere J-P, Benkadour H (1995) Theoretical approach to the thermochemistry of geminal interactions in XY_2H_n compounds (X = C, N, O, Si, P, S; Y = NH_2, OH, F, SiH_3, PH_2, SH). J Molec Struct Theochem 334:137–143
363. Ochterski JW, Peterson GA, Wiberg KB (1995) A comparison of model chemistries. J Am Chem Soc 117:11299–11308

364. Smith DW (1998) Group electronegativities from electronegativity equilibration. Faraday Trans 94:201–205
365. Smith DW (2007) A new approach to the relationship between bond energy and electronegativity. Polyhedron 26:519–523
366. Matsunaga N, Rogers DW, Zavitsas AA (2003) Pauling's electronegativity equation and a new corollary accurately predict bond dissociation enthalpies and enhance current understanding of the nature of the chemical bond. J Org Chem 68:3158–3172
367. Ionov SP, Alikhanyan AS, Orlovskii VP (1992) On the determination of the electronegativity of both the chemical bond and atom in molecule. Doklady Phys Chem 325:455–456
368. Batsanov SS (2000) Thermochemical electronegativities of metals. Russ J Phys Chem 74:267–270
369. Howard JAK, Hoy VJ, O'Hagan D, Smith GTS (1996) How good is fluorine as a hydrogen bond acceptor? Tetrahedron 52:12613–12622
370. Dunitz JD, Taylor R (1997) Organic fluorine hardly ever accepts hydrogen bonds. Chem Eur J 3:89–98
371. Bykov GV, Dobrotin RB (1968) Calculation of the electronegativity of fluorine from thermochemical data. Russ Chem Bull 17:226–2271
372. Batsanov SS (1989) Structure and properties of fluorine, oxygen, and nitrogen atoms in covalent bonds. Russ Chem Bull 38:410–412
373. Finemann MA (1958) Correlation of bond dissociation energies of polyatomic molecules using Pauling's electronegativity concept. J Phys Chem 62:947–951
374. Datta D, Singh SN (1990) Evaluation of group electronegativity by Pauling's thermochemical method. J Phys Chem 94:2187–2190
375. Batsanov SS (1962) Electronegativity of elements and chemical bond. Nauka, Novosibirsk (in Russian)
376. Batsanov SS (1990) The concept of electronegativity and structural chemistry. Sov Sci Rev B Chem Rev 15(4):3
377. Batsanov SS (1975) System of electronegativities and effective atomic charges in crystalline compounds. Russian J Inorg Chem 20:1437–1440
378. Batsanov SS (1990) Polar component of the atomization energy and electronegativity of atoms in crystals. Inorg Mater 26:569–572
379. Batsanov SS (2001) Electronegativities of metal atoms in crystalline solids. Inorg Mater 37:23–30
380. Vieillard P, TardyY (1988) Une nouvelle échelle d'électronégativité des ions. Compt Rend Ser II 308:1539–1545
381. Ionov SP, Sevast'yanov DV (1994) Relative chemical potential and structural-thermochemical model of metallic bonds. Zh Neorg Khim 39:2061–2067 (in Russian)
382. Mulliken RS (1934) A new electroaffinity scale; together with data on valence states and on valence ionization potentials and electron affinities. J Chem Phys 2:782–793
383. Mulliken RS (1935) Electroaffinity, molecular orbitals and dipole moments. J Chem Phys 3:573–585
384. Mulliken RS (1937) Discussion of the papers presented at the symposium on molecular structure. J Phys Chem 41:318–320
385. Pritchard HO (1953) The determination of electron affinities. Chem Rev 52:529–563
386. Pritchard HO, Skinner HA (1955) The concept of electronegativity. Chem Rev 55:745–786
387. Skinner HA, Sumner FH (1957) The valence states of the elements V, Cr, Mn, Fe, Co, Ni, and Cu. J Inorg Nucl Chem 4:245–263
388. Pilcher G, Skinner HA (1962) Valence-states of boron, carbon, nitrogen and oxygen. J Inorg Nucl Chem 24:93–952
389. Batsanov SS (1960) Structural-chemical problems of the electronegativity concept. Proc Sibir Branch Acad Sci USSR 1:68–83 (in Russian)
390. Iczkowski RP, Margrave JL (1961) Electronegativity. J Am Chem Soc 83:3547–3551
391. Hinze J, Jaffe HH (1962) Orbital electronegativity of neutral atoms. J Am Chem Soc 84:540–546

392. Hinze J, Whitehead MA, Jaffe HH (1963) Bond and orbital electronegativities. J Am Chem Soc 85:148–154
393. Hinze J, Jaffe HH (1963) Orbital electronegativities of the neutral atoms of the period three and four and of positive ions of period one and two. J Phys Chem 67:1501–1506
394. Parr RG, Donnelly RA, Levy M, Palke WE (1978) Electronegativity: the density functional approach. J Chem Phys 68:3801–3807
395. Parr RG, Yang W (1989) Density-functional theory of atoms molecules. Oxford University Press, New York
396. Parr RG, Bartolotti L (1982) On the geometric mean principle for electronegativity equalization. J Am Chem Soc 104:3801–3803
397. Polizer P, Murray JS (2006) A link between the ionization energy ratios of an atom and its electronegativity and hardness. Chem Phys Lett 431:195–198
398. Sen KD, Jørgensen CK (eds) (1987) Structure and Bonding, vol 66. Springer-Verlag, Berlin
399. Allen LC (1994) Chemistry and electronegativity. Int J Quantum Chem 49:253–277
400. Bergmann D, Hinze J (1996) Electronegativity and molecular properties. Angew Chem Int Ed 35:150–163
401. Sacher E, Currie JF (1988) A comparison of electronegativity series. J Electr Spectr Relat Phenom 46:173–177
402. Valone SM (2011) Quantum mechanical origins of the Iczkowski–Margrave model of chemical potential. J Chem Theory Comput 7:2253–2261
403. Pearson RG (1988) Absolute electronegativity and hardness: application to inorganic chemistry. Inorg Chem 27:734–740
404. Pearson RG (1990) Electronegativity scales. Acc Chem Res 23:1–2
405. Politzer P, Shields ZP-I, Bulat FA, Murray JS (2011) Average local ionization energies as a route to intrinsic atomic electronegativities. J Chem Theory Comput 7:377–384
406. Allen LC (1994) Chemistry and electronegativity. Int J Quant Chem 49:253–277
407. Mann JB, Meek TL, Allen LC (2000) Configuration energies of the main group elements. J Am Chem Soc 122:2780–2783
408. Mann JB, Meek TL, Knight ET et al (2000) Configuration energies of the d-block elements. J Am Chem Soc 122:5132–5137
409. Brown ID, Skowron A (1990) Electronegativity and Lewis acid strength. J Am Chem Soc 112:3401–3403
410. Martynov AI, Batsanov SS (1980) New approach to calculating atomic electronegativities. Russ J Inorg Chem 25:1737–1740
411. Giemza J, Ptak WS (1984) An empirical chemical potential of the atomic core for non-transition element. Chem Phys Lett 104:115–119
412. Bergmann D, Hinze J (1987) Electronegativity and charge distribution. In: Sen KD, Jörgensen CK (eds) Structure and Bonding, vol. 66. Springer-Verlag, Berlin
413. True JE, Thomas TD, Winter RW, Gard GL (2003) Electronegativities from core ionization energies: electronegativities of SF_5 and CF_3. Inorg Chem 42:4437–4441
414. Stevenson DP (1955) Heat of chemisorption of hydrogen in metals. J Chem Phys 23:203–203
415. Trasatti S (1972) Electronegativity, work function, and heat of adsorption of hydrogen on metals. J Chem Soc Faraday Trans I 68:229–236
416. Trasatti S (1972) Work function, electronegativity, and electrochemical behaviour of metals. J Electroanalytical Chem 39:163–184
417. Dritz ME (2003) Properties of elements. Metals, Moscow (in Russian)
418. Miedema AR, De Boer FR, De Chatel PF (1973) Empirical description of the role of electronegativity in alloy formation. J Phys F 3:1558–1576
419. Miedema AR, De Chatel PF, De Boer FR (1980) Cohesion in alloys—fundamentals of a semi-empirical model. Physica B 100:1–28
420. Ray PK, Akinc M, Kramer MJ (2010) Applications of an extended Miedema's model for ternary alloys. J Alloys Comp 489:357–361
421. Parr RG, Pearson RG (1983) Absolute hardness: companion parameter to absolute electronegativity. J Am Chem Soc 105:7512–7516

422. Pearson RG (1993) Chemical hardness—a historical introduction. Structure and Bonding 80:1–10
423. Batsanov S.S. (1986) Experimental foundations of structural chemistry. Standarty, Moscow (in Russian)
424. Cottrell TL, Sutton LE (1951) Covalency, electrovalency and electronegativity. Proc Roy Soc London A 207:49–63
425. Pritchard HO (1953) The determination of electron affinities. Chem Rev 52:529–563
426. Allred AL, Rochow EG (1958) A scale of electronegativity based on electrostatic force. J Inorg Nucl Chem 5:264–268
427. Batsanov SS (1993) A new scale of atomic electronegativities. Russ Chem Bull 42:24–29
428. Batsanov SS (2004) Geometrical electronegativity scale for elements taking into account their valence and physical state. Russ J Inorg Chem 49:1695–1701
429. Sanderson RT (1951) An interpretation of bond lengths and a classification of bonds. Science 114:670–672
430. Sanderson RT (1982) Radical reorganization and bond energies in organic molecules. J Org Chem 47:3835–3839
431. Sanderson RT (1988) Principles of electronegativity: general nature. J Chem Educat 65:112–118
432. Sanderson RT (1988) Principles of electronegativity: applications. J Chem Educat 65:227–231
433. Batsanov SS (1988) Refinement of the Sanderson procedure for calculating electronegativities of atoms. J Struct Chem 29:631–635
434. Batsanov SS (1978) A new approach to the geometric determination of the electronegativities of atoms in crystals. J Struct Chem 19:826–829
435. Gorbunov AI, Kaganyuk DS (1986) A new method for the calculation of electronegativity of atoms. Russ J Phys Chem 60:1406–1407
436. Batsanov SS (1971) Electronegativity and effective charges of atoms. Znanie, Moscow (in Russian)
437. Ray N, Samuels L, Parr RG (1979) Studies of electronegativity equalization. J Chem Phys 70:3680–3684
438. Batsanov SS (1994) Equalization of interatomic distances in polymorphous transformations under pressure. J Struct Chem 35:391–393
439. Batsanov SS (1975) Electronegativity of elements and chemical bond (in Russian). Nauka, Novosibirsk
440. Phillips JC (1968) Covalent bond in crystals: partially ionic binding. Phys Rev 168:905–911
441. Phillips JC (1968) Covalent bond in crystals: anisotropy and quadrupole moments. Phys Rev 168:912–917
442. Phillips JC (1968) Covalent bond in crystals: lattice deformation energies. Phys Rev 168:917–921
443. Phillips JC (1974) Chemical bonding at metal-semiconductor interfaces. J Vacuum Sci Technol 11:947–950
444. Phillips JC, Lucovsky G. (2009) Bonds and bands in semiconductors 2nd ed. Momentum Press
445. Li K, Xue D (2006) Estimation of electronegativity values of elements in different valence states. J Phys Chem A110;11332–11337
446. Li K, Wang X, Zhang F, Xue D (2008) Electronegativity identification of novel superhard materials. Phys Rev Lett 100:235504
447. Pettifor DG (1984) A chemical scale for crystal-structure maps. Solid State Commun 51:31–34
448. Pettifor DG (1985) Phenomenological and microscopic theories of structural stability. J Less-Common Metals 114:7–15
449. Pettifor DG (2003) Structure maps revisited. J Phys Cond Matter 15:V13–V16
450. Campet G, Portiera J, Subramanian MA (2004) Electronegativity versus Fermi energy in oxides: the role of formal oxidation state. Mater Lett 58:437–438
451. Carver JC, Gray RC, Hercules DM (1974) Remote inductive effects evaluated by X-ray photoelectron spectroscopy. J Am Chem Soc 96:6851–6856

452. Gray R, Carver J, Hercules D (1976) An ESCA study of organosilicon compounds. J Electron Spectr Relat Phenom 8:343–357
453. Gray R, Hercules D (1977) Correlations between ESCA chemical shifts and modified Sanderson electronegativity calculations. J Electron Spectr Relat Phenom 12:37–53
454. Ray NK, Samuels L, Parr RG (1979) Studies of electronegativity equalization. J Chem Phys 70:3680–3684
455. Parr RG, Bartolotti LJ, Gadre SR (1980) Electronegativity of the elements from simple $\chi\alpha$ theory. J Am Chem Soc 102:2945–2948
456. Pearson RG (1985) Absolute electronegativity and absolute hardness of Lewis acids and bases. J Am Chem Soc 107:6801–6806
457. Fuentealba P, Parr RG (1991) Higher-order derivatives in density-functional theory, especially the hardness derivative $\partial\eta/\partial N$. J Chem Phys 94:5559–5564
458. Politzer P, Weinstein H (1979) Some relations between electronic distribution and electronegativity. J Chem Phys 71:4218–4220
459. Ferreira R, Amorim AO (1981) Electronegatlvity and the bonding character of molecular orbitals.Theor Chim Acta 58:131–136
460. Amorim AO de, Ferreira R (1981) Electronegativities and the bonding character of molecular orbitals: A remark. Theor Chim Acta 59:551–553
461. Pearson RG (1989) Absolute electronegativity and hardness: applications to organic chemistry. J Org Chem 54:1423–1430
462. Mortier WJ, van Genechten K, Gasteiger J (1985) Electronegativity equalization: application and parametrization. J Am Chem Soc 107:829–835
463. Mortier WJ, Ghosh SK, Shankar S (1986) Electronegativity-equalization method for the calculation of atomic charges in molecules. J Am Chem Soc 108:4315–4320
464. Van Genechten KA, Mortier WJ, Geerlings P (1987) Intrinsic framework electronegativity: a novel concept in solid state chemistry. J Chem Phys 86:5063–5071
465. Uytterhoeven L, Mortier WJ, Geerlings P (1989) Charge distribution and effective electronegativity of aluminophosphate frameworks. J Phys Chem Solids 50:479–486
466. De Proft F, Langenaeker W, Geerlings P (1995) A non-empirical electronegativity equalization scheme: theory and applications using isolated atom properties. J Mol Struct Theochem 339:45–55
467. Bultinck P, Langenaeker W, Lahorte P et al (2002) The electronegativity equalization method: parametrization and validation for atomic charge calculations. J Phys Chem A 106:7887–7894
468. Bultinck P, Langenaeker W, Lahorte P et al (2002) The electronegativity equalization method: applicability of different atomic charge schemes. J Phys Chem A 106:7895–7901
469. von Szentpály L (1991) Studies on electronegativity equalization: consistent diatomic partial charges. J Mol Struct Theochem 233:71–81
470. Donald KJ, Mulder WH, von Szentpály L (2004) Valence-state atoms in molecules: influence of polarization and bond-charge on spectroscopic constants of diatomic molecules. J Phys Chem A 108:595–606
471. Speranza G, Minati L, Anderle M (2006) Covalent interaction and semiempirical modeling of small molecules. J Phys Chem A 110:13857–13863
472. Boudreaux EA (2011) Calculations of bond dissociation energies: new select applications of an old method. J Phys Chem A 115:1713–1720
473. Islam N, Ghosh DC (2010) Evaluation of global hardness of atoms based on the commonality in the basic philosophy of the origin and the operational significance of the electronegativity and the hardness. Eur J Chem 1:83–89
474. Urusov VS (1961) On the calculation of bond ionicity in binary compounds. Zh Neorg Khim 6:2436–2439 (in Russian)
475. Batsanov SS (1964) Calculating the degree of bond ionicity in complex ions by electronegativity method. Zh Neorg Khim 9:1323–1327 (in Russian)
476. Waber JT, Cromer DT (1965) Orbital radii of atoms and ions. J Chem Phys 42:4116–4123
477. Batsanov SS (2011) Calculating atomic charges in molecules and crystals by a new electronegativity equalization method. J Mol Struct 1006:223–226

478. Batsanov SS (2011) Thermodynamic determination of van der Waals radii of metals. J Mol Struct 990:63–66
479. Pauling L (1952) Interatomic distances and bond character in the oxygen acids and related substances. J Phys Chem 56:361–365
480. Pauling L (1929) The principles determining the structure of complex ionic crystals. J Am Chem Soc 51:1010–1026
481. Pauling L (1948) The modern theory of valency. J Chem Soc 1461–1467
482. Sanderson RT (1954) Electronegativities in inorganic chemistry. J Chem Educat 31:238–245
483. Reed JL (2003) Electronegativity: coordination compounds. J Phys Chem A 107:8714–8722
484. Suchet JP (1965) Chemical physics of semiconductors. Van Nostrand, London
485. Suchet JP (1977) Electronegativity, ionicity, and effective atomic charge. J Electrochem Soc 124:30C–35C
486. Noda Y, Ohba S, Sato S, Saito Y (1983) Charge distribution and atomic thermal vibration in lead chalcogenide crystals. Acta Cryst B 39:312–317
487. Feldmann C, Jansen M (1993) Cs_3AuO, the first ternary oxide with anionic gold. Angew Chem Int Ed 32:1049–1050
488. Pantelouris A, Kueper G, Hormes J et al (1995) Anionic gold in Cs_3AuO and Rb_3AuO established by X-ray absorption spectroscopy. J Am Chem Soc 117:11749–11753
489. Feldmann C, Jansen M (1995) Zur kristallchemischen Ähnlichkeit von Aurid- und Halogenid-Ionen. Z anorg allgem Chem 621:1907–1912
490. Mudring A-V, Jansen M (2000) Base-induced disproportionation of elemental gold. Angew Chem Int Ed 39:3066–3067
491. Nuss J, Jansen M (2009) BaAuP and BaAuAs, synthesis via disproportionation of gold upon interaction with pnictides as bases. Z allgem anorg Chem 635:1514–1516
492. Karpov A, Nuss J, Wedig U, Jansen M (2003) Cs_2Pt: a platinide(-II) exhibiting complete charge separation. Angew Chem Int Ed 42:4818–4821
493. Batsanov SS, Ruchkin ED (1959) Mixed halogenides of tetravalent platinum. Zh Neorg Khim 4:1728–1733 (in Russian)
494. Batsanov SS, Ruchkin ED (1965) On the isomerism of mixed halogenides of platinum. Zh Neorg Khim 10:2602–2605 (in Russian)
495. Batsanov SS, Sokolova MN, Ruchkin ED (1971) Mixed halides of gold. Russ Chem Bull 20:1757–1759
496. Batsanov SS (1986) Experimental foundations of structural chemistry. Standarty, Moscow (in Russian)
497. Batsanov SS, Rigin VI (1966) Isomerism of thallium selenobromides. Doklady Akad Nauk SSSR 167:89–90
498. Dehnicke K (1965) Synthesis of oxide halides. Angew Chem Int Ed 4:22–29
499. Custelcean R, Jackson JE (1998) Topochemical control of covalent bond formation by dihydrogen bonding. J Am Chem Soc 120:12935–12941
500. Batana A, Faour J (1984) Pressure dependence of the effective charge of ionic crystals. J Phys Chem Solids 45:571–574
501. Ves S, Strössner K, Cardona M (1986) Pressure dependence of the optical phonon frequencies and the transverse effective charge in AlSb. Solid State Commun 57:483–486
502. Katayama Y, Tsuji K, Oyanagi H, Shimomura O (1998) Extended X-ray absorption fine structure study on liquid selenium under pressure. J Non-Cryst Solids 232–234:93–98
503. Gauthier M, Polian A, Besson J, Chevy A (1989) Optical properties of gallium selenide under high pressure. Phys Rev B 40:3837–3854
504. Talwar DN, Vandevyver M (1990) Pressure-dependent phonon properties of III-V compound semiconductors. Phys Rev B 41:12129–12139
505. Kucharczyk W (1991) Pressure dependence of effective ionic charges in alkali halides. J Phys Chem Solids 52:435–436
506. Errandonea D, Segura A, Muoz V, Chevy A (1999) Effects of pressure and temperature on the dielectric constant of GaS, GaSe, and InSe: role of the electronic contribution. Phys Rev B 60:15866–15874

507. Goi AR, Siegle H, Syassen K et al (2001) Effect of pressure on optical phonon modes and transverse effective charges in GaN and AlN. Phys Rev B 64:035205
508. Yamanaka T, Fukuda T, Mimaki J (2002) Bonding character of SiO_2 stishovite under high pressures up to 30 GPa. Phys Chem Miner 29:633–641
509. Batsanov SS (1999) Pressure effect on the heat of formation of condensed substances. Russ J Phys Chem 73:1–6
510. Ferrante J, Schlosser H, Smith JR (1991) Global expression for representing diatomic potential-energy curves. Phys Rev A 43:3487–3494
511. Ghandehari K, Luo H, Ruoff AL et al (1995) Crystal structure and band gap of rubidium hydride to 120 GPa. Mod Phys Lett B 9:1133–1140
512. Ghandehari K, Luo H, Ruoff AL et al (1995) New high pressure crystal structure and equation of state of cesium hydride to 253 GPa. Phys Rev Lett 74:2264–2267
513. Batsanov SS (2005) Chemical bonding evolution on compression of crystals. J Struct Chem 46:306–314
514. Batsanov SS, Gogulya MF, Brazhnikov MA et al (1994) Behavior of the reacting system Sn + S in shock waves. Comb Explosion Shock Waves 30:361–365
515. Batsanov SS (2006) Mechanism of metallization of ionic crystals by pressure. Russ J Phys Chem 80:135–138
516. Reparaz JS, Muniz LR, Wagner MR et al (2010) Reduction of the transverse effective charge of optical phonons in ZnO under pressure. Appl Phys Lett 96:231906
517. Batsanov SS (2004) Determination of ionic radii from metal compressibilities. J Struct Chem 45:896–899
518. Batsanov SS (1994) Pressure dependence of bond polarities in crystalline materials. Inorg Mater 30:1090–1096
519. Batsanov SS (1997) Effect of high pressure on crystal electronegativities of elements. J Phys Chem Solids 58:527–532
520. Fujii Y, Hase K, Ohishi Y et al (1989) Evidence for molecular dissociation in bromine near 80 GPa. Phys Rev Lett 63:536–539
521. Takemura K, Minomura S, Shimomura O et al (1982) Structural aspects of solid iodine associated with metallization and molecular dissociation under high pressure. Phys Rev B 26:998–1004
522. Brown D, Klages P, Skowron A (2003) Influence of pressure on the lengths of chemical bonds. Acta Cryst B 59:439–448
523. Bokii GB (1948) Bond ionicity from atomic polarization and refraction. Moscow Univ Chem Bull 11:155–160

http://www.springer.com/978-94-007-4770-8

Introduction to Structural Chemistry
Batsanov, S.S.; Batsanov, A.S.
2012, X, 542 p., Hardcover
ISBN: 978-94-007-4770-8